National Library of Canada
Acquisitions and Bibliographic Services Branch
395 Wellington Street
Ottawa, Ontario
K1A 0N4

Bibliothèque nationale du Canada
Direction des acquisitions et des services bibliographiques
395, rue Wellington
Ottawa (Ontario)
K1A 0N4

Your file Votre référence

Our file Notre référence

NOTICE

The quality of this microform is heavily dependent upon the quality of the original thesis submitted for microfilming. Every effort has been made to ensure the highest quality of reproduction possible.

If pages are missing, contact the university which granted the degree.

Some pages may have indistinct print especially if the original pages were typed with a poor typewriter ribbon or if the university sent us an inferior photocopy.

AVIS

La qualité de cette microforme dépend grandement de la qualité de la thèse soumise au microfilmage. Nous avons tout fait pour assurer une qualité supérieure de reproduction.

S'il manque des pages, veuillez communiquer avec l'université qui a conféré le grade.

La qualité d'impression de certaines pages peut laisser à désirer, surtout si les pages originales ont été dactylographiées à l'aide d'un ruban usé ou si l'université nous a fait parvenir une photocopie de qualité inférieure.

Canada

Dynamic modelling and on-off switching control of a chilled water cooling system with storage

Wei Ling Jian

A thesis

in

The Centre for Building Studies

Presented in Partial Fulfilment of the

Requirements for the Degree of Master of Engineering at

Concordia University

Montreal, Quebec, Canada

January 1996

ISBN 0-612-10863-5

ABSTRACT

Dynamic modelling and on-off switching control of a chilled water cooling system with storage

by

Wei Ling Jian

A dynamic model of vapour compression refrigeration system is developed. The overall model consists of the following basic components: compressor, condenser, expansion valve, evaporator, evaporative cooler and cool storage. The integrated system is referred to as chilled water cooling system with storage (CWCS).

The mathematical modelling of the CWC system under taken in this study predicts the change in state of refrigerant in the system with respect to time. A computer program is developed to solve the equations by combining basic engineering principles with some empirical parameters and using correlations for the refrigerant properties. Open-loop tests are carried out to study the performance characteristics of the system under varied cooling load, compressor speed, and refrigerant mass flow rate. The model is intended to serve as an analytical design tool and to provide a basis for control analysis.

Based on heuristic method, some "optimal on-off control" strategies for the chilled water cool storage system are developed using reduced order models. The methodology of generating such control profiles is illustrated and the results of tests for optimality

show that the heuristic control profiles are near optimal.

The on-off control scheme is implemented on the full order CWC system. The operating performance of the system is described under several simulated cases. The results indicate that the control scheme is capable of maintaining the chilled water temperature close to the chosen setpoint range.

ACKNOWLEDGEMENTS

I take this opportunity to express my gratitude to my supervisor, Dr. M. Zaheer-uddin for his invaluable guidance, encouragement and suggestions during the whole course of this study.

Gratitude is also extended to Concordia University Centre for Building Studies for the use of computer facilities, and the technical stuff who provided a great deal of technical help and advice.

With respect, love and admiration, Sincerely thank my parents, and sister for their moral support.

Finally, special thanks and appreciation due to my husband Wei Zhang, for his devoted love, understanding, encouragement and support.

TABLE OF CONTENTS

ABSTRACT iii

LIST OF FIGURES ix

LIST OF TABLES xiv

NOMENCLATURE xv

CHAPTERS **PAGE**

1 INTRODUCTION 1

1.1 Motivation 2

1.2 A basic refrigeration cycle 2

1.3 Layout of the thesis 4

2 LITERATURE REVIEW 6

2.1 Modelling of vapour compression refrigeration system 7

2.1.1 Transient modelling 7
2.1.2 Steady state model 10
2.1.3 Brief review of some models 14

2.2 Control strategies for chiller and cool storage systems 15

2.3 Discussion 22

3 ANALYTICAL MODEL 25

3.1 Introduction 26

3.2 Physical model 26

TABLE OF CONTENTS

3.3 Basic modelling technique 28

3.4 Compressor model 30

3.5 Condenser model 32

3.5.1 Dynamic equations 33
3.5.2 Heat transfer coefficients 38

3.6 Evaporator model 39

3.6.1 Evaporation region 41
3.6.2 Superheat region 45
3.6.3 Heat transfer coefficients 48

3.7 Thermostatic expansion valve model 49

3.8 Evaporative cooler model 53

3.9 Chilled water storage tank model 54

4 SIMULATION RESULTS 56

4.1 Numerical technique 57

4.2 Simulation results and discussion 57

5 ON-OFF SWITCHING CONTROL STRATEGIES FOR THE CWC SYSTEM 74

5.1 Introduction 75

5.2 Construction of reduced-order model 75

5.3 Heuristic on-off control technique 77

5.4 ON time search methodology 79

5.5 Test for optimality of control profiles 80

5.6 Optimization method for searching problem 82

TABLE OF CONTENTS

5.7 Further investigation of the on-off control profiles 84

5.8 Application of heuristic on-off control profiles 85

5.8.1 Multiple usage of heuristic on-off control technique for daily load 86

5.8.2 Lead time switching approach for constrained near-optimal solution 87

5.9 Implementation 89

5.9.1 Results and discussion 90

6 CONCLUSIONS AND RECOMMENDATIONS 120

6.1 Conclusions 121

6.2 Recommendations for future work 123

REFERENCE 125

APPENDIX 131

LIST OF FIGURES

Figures Page

1.1 Single stage vapour compression system schematic diagram 3

1.2 Diagram of state changes of the refrigerant (for unit mass of refrigerant) 3

3.1 Schematic diagram of the CWC system 27

3.2 Condenser model 35

3.3 Evaporator model 40

3.4 Evaporation region 42

3.5 Superheat region 46

3.6 Typical gradient curve for thermostatic expansion valves 50

4.1 Flow chart of system computer program 63

4.2 Evaporation temperature as function of time 64

4.3 Condensation temperature as function of time 65

4.4 Chilled water storage tank temperature as function of time 66

4.5 Heat exchange rate of condenser and evaporator 67

4.6 Refrigerant states as function of time 68

4.7 Degree of superheat as function of percent load 69

4.8 Compressor power input as function of percent load and the speed 70

4.9 COP as function of percent mass flow rate 71

4.10a Temperatures in condenser as function of time 72

LIST OF FIGURES

Figures Page

4.10b Temperatures in evaporator as function of time 72

4.11 Tch as function of motor speed and percent load 73

5.1 Comparison of Tch and U3 responses between optimal (Jmin) and not optimal (other) case for load profile1

(a) Load profile1 92
(b) Tch response 92
(c) U3 responses 92

5.2 Steady-state optimal value of U3 as function of Um 93

5.3 Flow chart of the program for searching optimal on time 94

5.4 Flow chart of the program for searching optimal lead time 95

5.5 Chiller energy cost as function of lead time and on time for load profile1

(a) Load profile1 96
(b) Cost configuration 96

5.6 Flow chart of the program for finding Jmin and Tl by "Golden section" optimization method 97

5.7 Chiller energy cost as function of lead time and on time for load profile2

(a) Load profile2 98
(b) Cost configuration 98

5.8 Chiller energy cost as function of lead time and on time for load profile3

(a) Load profile3 99
(b) Cost configuration 99

LIST OF FIGURES

Figures Page

5.9 Comparison of Tch and U3 responses between optimal (Jmin) and not optimal (other) case for load profile2

(a) Load profile2 100
(b) Tch response 100
(c) U3 responses 100

5.10 Comparison of Tch and U3 responses between optimal (Jmin) and not optimal (other) case for load profile3

(a) Load profile3 101
(b) Tch response 101
(c) U3 responses 101

5.11a,b,c Optimal unconstrained Tch and U3 responses

(a) Daily load case1 profile 102
(b) Tch response 102
(C) U3 response 102

5.11d,e Optimal unconstrained Tch and U3 responses (first trial)

(d) Tch response 103
(e) U3 response 103

5.11f,g Optimal unconstrained Tch and U3 responses (second trial)

(f) Tch response 104
(g) U3 response 104

5.11h,i Optimal unconstrained Tch and U3 responses (third and final trial)

(h) Tch response 105
(i) U3 response 105

5.12 Lead time as a function of net overshoot in temperature 106

LIST OF FIGURES

Figures Page

5.13a,b,c Optimal unconstrained Tch and U3 responses

(a) Daily load case2 profile 107
(b) Tch response 107
(C) U3 response 107

5.13d,e Optimal unconstrained Tch and U3 responses (first trial using the results from Fig. 5.12)

(d) Tch response 108
(e) U3 response 108

5.13f,g Optimal unconstrained Tch and U3 responses (second and final trial using results from Fig. 5.12)

(f) Tch response 109
(g) U3 response 109

5.14a,b,c Optimal unconstrained Tch and U3 responses

(a) Daily load case3 profile 110
(b) Tch response 110
(C) U3 response 110

5.14d,e Optimal unconstrained Tch and U3 responses (using the results from Fig.5.12)

(d) Tch response 111
(e) U3 response 111

5.15 Open loop responses of Tch for three load cases

(a) Tch response at Um=0.3 (b) Tch response at Um=0.5
(c) Tch response at Um=0.8 112

5.16 Steady-state optimal value of An as function of Um 113

LIST OF FIGURES

Figures Page

5.17 Comparison of Tch responses between two models
for load profile1

(a) Load profile1 114
(b) Tch response 114

5.18 Comparison of Tch responses between two models
for load profile2

(a) Load profile2 115
(b) Tch response 115

5.19 Comparison of Tch responses between two models
for load profile3

(a) Load profile3 116
(b) Tch response 116

5.20 Comparison of Tch and energy input repones
of two models for daily load (case1)

(a) Daily load case1 profile 117
(b) Tch responses 117
(c) U3 and An responses 117

5.21 Comparison of Tch and energy input repones
of two models for daily load (case2)

(a) Daily load case1 profile (b) Tch responses 118
(c) U3 and An responses 118

5.22 Comparison of Tch and energy input repones
of two models for daily load (case3)

(a) Daily load case1 profile (b) Tch responses 119
(c) U3 and An responses 119

LIST OF TABLES

Tables	Page
3.1 Compressor parameters used in simulation	32
3.2 Condenser parameters used in simulation	39
3.3 Evaporator parameter used in simulation	49
3.4 Expansion valve parameters used in simulation	53
3.5 Evaporative cooler parameters used in simulation	54
3.6 Storage tank parameters used in simulation	55
5.1 System parameters of the reduced order model	80

NOMENCLATURE

A	heat transfer area of heat exchangers (m^2)
b_{fac}	thermal expansion valve bleed factor
C	thermal capacity (kJ/K), specific heat (kJ/kg·K), constant
C1	constant in equation (3.40)
COP	coefficient of performance
C_{txv}	general orifice flow area coefficient
D	diameter (m)
d	diameter (m)
dT	temperature differential
dt	time differential
E	function
F	$\pi \times$ diameter of inner or outer wall of the tube (m)
f	symbol of the function
ft	terminal time
G	mass velocity ($kg/s \cdot m^2$)
g	gravitational acceleration (m/s^2)
h	heat transfer coefficient ($kJ/s \cdot m^2 \cdot K$), enthalpy of refrigerant (kJ/kg)
H_c	heat transfer coefficient between tube surface and spray water ($kJ/s \cdot m^2 \cdot K$)
h_e	heat transfer coefficient between refrigerant and tubes in evaporation region ($kJ/s \cdot m^2 \cdot K$)

h_{es} heat transfer coefficient between refrigerant and tubes in superheat region ($kJ/s \cdot m^2 \cdot K$)

h_{fg} latent heat of evaporation (kJ/g)

High maximum value of search interval

H_l enthalpy of refrigerant leaving the discharge port (kJ/kg)

h_l enthalpy of saturated liquid refrigerant (kJ/kg)

h_o enthalpy of refrigerant at 0°C

h_s enthalpy of vapour entering the suction port (kJ/kg)

h_v enthalpy of saturated vapour refrigerant (kJ/kg)

i number of node

J energy cost, mechanical equivalent of heat

K polytrophic constant, assumed equal to specific heat ratio, thermal conductivity ($kJ/s \cdot m \cdot °C$)

k thermal conductivity ($kJ/s \cdot m \cdot °c$)

L length (m)

L_e length of the evaporator tubes in evaporation region (m)

Low minimum value of search interval

M mass of refrigerant (kg)

$\dot{M}$ mass flow rate of refrigerant (kg/h)

N compressor motor speed (rpm)

N_μ Nusselt number

P pressure (Pa)

P_r Prandtl number

Q capacity of the thermal expansion valve (Tons)

R_e Reynolds number

T temperature (°C), (K)

T(i) temperature at each node of superheat region

t time (s), (h)

t_0 starting time of cost function evaluation period

t_z ending time of cost function evaluation period

U_i mass flow rate ratio

U_{imax} maximum mass flow rate (kg/h)

U_m mass flow rate ratio of water from application facilities

U_{mmax} maximum mass flow rate of water from building (kg/h)

V_c volume of condenser (m^3)

V_{cl} clearance volume of the compressor cylinder (m^3)

V_d maximum volume of the compressor cylinder (m^3)

W_c work done by compressor motor (kJ/kg)

x variable in optimization search problem

y distance of the superheat volume node to the bondage between evaporation and superheat region

Subscripts

a upper

ao outgoing air from evaporative cooler

ac	ambient air of the evaporative cooler
c	condenser, condenser tubes, condensation, evaporative cooler
ci	inlet of the condenser
ch	chilled water
city	city water
chset	setpoint value of chilled water temperature
chss	steady-state condition of chilled water
co	outlet of the condenser
d	discharge section
e	evaporator tubes of evaporation region, evaporation
ei	inlet of the evaporator
eo	outlet of evaporator
es	evaporator tubes of superheat region
g	refrigerant vapour
i	inlet
ic	inside of condenser tubes
ie	inside of evaporator tubes
i,rt	inlet, rated
l	refrigerant liquid
La	test point close to low limit of the search interval
Lb	test point close to upper limit of the search interval
ld	lead

min	minimum
max	maximum
o	outlet
oc	between the condenser tubes and cycling water
oe	between the evaporator tubes and cycling water
on	on-mode
ope	operation condition
o,rt	outlet, rated
pa	air
r	cross section of inner tube of evaporator
rc	refrigerant in condenser
re	refrigerant in evaporator
rt	rated
r,rt	refrigerant, rated
r,txv	rated, thermal expansion valve
s	suction, superheat
sh	superheat
ss	steady-state
t	total
v	saturated refrigerant vapour
w	condenser and evaporator tube wall
wa	water

wac cycling water in condenser

wae cycling water in evaporator

was cycling water in superheat region of evaporator

wat water

wo water in evaporative cooler

∞ environment

Superscripts

* optimal

Greek

α Mean void fraction, weighting factors

Δ Finite difference

Δp pressure drop (Pa)

ΔT superheat temperature (K)

Δx quantity of vapour

ε small positive value

η_v clearance volumetric efficiency

μ dynamic viscosity (Pa·s)

ξ fraction of heat exchange

ρ density (kg/m^3)

τ time constant

Φ mass flow rate of refrigerant (kg/h)

∂ partial differential

CHAPTER 1

INTRODUCTION

1.1 Motivation

The utilization of refrigeration plants, air conditioning units and heat pumps has been remarkably increased since they were first produced based on the theory of vapour compression refrigeration system. This requires the design practice to be more efficient in order to predict the instabilities or other undesired behaviour of the system. Many of the present studies are based upon steady-state analysis of the system components. The seemingly steady-state behaviour of a refrigeration system is actually the superposition of a number of transient phenomena of varying time lengths. It will never show adequate system responses. Thus, it has become necessary to study transient performance characteristic of the system to find out the influence of parameters and different operating conditions on the system. With the energy conservation becoming increasingly important, more effort should be carried out in the control analysis of the system. Consequently, improvement in the design and control of refrigeration system are required. To this end, the motivation of this research is to develop a computer simulation model of the tools required for the prediction of the transient response of chilled water cooling systems and to find simple and efficient control strategies for improving system performance.

1.2 A basic refrigeration cycle

Figure 1.1 illustrates the schematic diagram of the basic vapour compression refrigeration cycle, consisting of the minimum required components of the system.

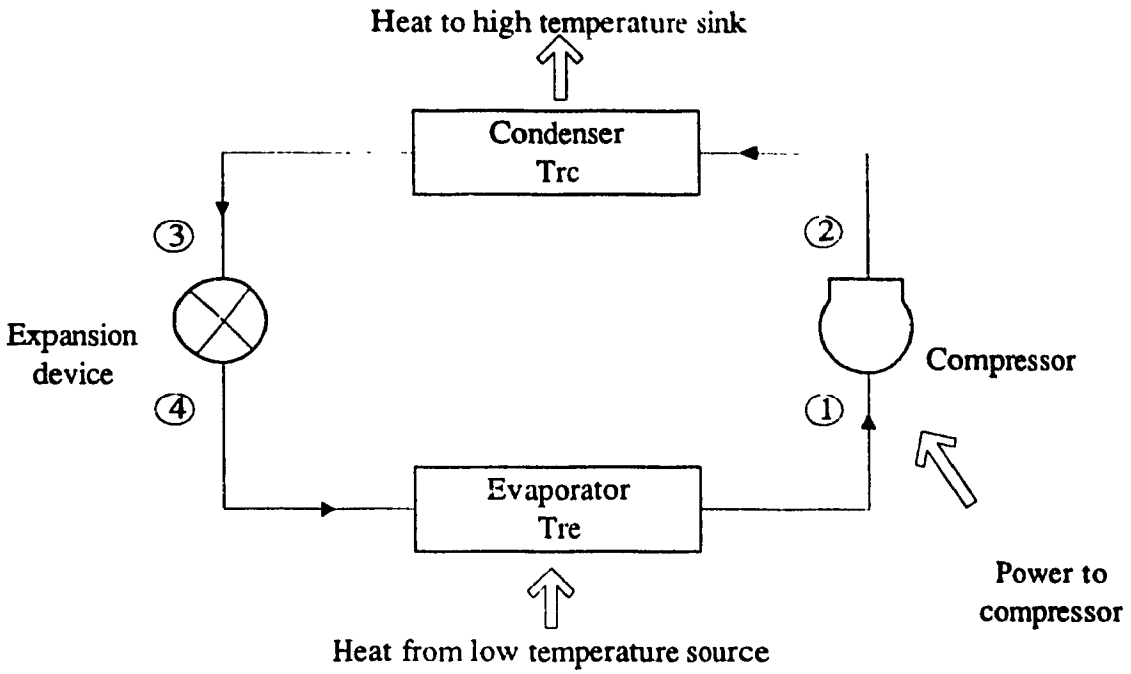

Figure 1.1 Single stage vapor compression system schematic diagram

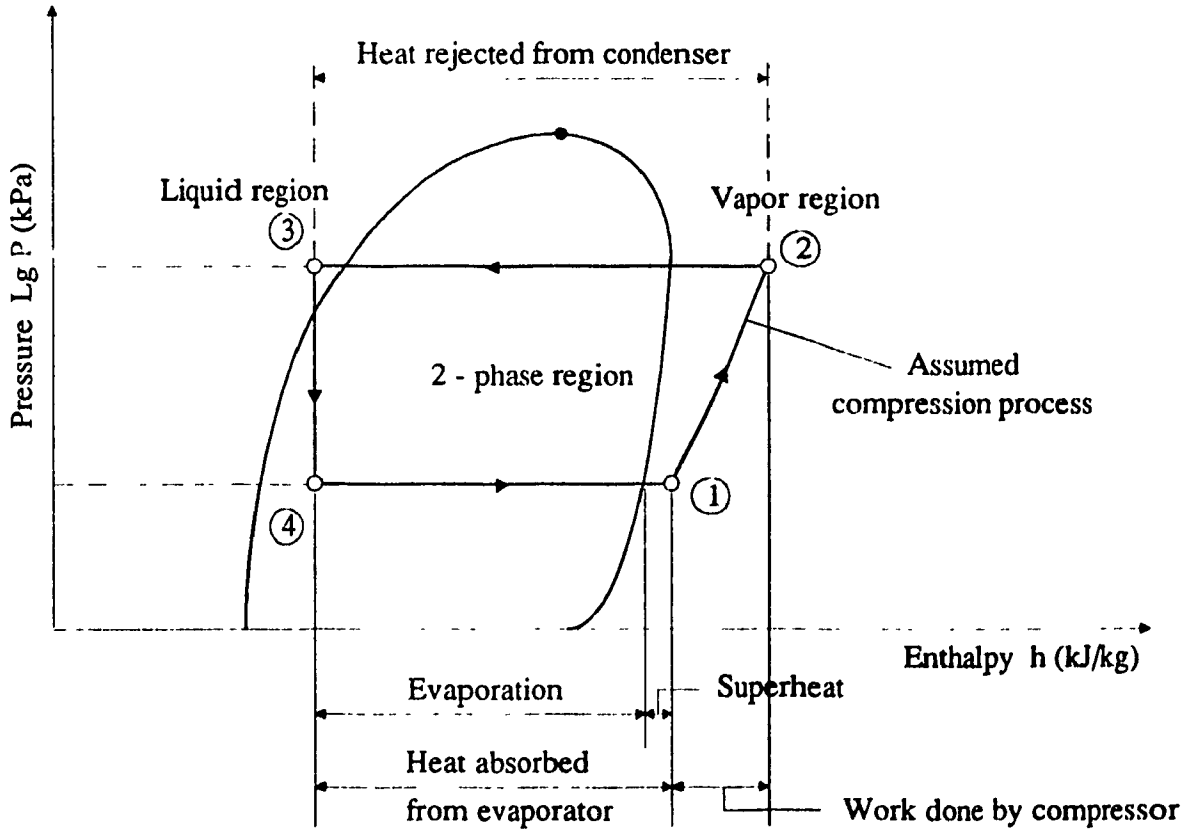

Figure 1.2 Diagram of state changes of the refrigerant (for unit mass of refrigerant)

Figure 1.2 shows the basic refrigeration cycle on the pressure-enthalpy diagram. From the thermodynamic point of view, the basic refrigeration system components needed to make this heat transfer feasible are: a condenser, an evaporator, a compressor, and an expansion device. A thermodynamic cycle of the system can be explained considering the processes that the refrigerant undergoes in these four components.

Refrigerant leaves the evaporator at state "1" as low temperature, low pressure, superheated vapour and enters the compressor in which it is compressed adiabatically. This compression process is associated with an increase of refrigerant temperature. At state "2", the high pressure and high temperature vapour enters the condenser. The refrigerant passing through the condenser rejects heat to the high temperature sink and condenses, usually, to a subcooled liquid at state "3". Then the refrigerant flows through the expansion device undergoing a drop in pressure and temperature. Finally, the low pressure, low temperature, low quality refrigerant at state "4" enters the evaporator, where it picks up heat from the low temperature source, reaching a superheated vapour state "1" at the evaporator exit. In the explanation above, the low and high temperature source and sink are the indoor and outdoor environments respectively. To the basic vapour compression system an evaporative cooler and a chilled water storage tank are added. The resulting system is referred to as chilled water cooling system (CWCS). This thesis deals with dynamic modelling and on-off control strategies for a typical CWCS.

1.3 Layout of the thesis

In chapter 2, the previous work done on modelling of the refrigerating systems is

presented. Then the overall CWCS model including the physical and analytical models are presented in chapter 3. The development of a computer program and the results obtained are explained in chapter 4. The methodology of determining the control strategies is described in chapter 5. In chapter 6, a summary of the analysis is given along with the recommendations for future research.

CHAPTER 2

LITERATURE REVIEW

2.1 Modelling of vapour compression refrigeration systems

A number of researchers have studied either through experiment or theoretical simulations the modelling of vapour compression refrigeration system. However, most of the current studies are concerned mainly with steady state performance in spite of the fact that the steady-state conditions are hardly ever reached and actual coefficient of performance (COP) may be considerably lower than that predicted by theoretical analysis. This chapter will review the modelling of the vapour compression refrigeration systems and heat pump systems.

2.1.1 Transient modelling

One of the first analysis on vapour compression refrigeration system has been presented by Dhar (1978), Dhar and Soedl (1979). The modelling techniques were illustrated by the use of diagrammatic graphs along with mathematical equations. The refrigeration system described was a window type room air conditioner. It consists of an air cooled condenser, a direct expansion evaporator, a hermetic compressor and a thermostatic expansion valve. The heat exchanger coils were modeled by zoning the heat exchanger coils into sub-control volumes, and using two phase flow analysis. The low pressure region was simulated by three "zones", an evaporator an accumulator and the compressor shell. The compressor model was constructed based on a number of simplifying assumptions to simulate steady-state operating conditions. The energy conservation principle was applied for the formulation of the components for the whole system. The objective of the study was to develop a computer program which can be used

as a design tool for matching the refrigeration system components for their optimum performance under both steady state and transient conditions. The numerical results and predicted responses of the system agree with the real system performance. At the end, the refinement of the simulation model has been pointed out by authors, so as to study various control schemes, especially for heat pumps.

Chi (1979) presented a computer model DEPAC for design and performance analysis of chillers. DEPAC model was made up of four component sub-programs CCOMP, CCOND, CEVAP and CTOWER for simulating compressors, condensers, evaporators and cooling towers respectively. The mathematical equations for the model were set up based on heat and mass transfer theory. DEPAC is applicable for selecting operation parameters for an existing chiller plant as well as required design parameters for a new plant, and it is also a tool for studies in energy conservation.

Chi and Didion (1982) developed a heat pump transient analysis computer program (TRPUMP). The mathematical models for the components were established from the conservation equations of mass, energy and momentum transfer. The model presented can be used to predict dynamic responses of the air-to-air heat pump of the type commonly used in residential applications. Simulation results were compared with test data taken at the National Bureau of Standards (NBS) and showed good agreement.

Yasuda et al (1983) presented a simulation model of a vapour compression refrigeration system. A mathematical model was developed to predict the transient behaviour of a laboratory-scale refrigerating system. The system components included a single-cylinder reciprocating compressor, a shell-and-tube condenser, a thermostatic

expansion valve, and a dry evaporator. The basic equations of the model components were derived from the mass and energy conservation theory. Simulation and experimental results of transient behaviour were compared for three cases by tuning of the static superheat of expansion valve. The comparative results showed good agreement regarding absolute values and tendency.

A detailed mathematical model of vapour compression heat pump was described by MacArthur (1984). The equations developed for model components were based on energy conservation principles. The component models were composed of condenser, evaporator, accumulator, expansion device and compressor. The heat pump model was capable of predicting the spatial values of temperature and enthalpy as functions of time for the two heat exchangers. The temperature and enthalpy in other components were simulated using lumped-parameter form. Simulation results showed that the model is internally consistent. However, in order to improve the model accuracy the corrections that define the heat transfer coefficients and pressure drop calculations have to be used.

An improved model to simulate the dynamic response of heat pumps has been reported by Sami et al (1987). The model is developed as lumped parameter model, using the control volume formulation for the system components. The equations for each control volume are written based on the conservation of mass, energy and momentum principles. Besides the main models of the computer program, other sub-models have also be developed to study the side effects of the various phenomena associated with heat pump operations, such as, thermodynamic properties of refrigerants, pressure drop, heat transfer coefficients and so on. Numerical results showed that the proposed model predicted fairly

well the heat pump dynamic response compared to experimental data.

2.1.2 Steady state model

Fiscker and Rice (1980) reported the steady state model for heat pumps (ORNL model). The model simulates the steady-state performance of conventional, vapour compression electrically-driven, air-to-air heat pumps in both heating and cooling modes. It contains all general components of heat pump systems, including compressors, refrigerant flow control devices fin-and-tube heat exchangers, fan and indoor ducts. The model can be utilized as an analytical design tool by heat pump manufacturers, consulting engineers and researchers. Based on the specifications of system operating conditions, system components and type of refrigerants the model would give the prediction of 1) system capacity and COP, 2) compressor and fan motor power consumptions, 3) coil outlet air dry- and wet-bulb temperatures, 4) air- and refrigerant-side pressure drops, 5) refrigerant-side states throughout the cycle and 6) overall compressor efficiencies and heat exchanger effectiveness. An important deficiency of the model was also pointed out by authors that the model is unable to simulate the refrigerant change inventory i.e how much refrigerant is in the heat exchangers, the compressor, and the lines.

Further investigations have been made based on Fiscker and Rice's steady-state model (ORNL model) by Dabiri (1982). The purpose of modifying the ORNL model was to enable the original model to simulate the performance of a given heat pump. Two additional models of heat pump components were presented, such as reversing valve model and refrigerant line heat loss model. Moveover, the compressor shell heat loss,

level of superheat at the evaporator exit were also discussed in the research. A sensitivity analysis was made and the results showed that 1) a relatively accurate data on compressor shell heat loss is necessary for the model, 2) a reversing valve factor of 0.25 was introduced as a constant in the model rather than an input parameter, 3) the heating capacity and COP of the heat pump were not affected by the level of superheat, 4) the liquid line heat loss term was neglected in the simulation model and 5) relatively accurate information on discharge line heat loss was necessary for the model.

Another steady-state model has been presented by Krakow and Lin (1983). The computer model of a multiple-source heat pump was developed in their investigation. The program is able to predict the steady-state performance characteristics of a heat pump interacting with the environment. The conditions of the environment referred to 1) source: ambient-air or storage-water conditions. 2) sink: space-air or storage-water conditions. Solving the equations for specified values of the parameters and environment conditions gave the steady-state performance characteristics of the heat pump system, which were temperatures, pressures, refrigerant flow rates, energy exchange rates and compressor power inputs.

Allen and Hamilton (1983) introduced in their study a steady-state model (NBC model) of reciprocating compressor water chillers of 10 to 200 Tons. In their study, two models were developed, one for the full load and another for part load operation. A full load chiller model predicts the operating characteristics of the chiller system when all compressors and cylinders are operating. On the other hand, a part load chiller model predicts the operation characteristics when compressors are cycled off or cylinders are

unloaded to provide capacity modulation. The model equations were written by applying basic physical laws. Besides above studies, authors have also examined two other existing water chiller models, BLAST and DOE-2 water chiller models. Comparison has been made among three models, the results showed that the DOE-2 model is the simplest one, but with largest predictive error, the NBC and BLAST models need approximately the same number of constants; however, the NBS model has a smaller predictive error.

Krakow and Lin (1987) also reported a numerical model of heat pump system with an evaporator, condenser, compressor and a throttling device. In their study, the equations governing the performance of the heat pump components and that of the state of the refrigerant were solved simultaneously in order to gain the steady-state performance characteristics of a heat pump. These steady-state performance characteristics include the condition of the refrigerant at the key points in the heat pump, the heat transfer rates for the heat exchangers, the power to the compressor, and the leaving temperatures of the source and sink fluids. Authors believe that their model will yield results within reasonable accuracy. Also, the model predicts the transition between refrigerant-dominant and source-dominant modes of operation of capillary-tube-controlled heat pumps. However, further refinement of the component models are expected to improve the overall accuracy of the heat pump model.

A system model for a centrifugal chiller was reported by Wong and Wang (1989). The simulation model was a two stage centrifugal chiller using a water-cooled condenser and R-11 as refrigerant. The purpose of the system simulations was 1) comparing the operating characteristics to find out an optimum scheme from various alternatives 2) to

search the potential energy saving improvement over the current system. The simulation results showed that when load is increased, the heat transfer coefficient of evaporator would increase, but that of condenser would decrease; The load ratio and the temperature of water entering the condenser have great influence on compression efficiency.

A general steady-state model for simulating an air-conditioning system was reported by Hamilton and Miller (1990). The components that formed the system model include: evaporators, compressors, condensers, capillary tubes, and heat exchanger fans. The equations describing each component in the system were based on a hypothetical steady-state condition and were combined to form a set of simultaneous equations describing the system response to a specific loading condition. To mathematically model the air-conditioning system, a method of using polynomial equations that fit the manufacturers' performance catalog data for each component along with thermodynamic relationships were developed. This study could provide assistance to air-conditioning system equipment manufactures for their system designs.

Cecchini and Marchal (1991) developed a simulation model of a refrigeration and air-conditioning system. The simulation focused on characterizing systems with small number of parameters obtained from experimental data. The system includes a compressor, a condenser, an evaporator, and a thermostatic expansion valve. Three objectives of the simulation program were highlighted. The first one was to predict the performance of the thermodynamic cycle of the refrigerant. Then the influence of the system components on the performance was also studied. Finally, the model was used to describe the performance of equipment in great number of sizes from minimum amount

of experimental data. The authors also illustrated a comparison between computed results and experimental data. The validation shows the uncertainty on capacity of the performances is about ±5% for water heat equipment. However, for air-to-air conditioners, the uncertainty was about ±10%.

A computer simulation model to analyze the performance of a water-cooled centrifugal chiller was presented by Jackson et al (1987). The model was developed based on the thermodynamic principles for a heat pump cycle and empirical correlations. The system simulated consisted of a variable speed centrifugal compressor and a hot-gas bypass option for capacity control, two heat exchangers and an expansion device. The parametric study was made for several cases to analyze the performance of an existing centrifugal chiller system. The simulation results showed that the most remarkable improvement in performance can be obtained by regulating the compressor speed and using the hot-gas bypass only when necessary. However, the authors have not designed a controller which can achieve such performance improvements.

2.1.3 Brief review of some models

More computer simulation models have been developed to investigate heat pumps, air conditioners, and chiller systems for design and performance improvements. The model that reported by Tobias (1973) simulated the direct expansion vapour-compression air-conditioning system. The mathematical model was developed based on differential equations describing the dynamics of the flow of boiling refrigerant. Oliver et al (1973) analyzed a commercial-sized air-conditioning system using reciprocating compressors. The

Freeman et al (1975) model compared solar system with air-to-air systems for residential applications. Ellison and Creswick (1978) introduced reciprocating compressor and flow expansion device subroutines, based on Hiller and Gluksman models (1976). The energy performance and cycling pattern of residential heat pumps were simulated by Bonne et al (1980). A simulation program HFROST has been used to analyze some control and operation mode functions. Hwang et al (1985) have developed a computer model for centrifugal chillers with refrigerant-to-water heat exchangers. Modelling and analysis of heat pumps were presented also by Lee et al (1971), Flower (1978), Young (1980), Allen and Hamilton (1980), Sami et al (1986), Tanaka et al (1982), Krakow and Lin (1983), Domanski et al (1983), Gupta and Prasad (1983), and Sami and Duong (1986).

2.2 Control strategies for chiller and cool storage systems

Since each chiller system is unique with a variety of chiller types, sizes, drives, manufactures, piping configurations, pumps, cooling towers, distribution systems, and loads. The control techniques could be very different for each individual system. In terms of control functions, they might be categorized in two types: capacity controls and safety controls.

Capacity controls: vary the thermal capacity of the system as function of the load

Safety controls: generally shut down the chiller unit and generate an alarm whenever an unsafe condition is detected

If the chiller system includes a cool storage, then there are basically five modes (ASHRAE Fundamental 1991) of operation of the storage for charging and release of

thermal energy:

(1) Charging storage -- involves operation of the refrigeration system to prepare the storage vessel for its cooling function.

(2) Simultaneous recharging storage and live-load chilling -- some of cooling capacity is used by the load at the same time that storage is being recharged.

(3) Live-load chilling -- identical to the normal operation of a conventional system, as it provides cooling capacity as needed.

(4) Discharging and live-load chilling -- The chiller system operates and storage vessel discharges at the same time to satisfy cooling demand.

(5) Discharging -- cooling needs are met only from storage, with no operation of the chiller system.

Many researcher have concentrated on the study of optimizing the chiller plant and heat pump energy consumption utilizing central energy management and control systems.

Wany, Y.T. et al (1983) developed the control algorithms, which provide for independent control of the valve, compressor speed and air mass flow rate so that the refrigerant pressure across the evaporator can be maintained to ensure maximum heat transfer in the evaporator. Three control inputs are considered in the control system: valve-orifice control, fan speed control and compressor-speed control. The aim of the valve control is to keep the superheat of the refrigerant leaving the evaporator constant. The optimum evaporator fan speed varies with the compressor speed and air temperature. The purpose of the compressor-speed control, which uses a conventional thyristor-drive DC motor, is to maintain the output hot-water temperature. The experimental results show

that the COP of the system can be improved.

Cascia, (1988) presented how an energy management system (EMS) can be used to adapt chiller plant control to optimize energy savings. Adaptive algorithms that can be programmed into a direct digital controller (DDC) are applied to three basic optimization control strategies: (1) optimizing the staging on or off of multiple chillers, (2) optimizing condenser water temperature, and (3) optimizing chilled water temperature when variable speed chilled water pumps are used. The data that collected from actual chiller plant performance such as chiller power in kilowatts, building load curves, variable speed pump power in kilowatts, and cooling tower power were used as feedback to update equipment part load performance curves as chiller plant conditions change. It was concluded that adaptive chiller control algorithms that optimize energy savings are superior to conventional control algorithms, because energy savings continued to be optimized over time as plant conditions change.

Zaheer-uddin and Wang (1991) made a study to evaluate the energy saving potential of a start-stop controlled water-loop heat pump (WLHP) system. The system model was formed by heat pumps for each zone; a storage tank; a boiler; and a evaporative cooler. In addition, using four energy input controllers and an equal number of mass flow rate controllers, a start-stop control strategy was developed. The switching criteria was defined to maintain the zone temperatures T_{z1}, T_{z2} close to some desired setpoint temperatures, and keep the storage tank temperature T_w in some arbitrary range. Simulation results indicate that the start-stop control strategy is able to maintain the zone temperatures to their respective setpoints under changing heating / cooling loads. Also,

adding a storage tank to the system offers 27% energy saving when the loop water temperature is maintained within near-optimal limits.

Johnson, G.A. (1985) defined and described some potential optimization techniques available to the centrifugal chiller plant operator and to the control system specifier. The control strategies include:

-- Optimize equipment start time by matching pull down load to chiller capacity

-- Electrical demand reduction during chiller pull down

-- Multiple chiller sequence control

-- Optimal cooling tower fan control

-- Reset chilled water temperature consistent with comfort requirements

The control strategies are applied to electric-driven centrifugal chiller plants with cooling tower fans and associated chilled and condenser water pumps. It was concluded that properly applying these strategies to the chiller plant can provide electrical cost savings over and above the savings associated with conventional independent electronic or pneumatic controllers. On a percentage bases, the chiller plant savings will typically be in the 10% to 25% range.

Another research concerning control strategies for a large chilled water plant was made by Lau, A.S. et al (1985). In the study, the chiller and cooling tower models were developed to be general models. The control functions to the system were simulated and following specific control strategies were considered:

-- chiller, tower, and pump strategies

-- storage mode regulation

-- reset of the chilled water set point

-- storage tank subcooling

-- overall impact

Simulation results show that demand limiting using the chilled water storage reduced annual peak demand by 16 kw, and saved an additional $5,500. Reset of the chilled water set point saved an additional $4,400 for a total combined savings of $14,300.

Utesch (1990) showed the direct digital control (DDC) system for a large centrifugal chiller. The operating control for the chiller unit consists of an industrial-type digital controller. The system control sequences utilized were:

-- chilled-water temperature cycle

__ low chilled-water flow cycle

-- thermal storage cycle

-- thermal storage flywheel cycle

-- chilled-water pumping control

-- condenser water pumping control

-- cooling tower fan control

The test results of this application were documented in another research project.

Among other studies, the optimizing of chiller plants energy consumption with central energy management and control system is examined by Williams (1985). Mitchell (1988) and Braun et al (1987) studied the performance and control characteristic of a large variable speed driven chiller system. Spethmann (1985) presented the optimized

control for multiple chillers by using the methods of establishing part load energy characteristics for individual chiller. Ulrich Bonne et al (1980) discussed the effects of the defrost control alternatives to the heat pump system. It was found out that the optimum length of frost build-up time leads to a higher efficiency of the systems performance than fixed timer systems and the ΔP-demand defrost systems.

Studies related to control performance with energy consumption and also thermal comfort to cool storage have been reported.

Spethmann (1989) developed an optimal controller for cool storage system. The variables considered in this optimization problem include: the utility rate structure, storage type and size, the plant configuration and load size and profile. Two strategies were suggested to minimize cost 1) demand minimization -- use storage to reduce the total of demand and energy charges each month 2) energy cost minimization -- the comparison of energy costs establishes whether a strategy of chiller priority or storage priority will be used. The cool storage supervisory controller (CSSC) has been implemented in a building automation system with direct digital control (DDC). The simulation results of the optimized control strategies show that large storage operated in storage priority saved 16% in cooling costs, and minimized storage and chiller size operated on chiller priority save 42% in cooling costs.

A general analysis concerning the principles of optimum control of cool storage and the application variations has been done by Spethmann (1993). The optimization variables mentioned in his previous work Spethmann (1989) has been examined to find out how the variables influence the nature of the optimal control strategies. This

information was than be used as a guide for control needs for specific types of projects. The logic of selecting control strategies was based on:

(1) storage priority and no inventory penalty

(2) storage priority with penalty for incomplete discharge

(3) chiller priority and no inventory penalty

(4) chiller priority and with inventory penalty

Some key factors have to be taken into consideration in order to establish the correct control strategy for different situations. One of them is the relative cost of stored versus direct cooling, and the other one is whether there is a cost penalty related to inventory level of stored cooling.

Simmonds (1994) made use of the work that was originated by Kirshenbaum (1991) and Braun (1992). The storage priority strategy was investigated in an ice-based thermal storage system, together with a upstream series chiller. The system in such an arrangement offers: 1) a constant chilled water temperature, and 2) higher compressor efficiency during a peak chiller operation. It has been pointed out that the storage priority control maximizes the ability of the ice storage systems to reduce a building's peak demand charges. Moreover, this strategy forces more usage of TES chiller at night in the ice making mode. However, the control equipment and sequences may be more complicated than chiller priority control.

A comparison of some control strategies has been presented by Braun (1992). Following control strategies has been described and compared:

(1) maximum energy cost control

(2) minimum demand control

(3) load-limit control

(4) chiller-priority control

The results indicate that the load-limiting strategy provides near-optimal control in terms of demand costs for all environmental conditions considered. The chiller-priority strategy required much greater demand costs and somewhat greater energy costs in the presence of time-of-day rates, but required lower energy costs while the time-of-day energy charges were not in effect.

Rawlings (1985) proposed three ice storage approaches in order to reduce the electrical demand charges and lower the installation costs. It was suggested that the chiller-priority control does not maximize the demand reduction of the system. Ice-priority control can maximize the demand reduction but may result in a higher installed cost. However, the constant proportion control offers a compromise between the two which has a low equipment cost and a good operation cost.

2.3 Discussion:

Review of the literature shows that quite a few applicable transient heat pump analytical models have been developed in the literature, such as Dhar (1978), Chi and Didion (1982), Yasuda et al (1983), MacArthur (1984), and Sami et al (1987). These models have examined the heat pump or vapour compression refrigerating system only; the transient modelling of a chilled water cooling system with storage and cooling tower have not been studied. Also, it is noted that in Chi and Didion (1982) heat pump model,

the evaporator was modeled in lumped parametric form, therefore, the refrigerant behaviour in superheat region of evaporator, such as the degree of superheat was not studied. It should be mentioned that, in the present study of chilled water cooling system (CWCS), condenser and evaporator models were derived based on the work reported by Yasuda (1983). However, there are some differences between these two studies. In CWCS model, refrigerant flows inside the tubes and cooling water circulates in the condenser shell, which is contrary to what was simulated in Yasuda's condenser model. In the evaporator model of CWCS, the water temperature is computed at each node. In Sami et al (1987) model of heat pump analysis, modelling of the components was only concerned about the prediction of transient response of refrigerant, such as the rate of mass and energy change of vapour and liquid refrigerant inside heat exchangers, but the simulation of heat flows between refrigerant and the heat exchanger material, and between the heat exchanger and secondary fluid were not modelled. Thus, in order to investigate the performance and the effect of control schemes on the chilled water cooling system with a storage, it is necessary to develop a new model based on the existing models of heat pump and incorporating a storage tank and an evaporative cooler so that the model is useful for control studies.

As far as control studies are concerned, Braun et al (1989) have examined optimal control strategies using steady state models of CWC systems. These optimal control strategies are referred to as supervisory control schemes. The use of PID controls for the local loop control of compressor is investigated by Zeng (1993).

Most CWC systems in practice use on-off control because of simplicity, reliability

and cost. Therefore, it is of interest to develop optimal or near optimal on-off control schemes for CWC systems. The advantage of such schemes is that they can readily be implemented on existing systems.

By predicting the cooling loads of the building we can determine the optimal on-off control schemes, such on-off control strategies act as supervisory control schemes which will be based on dynamic models as opposed to static models used in the literature.

To summarize the major objectives of the thesis are:

(1) development of a dynamic model of a CWC system which is suitable for control analysis,

(2) determining a methodology for computing optimal or near optimal on-off switching control strategies for CWC systems,

(3) demonstrating the application of control strategies by carrying out simulation studies under realistic operating conditions.

CHAPTER 3

ANALYTICAL MODEL

3.1 Introduction

The chilled water cooling system (CWCS) consists of several basic components, and each component has its own operating characteristic. To study the dynamic characteristics of the individual components, it would be necessary to develop a mathematical model describing the dynamic behaviour of the subsystems. The formulation of the component models has been achieved based on energy and mass balance principles. The state of refrigerant at every key point is modeled by using empirical correlations. Transient response of the system is obtained by solving the basic governing partial differential equations of the model as well as empirical equations for the properties of the refrigerant.

In this chapter, 1) Physical model of CWC system is described, and 2) individual models of the sub-systems of CWC system are developed.

3.2 Physical model

Figure 3.1 shows the schematic diagram of the CWC system used in this study. The main elements of the system are 1) a reciprocating compressor 2) a shell-and-tube condenser 3) a dry expansion evaporator 4) a thermostatic expansion valve 5) an evaporative cooler 6) a chilled water storage tank. The vapour compression refrigeration system comprises of elements 1) to 4). There are four controllers in the system, U_1 for evaporative cooler fan, U_2 for circulation water loop between condenser and evaporative cooler, U_3 for the energy input to the compressor and U_4 for chilled water loop between evaporator and storage tank. To understand the operation of the overall system, consider

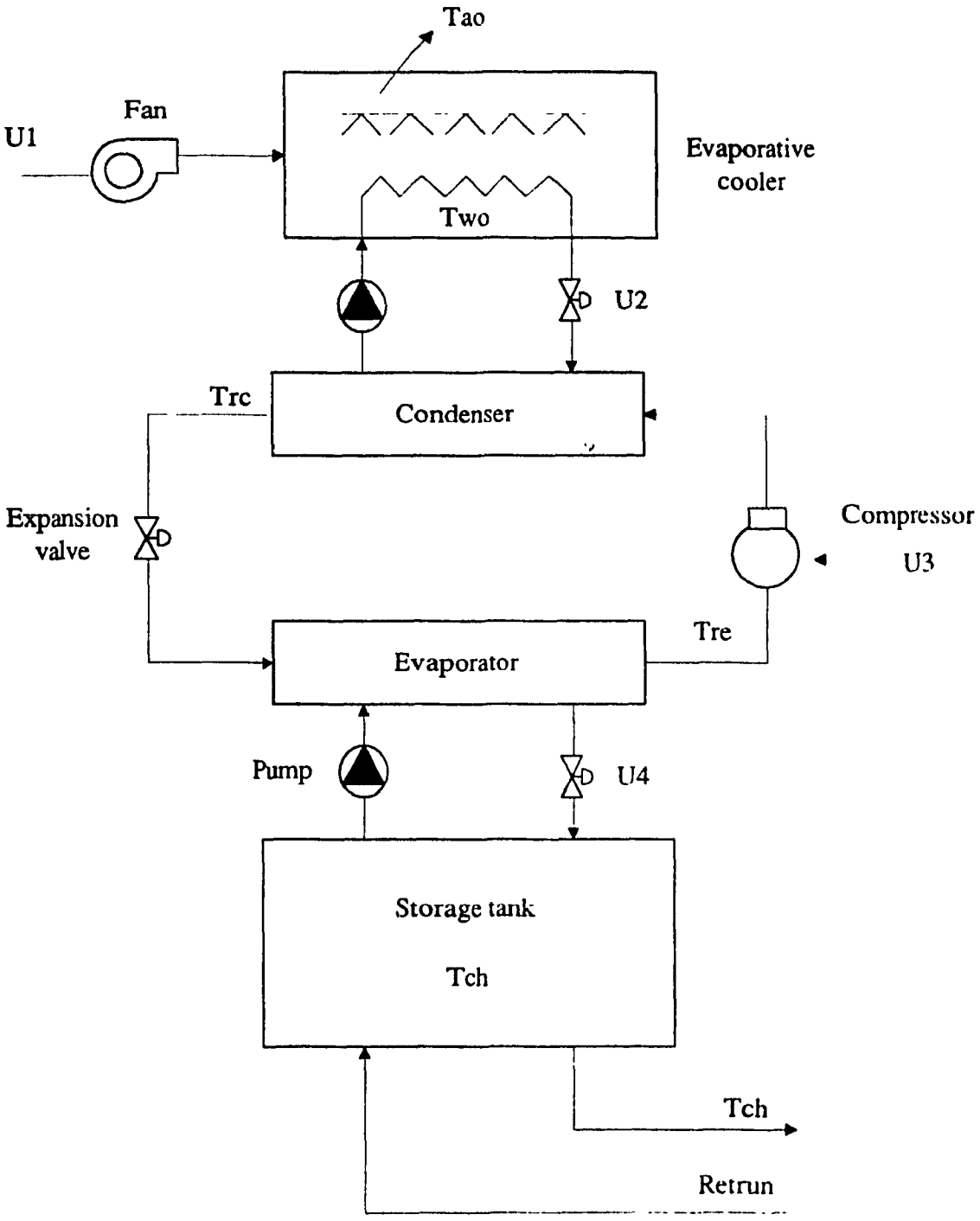

Figure 3.1 Schematic diagram of CWC system

the case of cooling required by a certain building. When system is started, refrigerant flows throughout the components of the system. Refrigerant gives up heat to the cooling water via a shell-and-tube condenser, in which refrigerant condenses from high pressure and temperature phase to high pressure but low temperature liquid phase, and this amount of heat will be extracted from circulating water by an evaporative cooler. The liquid refrigerant then passes though the thermostatic expansion valve, becomes low pressure liquid while entering the evaporator. The refrigerant absorbs heat from chilled water via a dry expansion evaporator. The amount of cool energy contained in chilled water is equal to the cooling energy required by the building. When cooling load is compensated by the cooling energy produced by refrigeration system, the whole system will reach balance condition, a steady state, until a new cooling requirement occurs.

3.3 Basic modelling technique

The analytical model has been formulated by representing the continuous physical process occurring in the system as a sequence of discrete small steps taken one at a time. Each system component was represented by one or more separate control volumes.

Many analytical models of individual refrigeration system components are available. Such as London et al (1952), Alves (1954), Anderson et al (1966), Saraf et al (1979), Daviri and Rice (1981) which made the detailed study of the individual components possible. However, the combination of the individual component model for simulation of the overall system performance would require very large computer memory and computational time.

The analysis of heat exchanger components is complicated because of two-phase refrigerant flow. While the various flow types may occur inside tubes of the heat exchanger, the local convective heat transfer coefficient at the inner wall of the tubes changes with both time and space coordinates. Previous studies conceming two-phase forced convective flow heat transfer are available. For example, Traviss et al (1973) performed experimental and analytical studies of vapour condensation in annular flow with refrigerants R-12, and R-22, resulting in an empirical correlation of the condensation heat transfer coefficient. Anderson (1966) performed laboratory measurements to obtain the forced convection evaporation heat transfer coefficient closely approximating those existing in refrigerant evaporators.

The mathematical model of the heat exchanger including refrigerant inside tubes has been developed by considering the tubes as one control-volume or some sub-control volumes. Every control volumes behaves as a "stirred tank" in which the outlet conditions from the control volume are equal to the bulk conditions within the control volume. The sizes and numbers of the control volumes are fixed.

Pressure drops in the heat exchanger pipes and refrigerant tubes due to refrigerant flow are neglected during the cycle calculations, since these pressure drops are small as compared to their mean pressures. Meanwhile the simplification also could save the computational time.

The refrigerant state formulations in each control volume is based on energy and mass conservation theory coupled with state equations which correlate the various refrigerant thermodynamic properties. The empirical correlations for refrigerant properties

have been developed by many researchers. Such as Mcharness et al (1955), Martin (1959), Downing (1974), Kartsounes and Erth (1971). The present study adopts some simplified correlations reported by Yasuda et al (1983).

The mathematical model equations were solved by the use of a digital computer, component equations of the system and each state equation for refrigerant properties are presented by separate subroutines. The state of the refrigerant and other system parameters are computed by simultaneous solution of the model equations.

3.4 Compressor model

The compressor is one of the essential parts of compression refrigeration system, along with condenser, the expansion valve, the evaporator and the interconnecting piping. The compressor model in this study consists of a single cylinder. The model equations are valid under the following assumptions:

1) the isentropic compression process is considered.
2) the refrigerant gas is assumed as an ideal gas.
3) the pressure losses of refrigerant flow through the expansion valves can be neglected.
4) motor speed is constant.
5) energy losses through compressor cylinder, suction and discharge ports are neglected.

The basic equations can be derived based on above assumptions. The clearance volumetric efficiency, η_v, is expressed as

$$\eta_v = 1 - \frac{V_{cl}}{V_d} \left[\left(\frac{p_d}{p_s}\right)^{\frac{1}{K}} - 1 \right] \quad (3.1)$$

where

V_{cl} = clearance volume of the cylinder (m^3)

V_d = maximum volume of the cylinder (m^3)

P_d = discharge pressure (Pa)

P_s = suction pressure (Pa)

K = polytrophic constant assumed equal to specific heat ratio

Mass flow rate through the compressor, ϕ_v (kg/h), is written as

$$\phi_v = \rho_s V_d N \eta_v \quad (3.2)$$

where

ρ_s = density of refrigerant vapour entering the suction port (kg/m^3)

N = compressor motor speed (RPM) ($N=AN \cdot AN_{max}$)

AN = compressor motor speed ratio

AN_{max} = maximum value of compressor motor speed (RPM)

The work done, W_c (kJ/kg), of compressor motor is given by

$$W_c = \frac{K}{K-1} P_s V_s \left[\left(\frac{p_d}{p_s}\right)^{\frac{K-1}{K}} - 1 \right] \quad (3.3)$$

where

V_s = specific volume of the refrigerant vapour entering the suction port (m^3/kg)

The enthalpy of the superheat vapour, H_1 (kJ/kg), leaving the discharge port is given by

$$H_l = H_s + W_c \tag{3.4}$$

where

H_s = enthalpy of vapour entering the suction port (kJ/kg)

The temperature, T_l of vapour discharged by the compressor into the condenser is given by

$$T_l = T_s \left(\frac{p_d}{p_s}\right)^{\frac{K-1}{K}} \tag{3.5}$$

where

T_s = temperature of refrigerant vapour entering the compressor suction port (K)

All parameters used in the simulation are listed in Table 3.1

Table 3.1 Compressor parameters used in simulation

Symbol	Magnitude	Units
AN_{max}	1200	RPM
V_{cl}	0.05	m^3
V_d	0.0006	m^3
K	1.15	dimensionless

3.5 Condenser model

The condenser in a refrigeration system removes the heat of compression and the heat absorbed by the refrigerant in the evaporator. The refrigerant is thereby converted back into the liquid phase at the condenser pressure and is available for re-expansion

through the expansion device into the evaporator.

A water cooled, shell-and-tube type condenser is considered in this study. In general, the heat transfer procedure inside the condenser tubes can be divided into three main phases. 1) de-superheating, 2) condensing, and 3) sub-cooling. Among these three states in a condenser tubes, de-superheating and sub-cooling hold relatively only small portion. Most of the condenser tube length occupied by condensation under a essentially constant temperature and pressure. In other words, the saturation region dominated over the superheat and liquid regions, therefore, it is reasonable to present the entire condenser section with a pure condensation process.

As in Yasuda et al (1981, 1983), a single control volume model for condenser is developed based on the following assumptions.

1) the condenser is considered as one lumped model which describes saturation characteristics of the refrigerant as the condenser behaviour.
2) pressure drop of refrigerant flow through condenser tubes is neglected.
3) heat losses through the condenser shell is neglected.
4) the refrigerant vapour and liquid inside the condenser tube are always in the thermodynamic equilibrium.

3.5.1 Dynamic equations

Basic equations are written based on continuity and energy conservation principle.

Figure 3.2 shows a lumped model of the condenser. The continuity equation for a combined vapour and liquid phase is given as:

$$\frac{d}{dt}\left(M_v + M_l \right) = \phi_i - \phi_o \tag{3.6}$$

and

$$M_v = V_c\ \alpha_c\ \rho_v \tag{3.7}$$

$$M_l = V_c\ \left(1 - \alpha_c \right)\ \rho_l \tag{3.8}$$

where

Φ_i = mass flow rate of refrigerant entering the condenser (kg/h)

Φ_0 = mass flow rate of refrigerant leaving the condenser (kg/h)

α_c = mean void fraction of vapour refrigerant

ρ_v = density of saturated vapour refrigerant (kg/m^3)

ρ_l = density of saturated liquid refrigerant (kg/m^3)

V_c = volume of condenser (m^3)

Equation (3.6) expresses that the refrigerant mass restored in the condenser equals to the difference of inlet and outlet mass flow rate. The energy balance equation for refrigerant is given as:

$$\frac{d}{dt}\left(M_v\ h_v + M_l\ h_l \right) = \phi_i h_{ci} - \phi_o h_{co} - h_{ic} A_{ic}\ \left(T_{rc} - T_c \right) \tag{3.9}$$

where

h_v = enthalpy of saturated vapour refrigerant (kJ/kg)

h_l = enthalpy of saturated liquid refrigerant (kJ/kg)

h_{ci} = enthalpy of gas refrigerant entering condenser (kJ/kg)

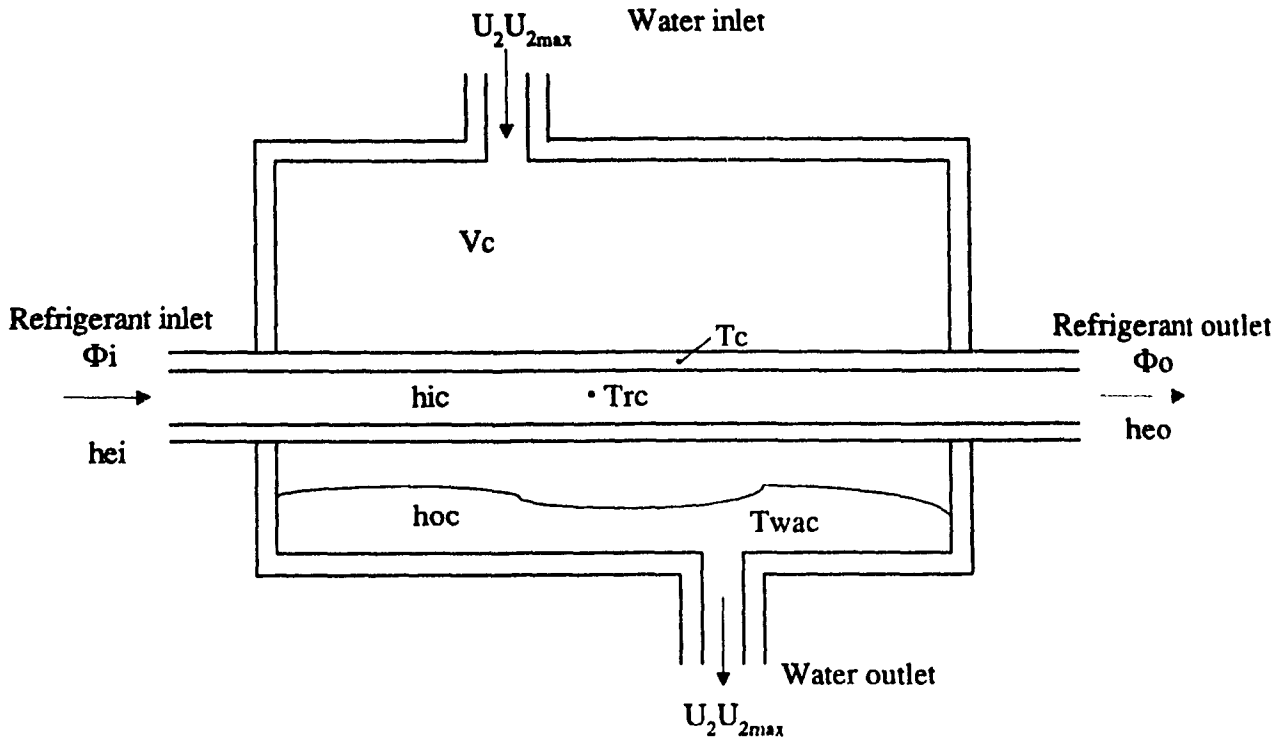

Figure 3.2 Condenser model

h_{co} = enthalpy of liquid refrigerant leaving condenser (kJ/kg)

h_{ic} = heat transfer coefficient between refrigerant and tubes ($kJ/s \cdot m^2 \cdot K$)

A_{ic} = inside heat transfer area of tubes (m^2)

T_{rc} = condensing temperature (K)

T_c = mean tube temperature (K)

This equation shows that the rate of energy change in refrigerant equals to the heat incoming from compressor $\Phi_i h_{ci}$ and the heat outgoing to the expansion valve $\Phi_o h_{co}$ as well as the heat lose through the tubes $h_{ic}A_{ic}(T_{rc}-T_c)$. The energy balance equation for the tube is given as:

$$C_c \frac{dT_c}{dt} = h_{ic} A_{ic} (T_{rc} - T_c) - h_{oc} A_{oc} (T_c - T_{wac}) \quad (3.10)$$

where

C_c = thermal capacity of tubes (kJ/K)

h_{oc} = heat transfer coefficient between water and tubes (kJ/s·m^2·K)

A_{oc} = external heat transfer area of tubes (m^2)

T_{wac} = cooling water temperature (K)

In this equation, the heat stored in condenser tubes equals to the heat gain from the refrigerant inside tubes $h_{ic}A_{ic}(T_{rc}-T_c)$ and the heat lose to the cooling water $h_{oc}A_{oc}(T_c-T_{was})$. The energy balance equation for cooling water is given as:

$$C_{wa} \frac{dT_{wac}}{dt} = h_{oc}A_{oc} (T_c - T_{wac}) - U_2U_{2max}C_{wat} (T_{wac} - T_{wo}) \quad (3.11)$$

where

C_{wa} = thermal capacity of cooling water (kJ/K)

C_{wat} = specific heat of cooling water (kJ/kg·K)

U_2U_{2max} = mass flow rate of cooling water (kg/h)

The equation presents that the rate of heat exchange in cooling water in the shell of the condenser is balanced to the heat coming from the refrigerant tubes $h_{oc}A_{oc}(T_c-T_{was})$ and the heat leaving for the evaporative cooler $U_2U_{2max}C_{wat}(T_{wac}-T_{wo})$.

By introducing following relations,

$$\frac{d\rho_v}{dt} = \frac{d\rho_v}{dT_{rc}} \frac{dT_{rc}}{dt} \tag{3.12}$$

$$\frac{d\rho_l}{dt} = \frac{d\rho_l}{dT_{rc}} \frac{dT_{rc}}{dt} \tag{3.13}$$

$$h_v = h_o + C_v T_{rc} \tag{3.14}$$

$$h_l = h_o + C_l T_{rc} \tag{3.15}$$

Equations (3.6), and (3.9) respectively become

$$(\rho_v - \rho_l) \frac{d\alpha_c}{dt} = \frac{1}{V_c} (\phi_i - \phi_o) - (\alpha_c \frac{d\rho_v}{dT_{rc}} + (1-\alpha_c) \frac{d\rho_l}{dT_{rc}}) \frac{dT_{rc}}{dt} \tag{3.16}$$

$$\begin{aligned} &[\alpha_c\rho_v C_v + (1-\alpha_c)\rho_l C_l + \alpha_c h_v \frac{d\rho_v}{dT_{rc}} + (1-\alpha_c) h_l \frac{d\rho_l}{dT_{rc}}] \frac{dT_{rc}}{dt} = \\ &\frac{1}{V_c} [(\phi_i h_{ci} - \phi_o h_{co}) - h_{ic} A_{ic} (T_{rc} - T_c)] - \\ &(\rho_v h_v - \rho_l h_l) \frac{d\alpha_c}{dt} \end{aligned} \tag{3.17}$$

where

C_v = specific heat of saturated vapour refrigerant (kJ/kg·K)

C_l = specific heat of saturated liquid refrigerant (kJ/kg·K)

If the mass of the liquid contained in the condenser is half of the total quantity during operation, then α_c takes a constant value of 0.5, and equation (3.16) can be removed due to $d\alpha_c/dt=0$. In this case, the left element of the first term in equation (3.17)

could be removed. Moveover, because the refrigeration system works under the condition within a certain range, this condition can be assumed to be fixed, therefore, the values of vapour and liquid refrigerant states would be considercd constant.

3.5.2 Heat transfer coefficients

Methods of evaluating heat transfer coefficients of various type of heat exchangers and that of fluid flow can be found in the literature, such as Holman (1986), ASHRAE Handbook of fundamentals (1991), Frank (1988), Bac et al (1971), Maim et al (1972) and so on. The approaches that have been applied in current study are discussed in following section.

Refrigerant side heat transfer coefficient

Refrigerant side heat transfer coefficient is determined by taking the empirical equation of the heat transfer coefficient for condensation of refrigerant inside the tubes (Holman, 1986)

$$h_{ic} = 0.555 \left[\frac{\rho(\rho - \rho_v)\, g\, k^3\, h'_{fg}}{\mu\, d\, (T_g - T_w)} \right]^{\frac{1}{4}} \qquad (3.18)$$

where

$$h'_{fg} = h_{fg} + 0.68\, C_p\, (T_g - T_w) \qquad (3.19)$$

Water side heat transfer coefficient

The heat transfer coefficient between cooling water and the condenser tube is assumed more or less remains constant at 6120 ($kJ/h \cdot m^2 \cdot K$)

All parameters used in the simulation are listed in Table 3.2.

Table 3.2 Condenser parameters used in simulation

Symbol	Magnitude	Units
U_{2max}	7000.0	Kg/h
A_{ic}	15.0	m^2
A_{oc}	2.33	m^2
H_{oc}	1.7	$kJ/s \cdot m^2 \cdot K$
C_c	20.7	$kJ/s \cdot m^2 \cdot K$
C_{wa}	500.0	kJ/K
C_{wat}	4.2	$kJ/kg \cdot K$
V_c	2.5	m^3

3.6 Evaporator model

Evaporator is that part of a refrigerating system in which refrigerant is vaporized to produce refrigeration for cooling fluid media. The fluid medium may be water or any other stable fluid used to transport cooling effect.

A direct expansion type evaporator is modeled as shown in Figure 3.3, and the fluid medium in this simulation is water. In a direct expansion evaporator the refrigerant is expanded inside tubes and vaporized completely before recirculation. The water which being cooled is circulated on the outside of the tube surface and within an enclosing shell.

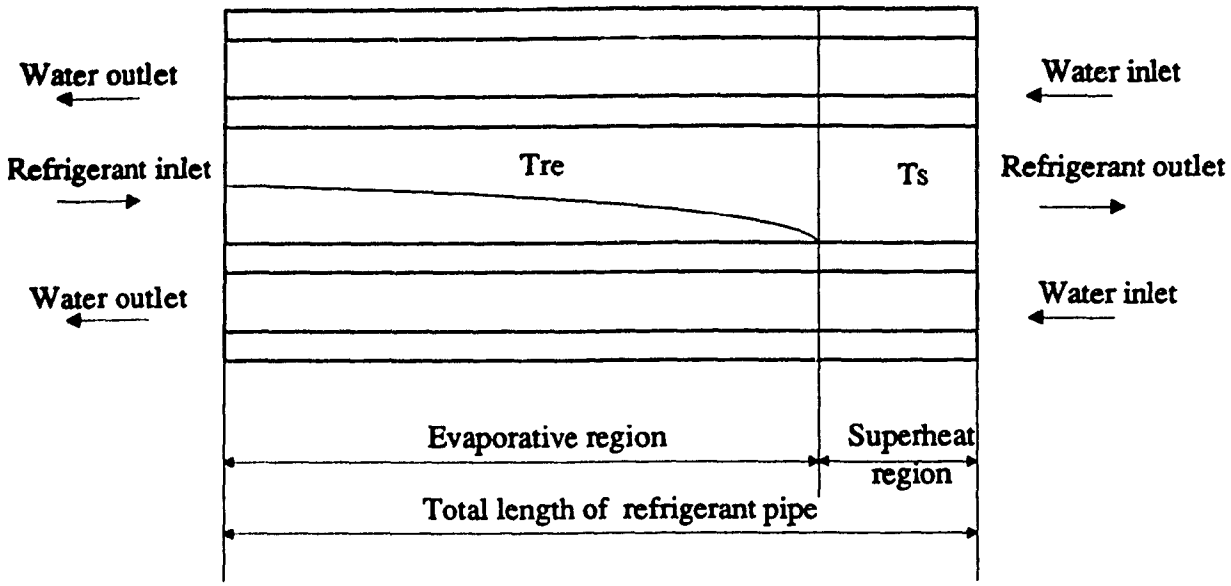

Figure 3.3 Evaporator model

The main purpose in this section is to investigate the dynamic behaviour of the evaporation temperature T_{re}, the superheating temperature T_{sh} (outlet refrigerant temperature) and the chilled water temperature in the storage tank T_{ch}. An evaporator with two regions is modeled using following assumptions.

1) for the refrigerant inside the tube, the evaporation region and superheat region is assumed to be separated by a distinct boundary, and the length of both region is fixed.

2) the chilled water entering the evaporator flows across the tubes with constant mass flow rate.

3) one control volume is considered for refrigerant tube wall and chilled water in evaporation region and two control volumes are taken for superheat region.

3.6.1 Evaporation region

Figure 3.4 shows the evaporation region which is considered as one control volume. For the lumped model of the refrigerant, the continuity equation is given in a combined form of vapour and liquid phases:

$$\frac{\partial}{\partial t}(M_v + M_L) = \phi_l - \phi_v \tag{3.20}$$

and

$$M_v = \alpha_e A_r \rho_v L_e \tag{3.21}$$

$$M_l = (1 - \alpha_e) A_r \rho_l L_e \tag{3.22}$$

where

Φ_l = mass flow rate of liquid refrigerant entering evaporator (kg/h)

Φ_v = mass flow rate of vapour refrigerant leaving evaporator (kg/h)

α_e = mean void fraction of vapour refrigerant in evaporation region

L_e = length of evaporation region (m)

A_T = cross section area of inner tube (m^2)

Equation (3.16) shows that the refrigerant mass stored inside the evaporator tubes equals the mass flow coming into the tubes Φ_i and that of going out of the tubes Φ_o. The energy balance equation for the refrigerant is given again in a combined form as

$$\frac{d}{dt}(M_v h_v + M_l h_l) = \phi_l h_{ei} - \phi_v h_{eo} + h_e A_{ie}(T_e - T_{re}) \tag{3.23}$$

where

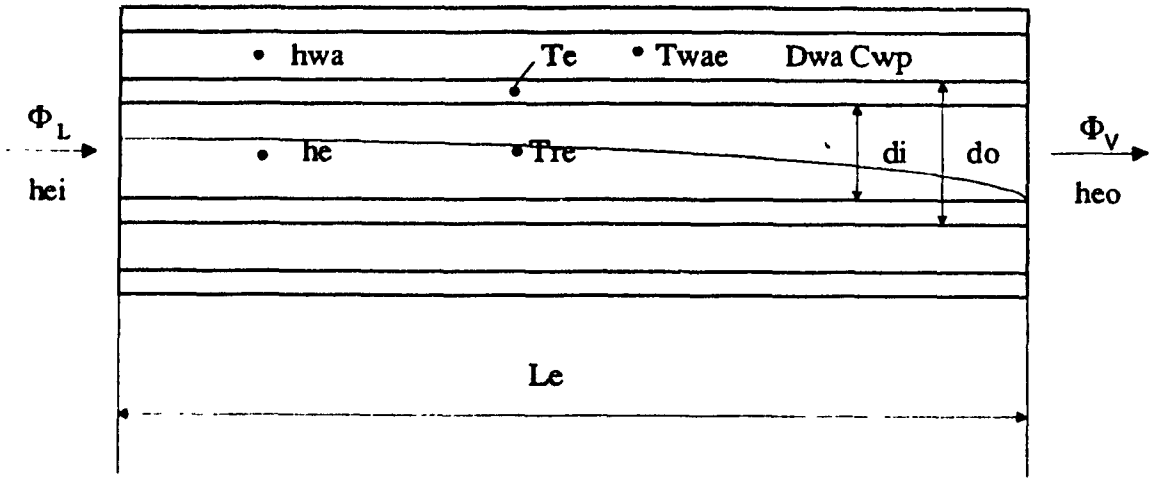

Figure 3.4 Evaporation region

h_{ei} = enthalpy of refrigerant entering evaporator (kJ/kg)

h_{eo} = enthalpy of refrigerant leaving evaporator (kJ/kg)

h_e = heat transfer coefficient between refrigerant and tubes in evaporation region ($kJ/s \cdot m^2 \cdot K$)

T_e = mean tube wall temperature of evaporation region (K)

T_{re} = evaporating temperature (K)

The energy that is stored in refrigerant is equal to the heat from the expansion valve outlet $\Phi_l h_{ei}$, the heat absorbed from the tubes $h_e A_{ie}(T_e - T_{re})$ and the heat out of the tubes $\Phi_v h_{eo}$. The energy balance equation for tube wall is given as:

$$\rho_w C_w A_w \frac{dT_e}{dt} = h_{wa} F_{oe} (T_{wae} - T_e) - h_e F_{ie} (T_e - T_{re}) \quad (3.24)$$

where

ρ_w = density of tube wall (kg/m^3)

C_w = specific heat of evaporator tube (kJ/kg·K)

A_w = cross sectional area of evaporator tube wall (m^2)

h_{wa} = heat transfer coefficient between water and tube wall ($kJ/s \cdot m^2 \cdot K$)

F_{ie} = $\pi \times$ inner diameter of tube (m)

F_{oe} = $\pi \times$ outer diameter of tube (m)

T_{wae} = water temperature in evaporation region (K)

The rate of energy change in evaporation region tubes equals to the heat gain from the chilled water outside the tubes $h_{wa}F_{oe}(T_{wae}-T_e)$ and the heat taken by the refrigerant inside tubes $h_eF_{ie}(T_e-T_{re})$. Chilled water in evaporation region is considered as a individual control volume as explained in the last section. The energy balance equation is written as:

$$\rho_{wa} C_{wa} A_{wa} \frac{dT_{wae}}{dt} = \frac{U_4 U_{4max} C_{wat}}{L_e} (T_{ch} - T_{wae}) - h_{wa} F_{oe} (T_{wae} - T_e) \quad (3.25)$$

where

ρ_{wa} = density of water (kg/m^3)

A_{wa} = cross sectional area of outside tube (m^2)

U_4U_{4max} = mass flow rate of chilled water between evaporator and storage (kg/h)

T_{ch} = chilled water storage tank temperature (K)

The heat exchange rate of chilled water is balanced to the heat obtained from chilled water storage tank $U_4U_{4max}C_{wat}(T_{ch}-T_{wae})$ and the heat lost to the evaporation region tubes $h_{wa}F_{oe}(T_{wae}-T_e)$. By using following relations:

$$\frac{d\rho_v}{dt} = \frac{d\rho_v}{dT_{re}} \frac{dT_{re}}{dt} \tag{3.26}$$

$$\frac{d\rho_l}{dt} = \frac{d\rho_l}{dT_{re}} \frac{dT_{re}}{dt} \tag{3.27}$$

$$h_v = h_o + C_v T_{re} \tag{3.28}$$

$$h_l = h_o + C_l T_{re} \tag{3.29}$$

The equation (3.20) and (3.23) respectively become

$$A_r[\ \alpha_e\rho_v+(1-\alpha_e)\rho_l\ ]\frac{dL_e}{dt} = \phi_l-\phi_v-[\ \alpha_e\frac{d\rho_v}{dT_{re}}+(1-\alpha_e)\frac{d\rho_l}{dT_{re}}\ ]A_rL_e\frac{dT_{re}}{dt} \tag{3.30}$$

and

$$[(\ \alpha_e\rho_vC_v+(1-\alpha_e)\rho_lC_l\ )+(\ \alpha_e\frac{d\rho_l}{dT_{re}}h_v+(1-\alpha_e)\frac{d\rho_l}{dT_{re}}h_l\ )]\ A_rL_e\frac{dT_{re}}{dt} = \phi_lh_{ei}-\phi_vh_{eo}+h_eA_{ie}(T_e-T_{re}) - [\alpha_e\rho_vh_v + (1-\alpha_e)\rho_lh_l\ ]Ar\frac{dL_e}{dt} \tag{3.31}$$

Investigations concerning the void fraction of two-phase flow in tube have been presented in the literature. For example Hughmark (1962), Egen (1957), Yasuda (1981) have shown that different methods can be used to determine the void fraction for two phases flow patten, such as empirical method, theoretical method and semi-theoretical method. In the present study, the mean void fraction of evaporator is taken as a constant value, therefore, equation (3.30) can be omitted and equation (3.31) is rewritten:

$$[\ (\alpha_e \rho_v C_v + (1-\alpha_e)\rho_l C_l) + \alpha_e \frac{d\rho_l}{dT_{re}} h_v + (1-\alpha_e)\frac{d\rho_l}{dT_{re}} h_l\ ]\ A_r L_e \frac{dT_{re}}{dt} = \phi_l h_{ei} - \phi_v h_{eo} + h_e A_{ie}(T_e - T_{re}) \tag{3.32}$$

3.6.2 Superheat region

Figure 3.5 shows the superheat region which is considered as two individual control volumes. Inside this region, the superheated vapour refrigerant is assumed incompressible.

The energy balance equation for superheated vapour is given as:

$$\rho_s C_s A_r \frac{\partial T_s(t,y)}{\partial t} + \frac{\phi_v C_s}{\Delta y} \partial T_s(t,y) = h_{es} F_{ie}\ [\ T_{es}(t,y) - T_s(t,y)\ ] \tag{3.33}$$

where

T_s = superheat temperature of refrigerant (K)

T_{es} = mean tube temperature of superheat region (K)

h_{es} = heat transfer coefficient between refrigerant and the tube wall in superheat

region (kJ/s·m^2·K)

C_s = specific heat of superheated refrigerant vapour (kJ/kg·K)

ρ_s = density of superheated refrigerant vapour (kg/m^3)

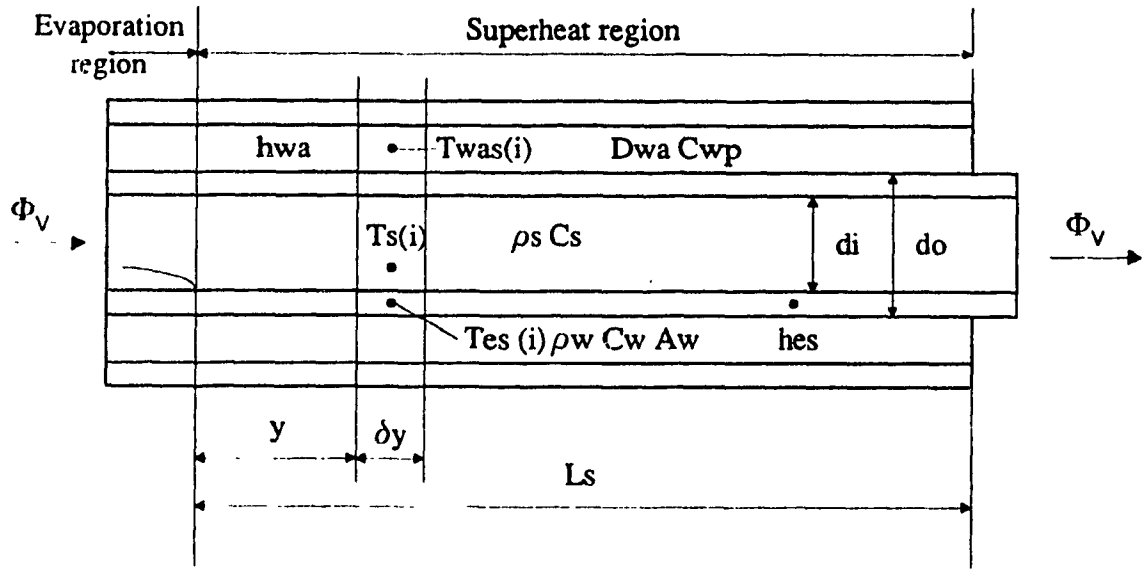

Figure 3.5 Superheat region

The energy exchange rate in refrigerant of each node in superheat region equals to the heat flow into and out of the node volume, $h_{es}F_{ie}[T_{es}(t,y)-T_s(t,y)]$. The energy balance equation for tube wall is:

$$\rho_w C_w A_w \frac{\partial T_{es}(t,y)}{\partial t} = h_{wa}F_{oe}\,[T_{was}(t,y)-T_{es}(t,y)] - h_{es}F_{ie}\,[T_{es}(t,y)-T_s(t,y)] \qquad (3.34)$$

where

T_{was} = water temperature in superheat region (K)

The heat stored in tube wall of each node is balanced to the heat gain from the chilled water $h_{wa}F_{oe}[T_{was}(t,y)-T_{es}(t,y)]$ and the heat absorbed by refrigerant $h_{ie}F_{ie}[T_{es}(t,y)-T_s(t,y)]$. The energy balance of chilled water is given as:

$$\rho_{we}A_{we}\Delta y \frac{\partial T_{wes}(t,y)}{\partial t} = U_4 U_{dwes}\,[\,T_{wes} - T_{wes}(t,y)\,] - \frac{h_{we}F_{oe}\,[\,T_{wes}(t,y) - T_{es}(t,y)\,]}{\rho_{we}C_{we}A_{we}} \tag{3.35}$$

where

Δy = length of control element in superheat region (m)

C_{wes} = specific heat of water (kJ/kg·K)

Before solving the equations by numerical analysis method, the equations were converted in to ordinary differential equations. The finite difference technique was used to get following approximation.

$$\frac{\partial T_s}{\partial y} = \frac{T_s(i+1) - T_s(i)}{\Delta y} \tag{3.36}$$

Then the equations (3.32), (3.33), and (3.34) become

$$\rho_s C_s A_s \frac{dT_s(i)}{dt} = -\frac{\phi_s C_s}{\Delta y}\,[\,T_s(i-1) + T_s(i)\,] + h_{ie}F_{is}\,[\,T_{ie}(i) - T_s(i)\,] \tag{3.37}$$

$$\rho_w C_w A_w \frac{dT_{ea}(i)}{dt} = h_{wa} F_{ea} [\, T_{wa}(i) - T_{ea}(i) \,] - h_{er} F_{ir} [\, T_{ea}(i) - T_s(i) \,] \qquad (3.38)$$

$$\rho_{wa} C_{wa} A_{wa} \Delta y \frac{dT_{wa}(i)}{dt} = U_i\, U_e \max\, C_{wa} [\, T_{wa} - T_{wa}(i) \,] - h_{wa}\, F_{ea}\, \Delta y [\, T_{wa}(i) - T_{ea}(i) \,] \qquad (3.39)$$

Where i from 1 to 2, the total length of superheat regions is $L_s = L_t - L_e$, Δy is the length of one single control volume.

3.6.3 Heat transfer coefficients

For evaporation region, the heat transfer coefficient is evalnated based on the ASHRAE fundamental (1991) for the evaporation in horizontal tubes:

$$h_e = C_1 \left(\frac{k}{d}\right) \left[\left(\frac{CD}{\mu}\right)^2 \frac{J\, \Delta X\, h_{fg}}{L} \right]^n \qquad (3.40)$$

where C_1=1.0082 and n=0.4 for a 6°C superheat at evaporator exit.

For superheat region, Domanski and Didion's (1983) equation is utilized to describe the single phase turbulent flow heated in a tube.

$$N_u = 0.023\, R_e^{0.8}\, P_r^{0.333} \qquad (3.41)$$

Heat transfer coefficient between water and tube wall is assumed to remain constant at 6200 (kJ/ h·m^2·°c). All parameters of evaporator used in simulation are listed in Table 3.3.

Table 3.3 Evaporator parameter used in simulation

Symbol	Magnitude	Units
A_{ic}	0.47	m^2
A_{oc}	1.068	m^2
A_w	0.0005	m^2
A_r	0.00177	m^2
H_{wa}	1.72	$kJ/s \cdot m^2 \cdot K$
H_{cs}	1.0	$kJ/s \cdot m^2 \cdot K$
D_w	8910	kg/m^3
C_w	0.39	$kJ/kg \cdot K$
C_s	0.6	$kJ/kg \cdot K$
L_t	8.0	m
N_s	2	dimensionless

3.7 Thermostatic expansion valve model

Thermostatic expansion valve (TXV) in a refrigeration system controls the flow rate of liquid refrigerant entering the evaporator in response to the superheat of the refrigerant gas leaving the evaporator. Its basic function is to keep practically the entire evaporator active, without permitting un-evaporated refrigerant liquid to be returned through the suction line to the compressor.

Stoecker (1966), Wedeking and Stoecker (1966), Fishcer (1980), Tate and Tree (1987), Yasuda (1981), Li et al (1990), Kuehl and Goldschmidt (1990), Kuehl and

Goldschmidt (1991) etc. have modelled the thermostatic expansion valve. In this study, the modelling method presented by Fisher and Rice is adopted. The model is based on the following assumptions

1) the condensation of the refrigerant is completed and there is certain degree of sub-cooling before it entering the TXV valve.

2) the pressure drops due to refrigerant flow through the nozzle and tube is neglected

3) the static superheat of the valve is taken a value of 6°C.

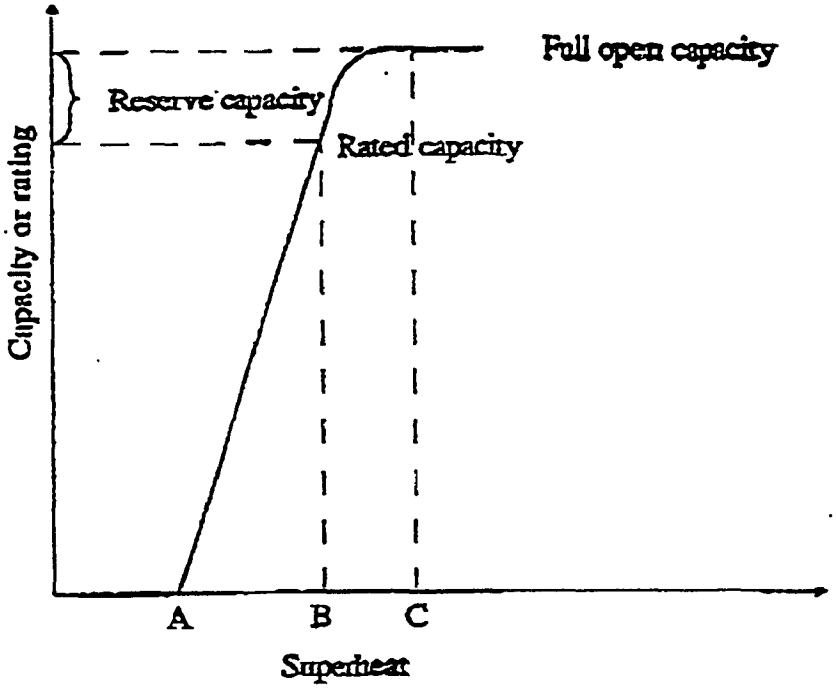

Figure 3.6 Typical gradient curve for thermostatic expansion valves

Figure 3.6 illustrates the superheat changes in response to change in load.

Superheat at no load A, static superheat, ensures sufficient spring force to keep the valve closed during equipment shutdown. An increase in valve capacity or load is approximately proportional to superheat until the valve is open fully. The opening superheat, represented by the distance AB may be defined as the superheat increase required to open the valve to match the load. Operation superheat is the sum of static superheat and opening superheat.

The general equation of TXV is given as

$$\dot{M}_{r,txv} = C_{txv} (\Delta T_{ope} - \Delta T_{ss}) (\rho_l \Delta P_{txv})^{\frac{1}{2}} \qquad (3.42)$$

In order to maintain the general form of the standard orifice equation, a dependence on the refrigerant liquid line density, ρ_l, has been added. Other parameters in equation (3.42) are

$M_{r,TXV}$ = mass flow rate that TXV will pass (kg/h)

C_{TXV} = general orifice flow area coefficient

ΔT_{ope} = actual operating superheat (°C)

ΔT_{ss} = static superheat (superheat at which (°C) the valve is just barely open)

ΔP_{txv} = available pressure drop from TXV inlet to outlet (Pa)

ΔT_{ope} is defined as the difference between superheat temperature at exit of evaporator and the saturation temperature of refrigerant inside the evaporation region (Pa).

$$\Delta T_{ope} = T_{sh} - T_{re} \qquad (3.43)$$

Before using equation (3.42), the flow area coefficient, C_{TXV}, and the available pressure drop across the TXV valve have to be calculated. In order to obtain C_{TXV} value,

the rated refrigerant mass flow rate has to be computed first.

$$\dot{M}_{r,rt} = \frac{12660\ \dot{Q}_{rt}\ b_{fac}}{h_{o,rt} - h_{i,rt}} \tag{3.44}$$

where

Q_{rt} = the capacity rating of the TXV valve (Tons)

b_{fac} = the valve bleed factor

$h_{o,rt}$ = the evaporator outlet refrigerant enthalpy at rated evaporator pressure and superheat (kJ/kg)

$h_{i,rt}$ = the refrigerant enthalpy at rated liquid line temperature (kJ/kg)

The constant 12,660 is used to convert from Tons of capacity to (kJ/h)

C_{txv} is then calculated from the following equation

$$C_{txv} = \frac{\dot{M}_{r,rt}}{(\Delta T_{rt} - \Delta T_{sp})} \left(\rho_{r,rt}\ \Delta P_{rt} \right)^{\frac{1}{2}} \tag{3.45}$$

where

ΔT_{rt} = the rated operating superheat (at 75% of maximum valve opening)(°C)

$\rho_{r,rt}$ = refrigerant density at rated liquid line temperature (kg/m^3)

ΔP_{rt} = rated pressure drop across expansion valve (Pa)

The available pressure drop cross the TXV valve ΔP_{txv} is computed by

$$\Delta P_{txv} = P_d - P_s \tag{3.46}$$

where

P_d = condensing pressure (Pa)

P_s = evaporating pressure (Pa)

All parameters of expansion valve used in simulation are listed in Table 3.4

Table 3.4 Expansion valve parameters used in simulation

Symbol	Magnitude	Units
C_{sv}	4.5	dimensionless
ΔT_{ss}	6	°C

3.8 Evaporative cooler model

Evaporative cooler in this system functions as a cooling tower. It is a device which uses a combination of mass and energy transfer to cool water by exposing it as an extended surface to the atmosphere. The evaporative cooler is assumed to be a single lumped model in which the temperature of the water is uniform, and the mass transfer is not considered. The energy balance equation for the circulating water between condenser and evaporative cooler is derived

$$C_{wo}\frac{dT_{wo}}{dt} = U_2 U_{2max} C_{wo}\xi\,(T_c - T_{wo}) - H_c A_c\,(T_{wo} - \frac{T_{ao}+T_{ai}}{2}) \qquad (3.47)$$

where

$$T_{ao} = T_{ai} + \frac{U_2 U_{2max} C_{wo}\xi (T_c - T_{wo})}{U_1 U_{1max} C_{pa}} \qquad (3.48)$$

C_{wo} = thermal capacity of evaporative cooler (kJ/K)

C_{pa} = specific heat of air (kJ/kg-K)

ξ = fraction of heat exchange between evaporative cooler tubes and water

T_c = temperature of evaporative cooler (K)

H_c = heat transfer coefficient between tube surface and spray water (kJ/s·m^2·K)

A_c = area of evaporative cooler (m^2)

T_{ao} = temperature of outgoing air from evaporative cooler (K)

T_{ac} = temperature of ambient air of evaporative cooler (K)

The equation (3.47) shows that the rate of energy change in cooling water equals to the heat extracted from condenser $U_2U_{2max}C_{wo}\xi(T_c-T_{wo})$ and the heat dumped to the air $H_cA_c(T_{wo}-(T_{ao}+T_{ac})/2)$ in the evaporative cooler. For the simplicity, the heat transfer coefficient between the tube surfaces and bulk spray water in the evaporative cooler, H_c, is constant 11037.6 (kJ/h·m^2·K). Table 3.5 lists the evaporative cooler parameters used in simulation.

Table 3.5 Evaporative cooler parameters used in simulation

Symbol	Magnitude	Units
H_c	3.066	kJ/s·m^2·K
A	60	m^2
T_{ac}	28	°C
U_{1max}	23686.9	kg/h
C_{wo}	83.7	kJ/kg
C_{pa}	1.0	kJ/kg·K

3.9 Chilled water storage tank model

Chilled water storage tank in the system preserves cooling energy temporarily for

later use. During the off-peak periods, cold water is generated and stored in the tank, and then withdrawn during peak periods as needed.

If the T_{ch} is the chilled water temperature and C_{ch} is the thermal capacity of the storage tank, the energy balance on the tank is given as

$$C_{ch}\frac{dT_{ch}}{dt} = -U_4 U_{4max} C_{wat}[T_{ch} - T_{was}(i)] + U_m U_{mmax} C_{wat}(T_{city} - T_{ch}) \qquad (3.49)$$

where i refers the last volume of the superheat region, the heat stored in the tank is equal to the energy withdrawn form the tank by refrigerant through the evaporator tubes, $U_4U_{4max}C_{wat}[T_{ch}-T_{was}(i)]$ and the rate of energy gained, $U_mU_{mmax}C_{wat}(T_{city}-T_{ch})$, from buildings which require cooling. All parameters of storage tank used in simulation are listed in Table 3.6.

To this end, the next step is to study the transient response characteristics of the sub-systems. It will not only to provide a check on the adequacy of the component models, but can also be used to determine the time required (for the variables of interest) to reach steady-state values.

Table 3.6 Storage tank parameters used in simulation

Symbol	Magnitude	Units
U_{mmax}	1150.0	kg/h
U_{4max}	6000.0	kg/h
C_{ch}	18.0	kJ/K
C_{wat}	4.2	kJ/kg·K
T_{city}	20.0	°C

CHAPTER 4

SIMULATION RESULTS

4.1 Numerical technique

The computer program has been developed by writing separate subroutines for each system component (compressor, evaporator, condenser, thermostatic expansion derive, evaporative cooler and storage tank).

Since the refrigerant properties for different states are repeatedly required in the system mathematical model, each refrigerant property correlation function has been built into as a separate subroutine.

The mathematical model of the CWC system consists of 49 ordinary differential and algebraic equations. During each time step every component subroutine is called respectively, and the equations of each subroutine are evaluated successively until all the equations has been solved once.

In order to numerically solve the ordinary differential equations, GEAR method (Gear 1971) is used. Figure 4.1 shows the flow chart of system computer program.

4.2 Simulation results and discussion

A 4.5 Ton CWC system is simulated. The parameters for the system components, and input data to the simulation program are listed in Tables 3.1~3.6. The dynamic characteristics of the system have been simulated for changes in the cooling load, compressor motor speed, mass flow rate through expansion valve, and so on. For example, Figure 4.2 shows the evaporating temperature T_{re} as function of time for three different cases (100%, 80%, and 60% full load). In the first 100 seconds, temperatures start from value of 2°C decrease rapidly and then gradually reach the steady-state value

of -3°C, -4.5°C, and -7°C in approximately 200s, 250s, and 450s respectively for three values of load as mentioned above. It can be noted, from the figure, that the higher the load value, the sooner the temperatures approach the steady-state. In addition, a higher cooling load causes the higher evaporating temperature in the system. The reason is that, under a certain condition of the system, if the cooling load is increased, more heat energy would be extracted from evaporator, since the size of evaporator is fixed, the only way of making more cooling is to increase the enthalpy difference of evaporator, therefore, the evaporating temperature goes up.

The condensing temperature T_{rc} as the function of time are shown in Figure 4.3 for the same three cases. From the figure, it is seen that, the temperatures rise rapidly from initial value until 200s, and then smoothly achieve the stead-state at about 450s. The values of steady-state condensing temperatures are 42.7°C, 42.2°C and 41.5°C respectively for the three different loads noted in the figure. It is also shown that, a low value of cooling load brings about a low steady-state condensing temperature. When load is deceased, the refrigerating capacity is reduced, and as the capacity falls off, the rate of heat rejection at the condenser also diminished permitting the condensing temperature to decline compared to outside air temperature.

In Figure 4.4, chilled water storage tank temperature T_{ch} responses are shown. The chilled water temperature T_{ch} entering the evaporator chills and gives up heat to the evaporator tubes. Since the T_{ch} and evaporating temperature T_{re} are closely depend on each other (superheat region is relatively small). The trend of the T_{ch} curves are similar as that of the T_{re}. Steady-state values of the T_{ch} are 8.5°C, 7.5°C and 4°C for the three

cases. Chilled water temperature of 4°C is likely to cause freezing, therefore for loads less than 60% of full load, it will be necessary to control the refrigeration capacity.

In Figure 4.5, the heat exchange rate in both evaporator Q_e, and in condenser Q_c, are shown. Q_e expresses the rate of heat absorbed by refrigerant in evaporator, and Q_c represents the rate of heat rejected from refrigerant. After the system starts running, both Q_e and Q_c decrease simultaneously from the initial value and meet the steady-state condition at almost same time 300s. The values of Q_e and Q_c are 61 (MJ/h) and 70 (MJ/h) respectively at steady-state.

Figure 4.6 shows refrigerant temperatures at four critical points within the refrigerant circuitry. Among four curves, the one with highest value is the compressor outlet temperature. The refrigerant leaving the compressor as a gas reaches a temperature of 55°C. The condenser outlet temperature, which is that of liquid refrigerant leaving the condenser, reaches a steady-state condition of about 40°C. The other two curves show the steady-state temperatures of compressor inlet and evaporator inlet. Both of them drop off gradually from the initial value, and reach the steady-state at 6°C and -3°C respectively, After the entire amount of refrigerant liquid is evaporated, the temperature starts rising until 9°C which is superheat temperature of vapour entering the compressor.

In Figure 4.7, degree of superheat in the evaporator as the function of percent cooling load is illustrated. From the figure, it can be realized that a higher degree of superheat is required as the cooling load is increased. During the operation of the system, when steady-state is achieved, the degree of superheat would also reach a certain value. If the load is increased, more liquid would evaporate to take the extra amount of heat,

therefor more quantity of refrigerant covers to vapour phase and this results in a higher degree of superheat. This response also agrees with the thermostatic expansion valve operating characteristic curve, in which, an increase in valve capacity or load is roughly proportional to superheat increase until the valve is fully open. ASHRAE Refrigeration Handbook (1994).

Compressor power input as function of percent load is plotted for 100%, 80%, and 60% of full motor speed as shown in Figure 4.8. It is shown that a lower power input is required when load is relatively high if compressor speed control is used. Besides, an increased in power consumption is caused by increase of compressor speed when load is constant.

In Figure 4.9, coefficient of performance COP of the system is plotted against percent mass flow rate of refrigerant. The figure shows that as mass flow rate increases, the system COP increases, The values of COP under given conditions which have been given in this evaluation is ranged between 3.8 to 4.9. They are quite reasonable by comparing with the results of other similar analysis.

Figure 4.10 a,b show the temperatures of refrigerant tube wall and circulating water for both condenser and evaporator. From Figure 4.10a, we can find that temperature curves of refrigerant and tube wall move with same trend with only a small difference during the whole process. The stead-state time is 400s, in that, temperatures reach 42.8°C and 42.2°C respectively. However, the cooling water temperature curve on the bottom is relatively smooth and quickly approaching the steady state compared with other two. In steady state the water temperature reaches 33°C. In Figure 4.10b, a larger temperature

difference between refrigerant and tube wall occurs. The temperature are -3°C and 5°C respectively which show a difference of 8°C. The reason for this is because in evaporator, separate regions for evaporation and superheat are simulated, a mean temperature difference of roughly 8°C is existed between these two regions, and this temperature would directly affect the metal temperatures of two regions since inner tubes are in contact with refrigerant mixture and gas. On the other hand chilled water with high temperature flowing outside the tubes would also influence the temperature of tube wall, due to the heat transfer in both radial and axial directions. Temperature of tube wall in evaporation region would not be close to refrigerant temperature in the presence superheat region. In addition, Figure 4.10b also shows the chilled water temperature as function of time. It reaches a steady state temperature of 8°C. The duration needed to achieve steady state for all three temperatures is 250s.

The effect of compressor motor speed N on chilled water temperature T_{ch} is plotted for three loads (100%, 80%, and 60% of full load). In Figure 4.11, it is obvious that as load decreases and motor speed increases, the chilled water temperature is decreased. If load is constant, increasing compressor motor speed would generate a higher quantity of gas refrigerant flow rate, therefore increasing the refrigerating capacity of the system, and produce more cooling energy which results in a lower chilled water temperature. On the other hand, if the compressor motor speed is fixed, but more cooling is required, the system has to generate higher cooling capacity in order to extract more heat through evaporator, and it would rise the temperature of evaporation, hence, the temperature of chilled water will also increase.

The open-loop simulation results presented above give the transient response characteristics of the system such as steady state time. Furthermore, the sensitivity of some important variable which affect the performance of the CWC system have been investigated. These results are useful in assessing the operating range of output parameters under various load conditions. It is apparent from the results that compressor speed control has significant potential in increasing the COP of the CWC system.

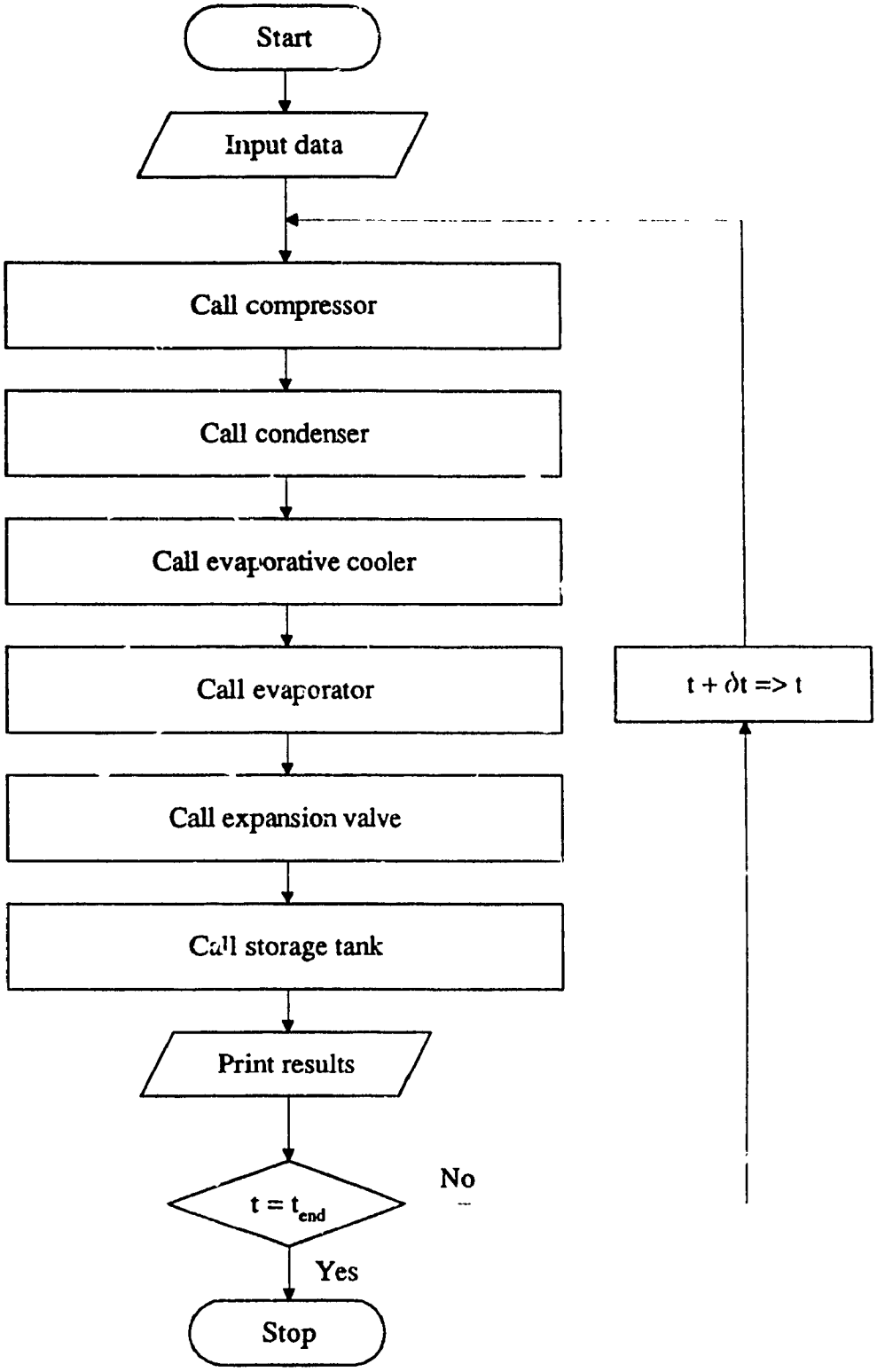

Figure 4.1 Flow chart of system computer program

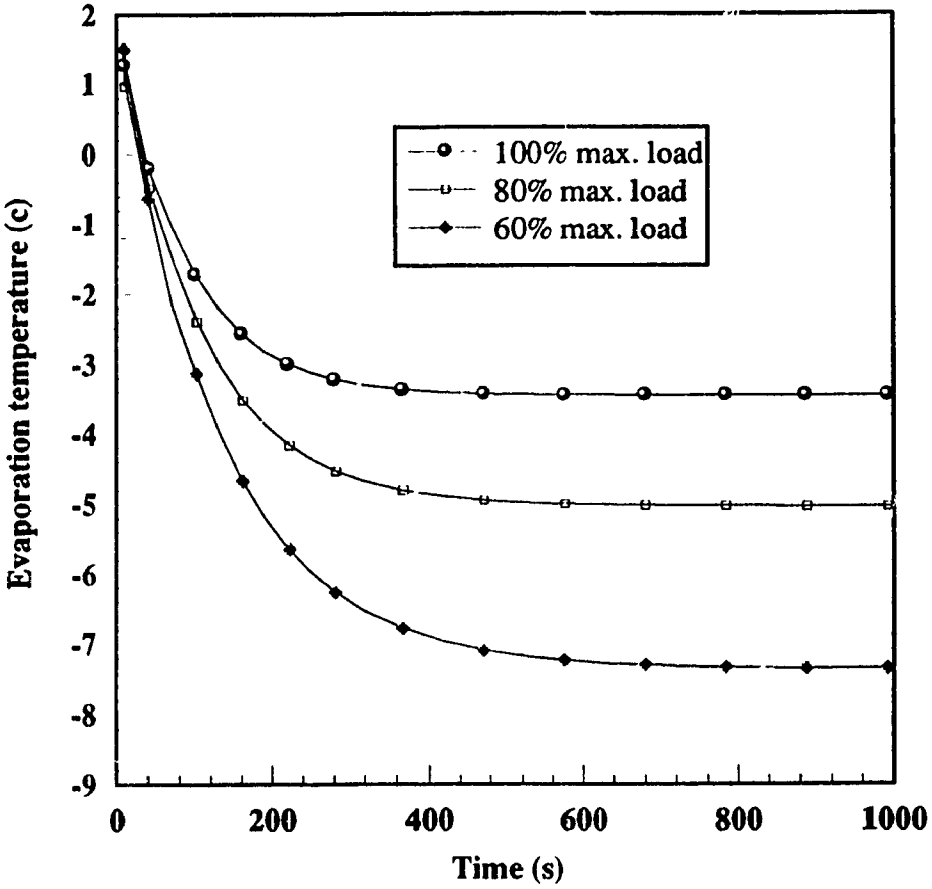

Figure 4.2 Evaporation temperature as function of time

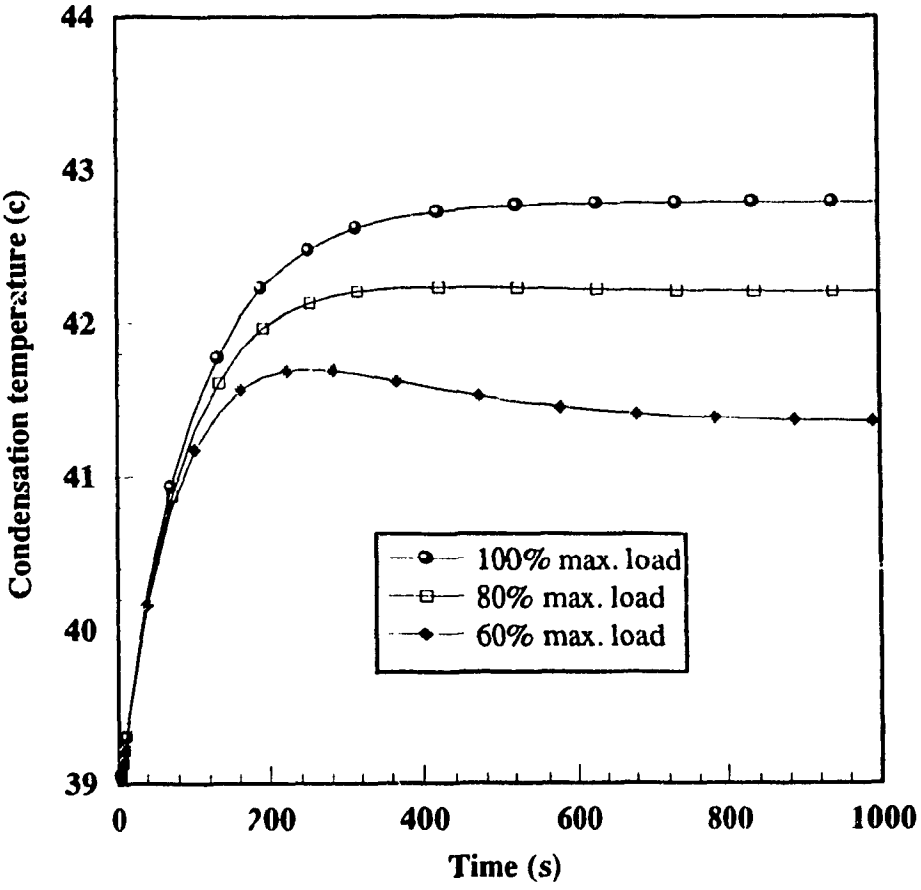

Figure 4.3 Condensation temperature as function of time

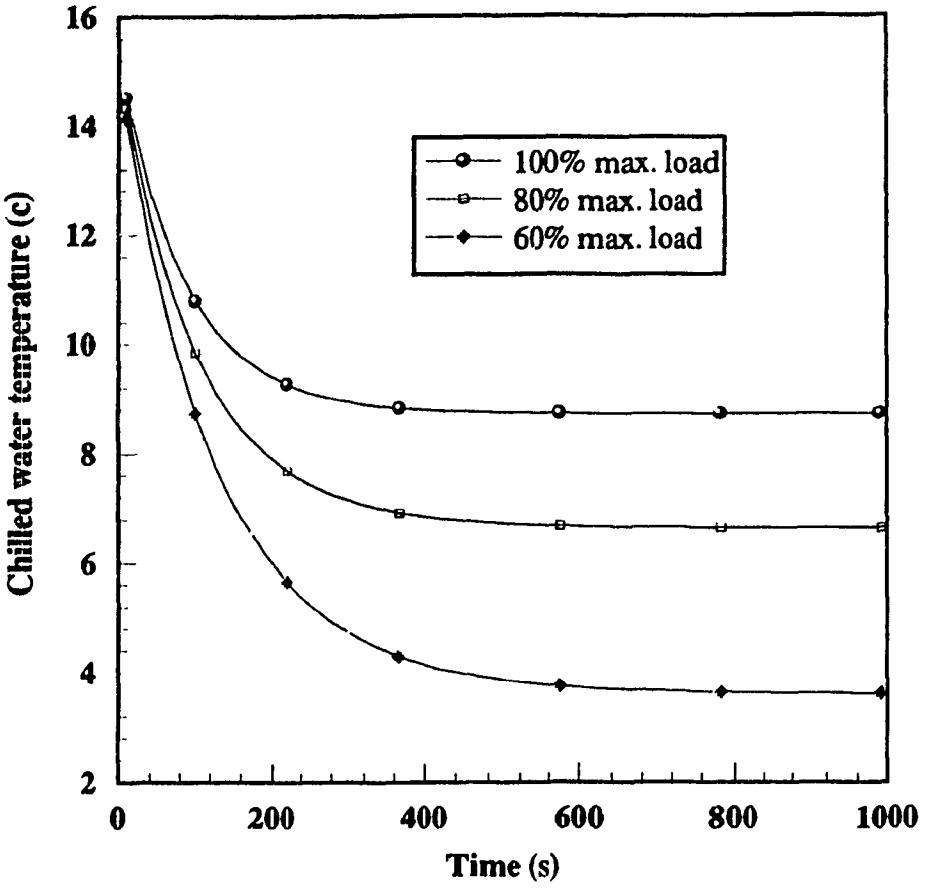

Figure 4.4 Chilled water storage tank temperature as function of time

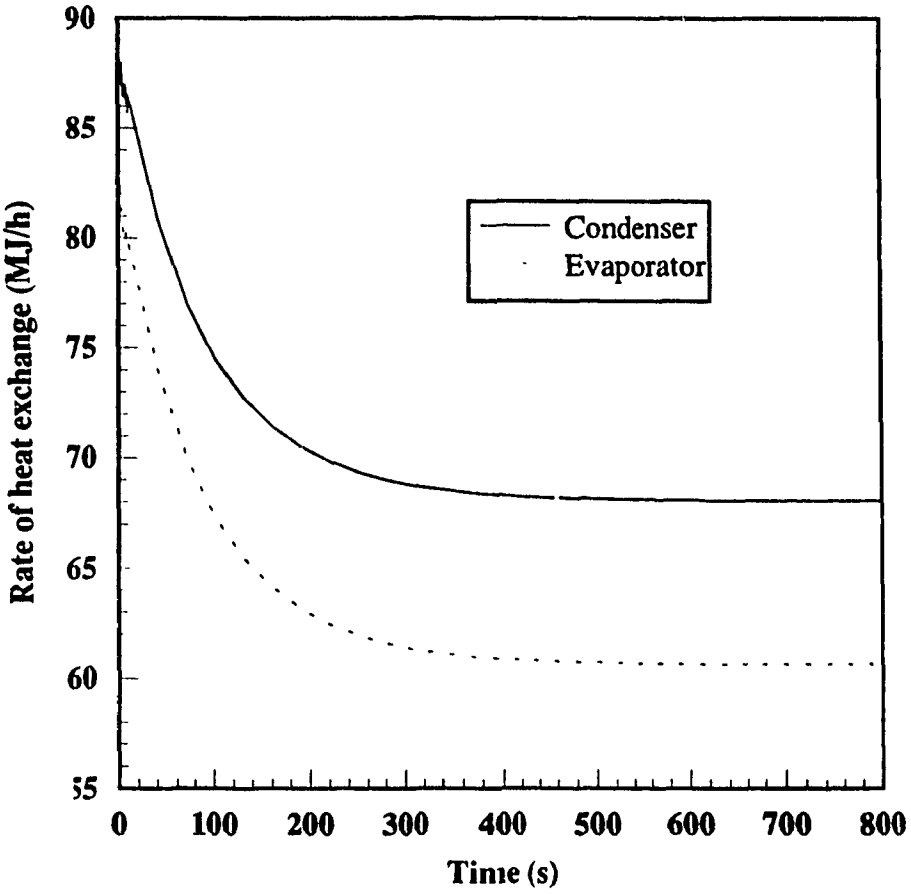

Figure 4.5 Heat exchange rate of condenser and evaporator

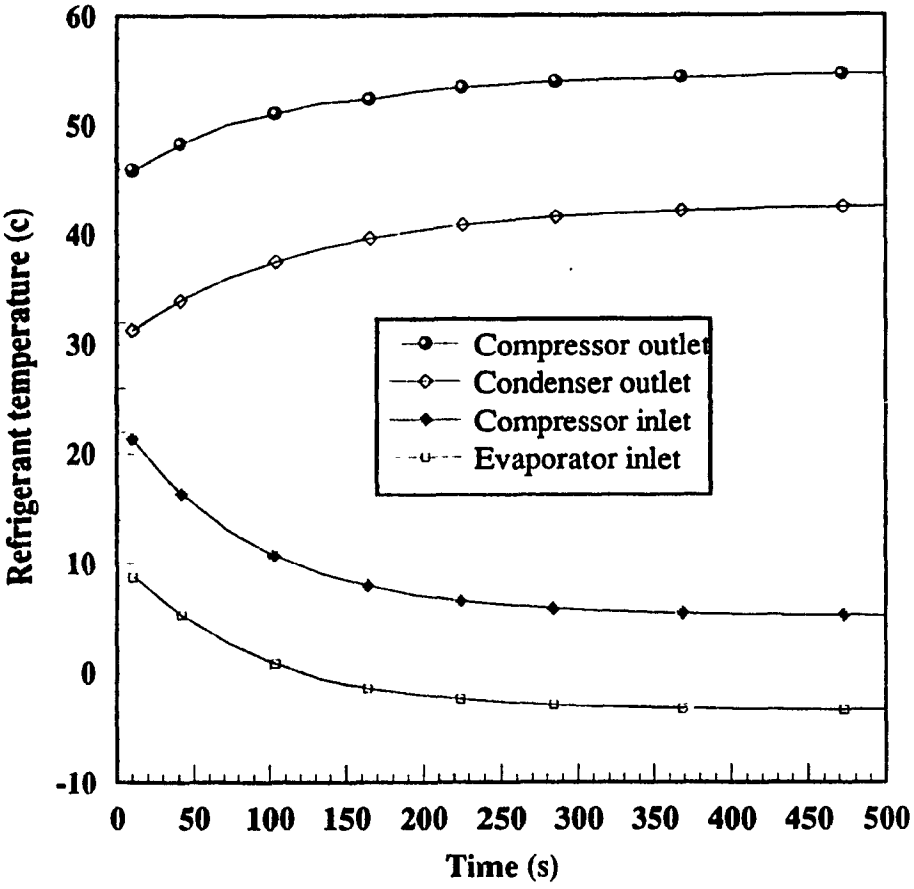

Figure 4.6 Refrigerant states as function of time

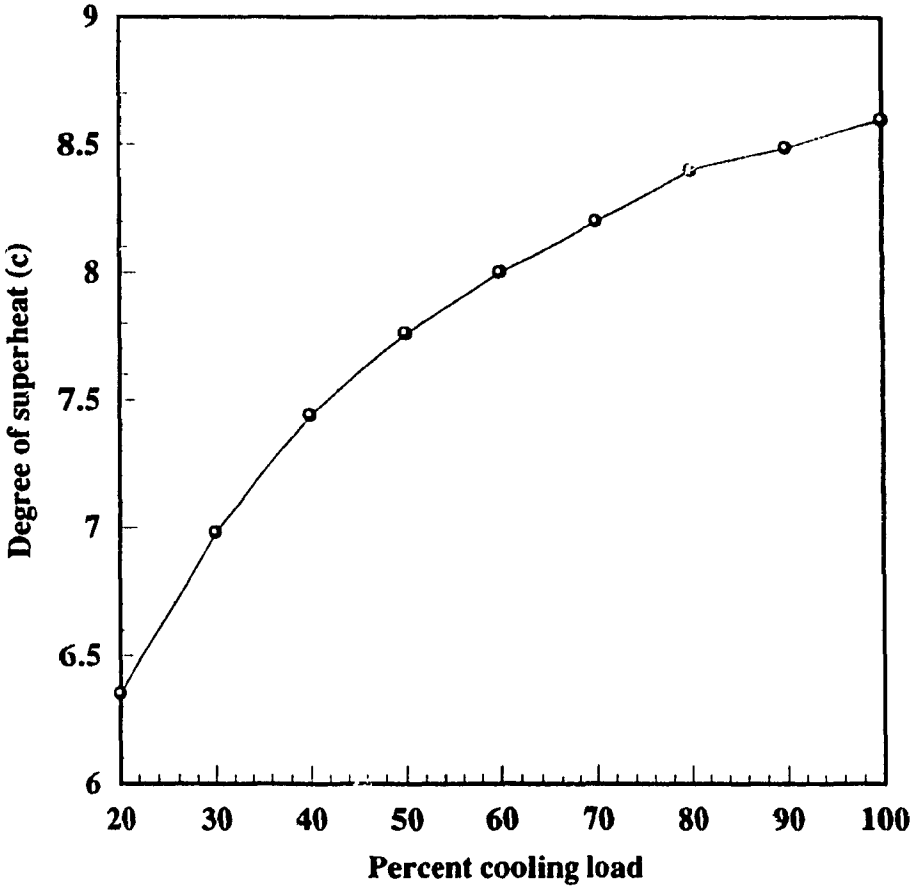

Figure 4.7 Degree of superheat as function of percent load

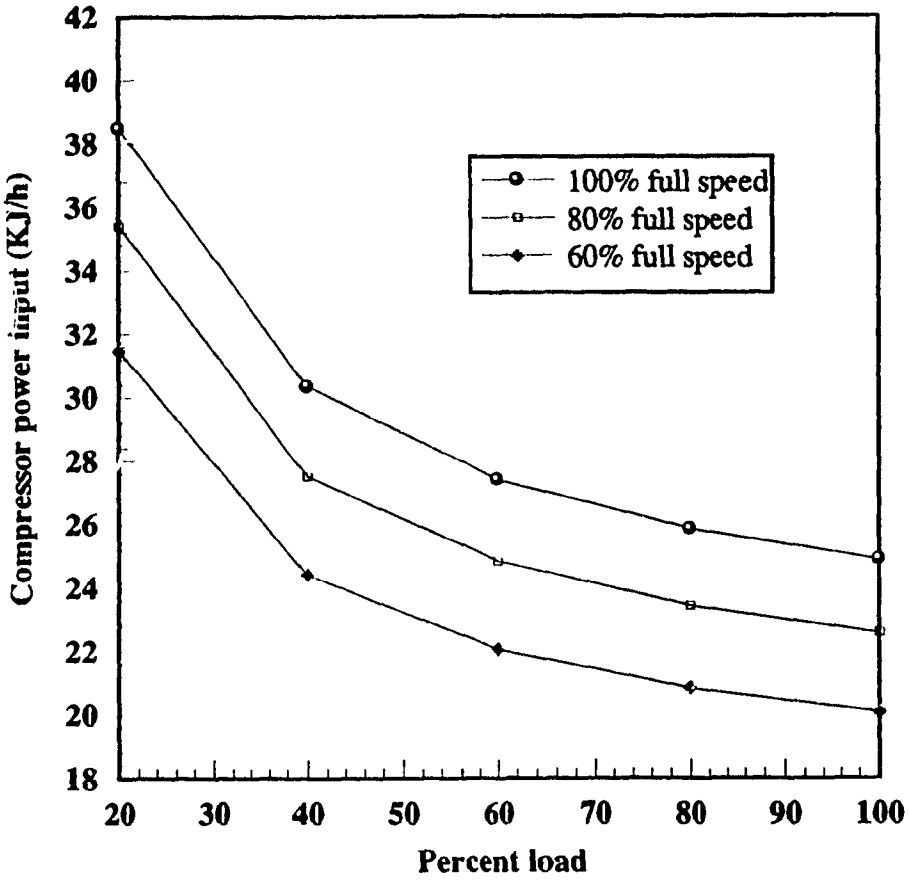

Figure 4.8 Compressor power input as function of percent load and the speed

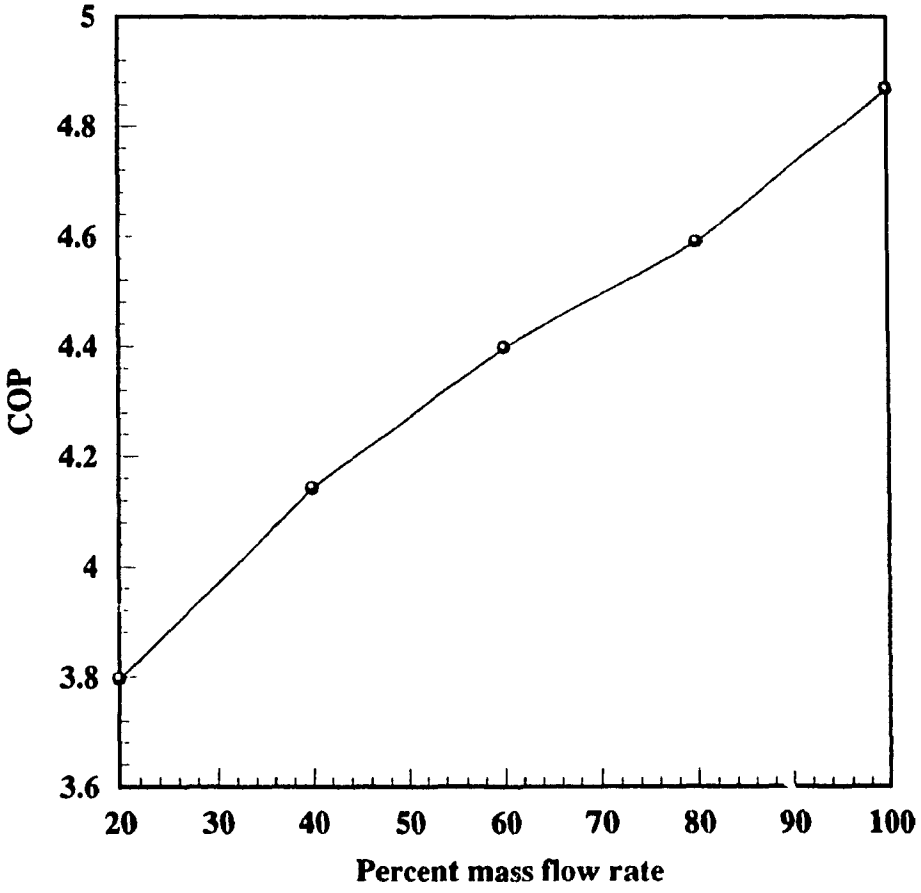

Figure 4.9 COP as function of percent mass flow rate

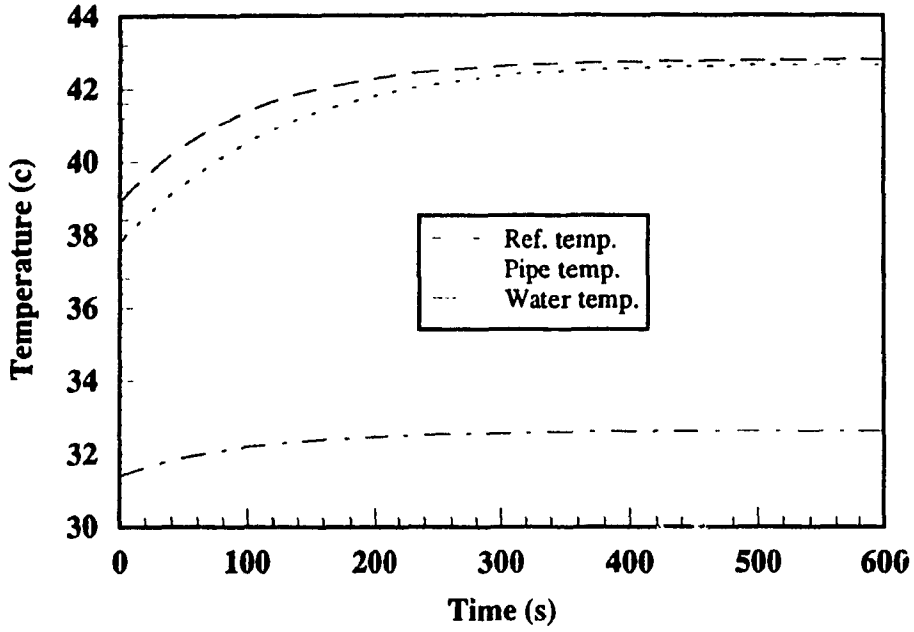

Figure 4.10a Temperatures in condenser as function of time

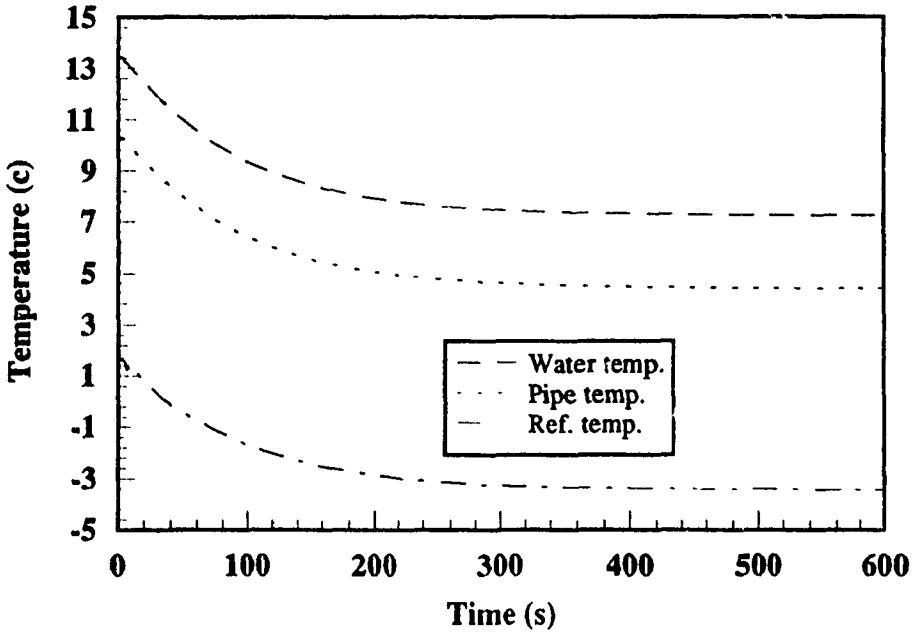

Figure 4.10b Temperatures in evaporator as function of time

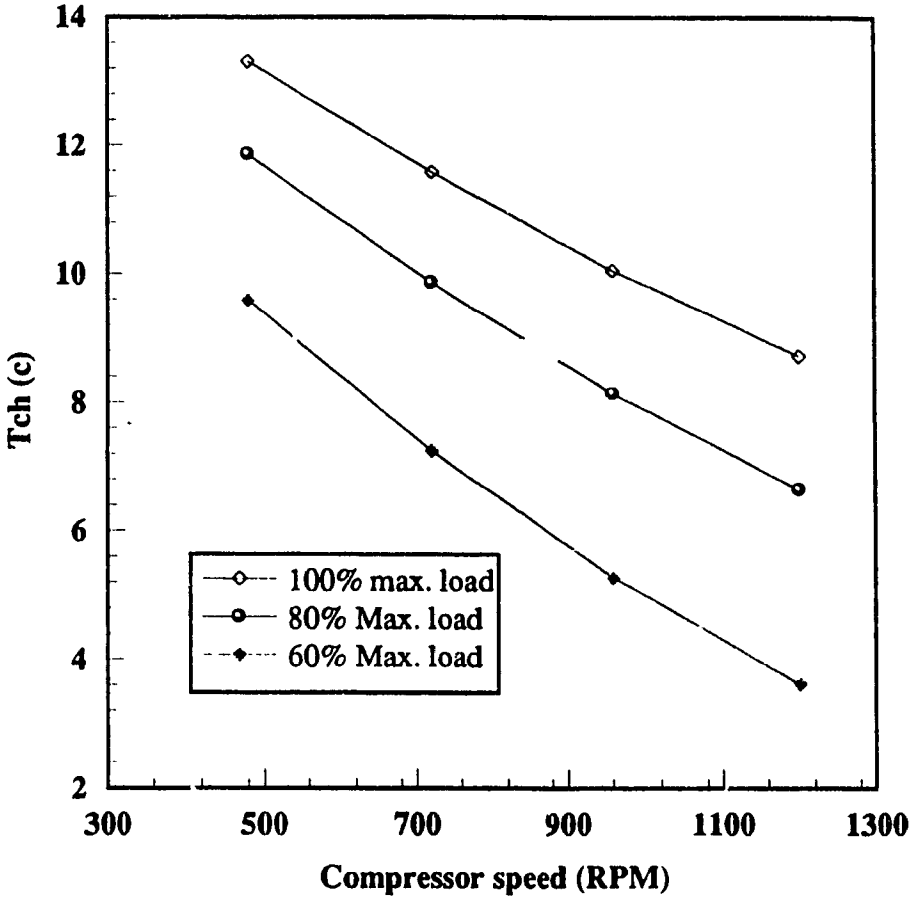

Figure 4.11 Tch as function of motor speed and load

CHAPTER 5

ON-OFF SWITCHING CONTROL STRATEGIES FOR THE CWC SYSTEM

5.1 Introduction

The dynamic responses of the system have been shown in previous chapters. The results reveal that the steady state values of state variables such as evaporating temperature T_{re}, condensing temperature T_{rc}, and cool storage temperature T_{ch}, vary depending on the load and operating conditions. For certain load profiles, chilled water temperature T_{ch} during the off cycle, could be somewhat higher or lower than the setpoint temperature. If it is higher, then thermal comfort condition would not be satisfied; On the other hand, if its lower, more energy will be consumed which means that the system is operating with low energy efficiency. In order to improve the entire system operation efficiency, a good control strategy is required to modulate the system control variables so that they are "optimal" or near optimal.

In this chapter, a heuristic on-off control strategy for the chilled water cool storage system is developed and a technique of creating such control profiles will be illustrated using a reduced-order model. Then the control profile will be examined for its optimality. The determination of optimal on-off control strategies for different but realistic load profiles will be given. Furthermore, the application of the heuristic on-off control profiles to the full order model (the model developed in previous chapters) will be also shown.

5.2 Construction of reduced-order model

For system shown in Figure 3.1 the heuristic on-off control strategy will be developed. If the T_{ch} is the chilled water temperature and C_{ch} is the storage capacity, the energy balance equation is written as:

$$C_{ch}\frac{dT_{ch}}{dt} = -U_3\, U_{3max}\, COP + U_m\, U_{mmax}\, C_{wat}\, (T_\infty - T_{ch}) \qquad (5.1)$$

where the rate of energy stored in the storage tank is equal to the rate of energy extracted from the chilled water $U_3\, U_{3max}$ COP and the heat gains from the return water coming from buildings $U_m\, U_{mmax}\, C_{wat}\, (T_\infty - T_{ch})$. U_m in the equation is mass flow rate of chilled water supplied to cooling coil, and U_3 is the input energy to the chiller. The coefficient of performance (COP) of the chiller is modelled as (Goh 1990):

$$COP = (\, COP_{max} - 1\,)\,(\, 1 - \frac{T_\infty - T_{ch}}{\Delta T_{max}}\,) \qquad (5.2)$$

where T_∞ is the sink temperature and ΔT_{max} is the maximum temperature differential the chiller is designed to work with.

The cost function for minimizing the energy use is defined as:

$$J = \int_{t_0}^{t_z} \alpha_1\, U_3\, dt + \alpha_2\, (T_{ch} - T_{chset})^2\, dt \qquad (5.3)$$

The purpose of this function is in evaluating and minimizing the energy cost through the chiller (U_3) and satisfying the setpoint temperature. The term $\alpha_1\, U_3\, dt$ represents the amount of chiller energy input, $\alpha_2\, (T_{ch} - T_{chset})^2\, dt$ refers to the deviations from the set point temperature, α_1 and α_2 are weighting factors.

Assuming the cooling load for period is known a priori, we propose a periodic solution for this problem to meet the following condition:

$$T_{ch\,(f)} - T_{chss} = \pm\ 0.05^{\circ}c \qquad (5.4)$$

where T_{chss} is steady-state temperature.

The constraint on the size U_3 is taken to be:

$$0 \le U_3 \le U_{3max} \qquad (5.5)$$

This model has been sized identical to the full-order model which was discussed in previous chapters, and the parameters such as U_3, U_{3max}, U_m, U_{mmax}, T_∞ are exactly same for both models. The purpose of building such a reduced-order model is for the development of the heuristic switching control scheme for the CWCS. Since the model is much simpler than the full-order model, computation time could be saved and the solution obtained could be easily analyzed. It is expected that the optimal on-off strategies designed with reduced-order model when implemented on the full-order model will result in near optimal performance. In next section, a set of heuristic on-off control profiles and the procedure of developing them will be presented for several load patterns.

5.3 Heuristic on-off control technique

Figure 5.1a shows the load profile which is used as an example for purpose of illustration. A time varying type load is selected rather than a constant load, because it is more close to the real case, also, if we assume the load is constant, then it would be considered that the steady-state control strategy for operating the chiller system will be optimal. In such a case, there is no advantage in having storage in the system, which will be a digression from time-varying loads with which we are concerned in the study.

Since the load is time varying as shown in Figure 5.1a, we have to look for dynamic optimal solution for it. Based on heuristic ideas, we present a set of "optimal" switching modes consisting of fully on portion and unsaturated steady-state profiles. The objective of the optimal switching strategy is that it should satisfy the boundary condition (5.4) and the minimum cost criterion. Before we illustrate the technique of developing such optimal switching profiles with examples, it should be noted that the numerical values in these examples are for a 4.5 Ton system whose design parameters were chosen based on steady-state sizing methods.

Figure 5.1c shows the optimal switching control profile for operating the chiller U_3 (in solid line) corresponding to the load profile shown in Figure 5.1a. The method to generate this control profile consists of the following two steps:

(1) finding the steady-state optimal solution and

(2) determining the lead time τ_{ld} and on time τ_{on} for control of the system such that

(a) the boundary condition is satisfied and

(b) the minimum cost criterion is met.

The steady-state optimal solution for chiller input U_3 is as a function of U_m (cooling load). The final value of U_3 for $T_{ch} = 8°C$ was obtained through simulation. The equation giving the relationship between U_m and U_3 can be written as:

$$U_3 = m\ U_M - c \qquad (5.6)$$

Note that this solution to U_3 is correlated with only one variable U_m, and the steady-state temperature is defined to be 8°C (Figure 5.2).

Equation (5.6) can be used to generate the unsaturated portions of the control

profile U_3 shown in Figure 5.1c. In order to determine the lead time τ_{ld} and on time τ_{on} for the full on portion while on-mode of U_3 is activated, an iterative numerical search method was used. The criterion for the optimal lead time τ_{ld}^* and on time τ_{on}^* were that the boundary condition (5.4) must be satisfied and at the same time the cost is minimized.

5.4 ON time search methodology

A numerical search technique has to be used in order to determine the lead time and on time shown in Figure 5.1c. In the methodology used, the search problem is considered as a one dimensional search problem. In Figure 5.1a, since the load is increasing at 1.5 hour, the chilled water storage has to be charged ahead of time so that water is available for supply at the set point temperature right at 1.5 hour. With this assumption, U_3 is turned on at time τ_{ld}, and it is held at maximum value for period of on-time τ_{on}, so that the chilled water temperature returns to its steady-state value at exactly 2.5 hour. With the τ_{ld} and τ_{on} thus determined, the cost during the period of 3.5 hour was computed.

Figure 5.3 shows the flow chart of the computer program for searching optimal on time period τ_{on}^*. It displays the steps that have been followed in the numerical search. Firstly, set up an arbitrary time as lead time slightly ahead of 1.5 hour, at this moment, U_3 is turned on and held until the period of τ_{on} is reached. The search for the length of on time starts right from the lead time point, and it must be so selected such that the state variables return to their respective steady-state values at 2.5 hour. In other words, the chilled water temperature T_{ch} has to be equal to 8°C at time 2.5 hour, as shown in Figure

5.1b. Once the on time is determined, U_3 is set back to its respective steady-state value computed from equation 5.6 or read from Figure 5.2.

For the system parameters defined in Table 5.1, it was found that search intervals as small as eighteen seconds were necessary. The magnitude of steady-state unsaturated control value is shown in Figure 5.2. The result plotted in Figure 5.1b shows that the temperature T_{ch} returned to its initial values at the end of the period. The figure also shows the optimal T_{ch} (J_{min}) as compared to a case which was not optimal. In next section, the switching control strategy will be examined and an optimization method will be suggested.

Table 5.1 System parameters of the reduced-order model

Variable	Magnitude	Units
U_{mmanx}	1150	kg/h
U_{3max}	30,000	kJ/h
COP_{max}	3	dimensionless
DT_{max}	45	°C
C_{ch}	8000	kJ/°C
T_{∞}	20	°C
T_{chset}	8	°C

5.5 Test for optimality of control profiles

It is reasonable to ask whether the control profile shown in Figure 5.1c (in solid

line) is optimal because there could be other solutions with different lead time τ_{ld}. In order to answer this question, an extended search method was used. This time, we again use the numerical search method but problem is extended to a two variable search problem. The search for both τ_{ld}^* and τ_{on}^* was executed over a wide range that is, from one hour before and a half hour later from the point of application of load (1.5h in Figure 5.1a). For each time interval $d\tau_2$, a search for the on time that minimized the cost was made.

Figure 5.4 shows the flow chart of the computer program for searching optimal τ_{ld}^* and τ_{on}^* by the methodology described above. When starting the program, initial value for lead time was assumed and U_3 is turned on, then for each small interval $d\tau_2$, a search for τ_{on} was made such that the state variable returns to its steady-state value at 2.5 hour, at this point U_3 is set back to its steady-state value. If such τ_{on} is determined, one set of iteration has been completed for the lead time that was set at beginning, and the corresponding cost value J is calculated for that iteration. Next round of searching will move ahead to the new lead time by adding a small amount $d\tau_1$ to the initial value, and this process will continue until the lead time is equal to 2.0 hour. While each step of searching is executed, the cost J will be found out and compared. The result of testing for optimality of the control method is shown in Figure 5.5b. In this figure, the cost J is plotted as a function of both lead time and on time. As it is shown in the figure, for each individual τ_{ld}, there is a τ_{on} which satisfies the condition such that the temperature of T_{ch} goes to the steady-state value 8°C at 2.5 hour. However, there is only one set of τ_{ld} and τ_{on} that gives the minimum cost J_{min} (4.06). The switching control profile for U_3 and the

temperature T_{ch} response for this optimal case are shown in Figure 5.1b,c (solid line).

5.6 Optimization method for searching problem

If cost J is treated as the function of lead time only, (since the on time is associated with lead time) then this problem becomes a single variable optimization problem. By expressing the cost by E, x as τ_{ld}, we can turn the problem to one of minimizing E of f which is a function of one variable only, i,e

$$\textit{minimize } E = f(x) \tag{5.7}$$

In order to solve this problem, the optimization methodology for one variable search problem called "golden section method" was used. The basic idea of the search technique is based on function evaluations that intend to maximize the reduction of interval known to contain the minimum in the least number of evaluations. Within a search interval defined by a lower limit of x at x_l and an upper limit at x_u. Two search points x_a and x_b are selected. The distance from x_l to x_a and from x_b to x_u is 0.618 (x_u-x_l). For next step of search, the two search points will be selected in the same way. The search will be terminated if the distance of interval reach a small number ε which was defined initially.

Figure 5.6 shows the flow chart of the computer program for the control problem by using "Golden section method". The steps can be summarized as follows:

1 Input data High, Low, ε

2 Compute the first two test points

T_{La} = High - 0.618 (High-Low)

T_{Lb} = Low + 0.618 (High-Low)

3 Evaluate the function f at the two test points

$J_a = f(T_{La})$

$J_b = f(T_{Lb})$

4 Test for the interval which contains the minimum

If $J_a \leq J_b$, go to step 5

If $J_a \leq J_b$, go to step 6

5 Use equations shown below to update all information for next iteration

$High = T_{Lb}$

$T_{Lb} = T_{La}$

$T_{La} = High - 0.618\ (High - Low)$

$J_a = f(T_{La})$

6 Use equations shown below to update all information for the next iteration

$Low = T_{La}$

$T_{La} = T_{Lb}$

$T_{Lb} = Low + 0.618\ (High - Low)$

$J_b = f(T_{Lb})$

7 Test for the end of the optimization

If $(High-Low) \geq \varepsilon$ then go to step 4

otherwise go to step 8

8 Check the interval which contains the minimum

If $J_a < J_b$, then $J_{min} = J_a$, $T_L = T_{La}$

otherwise $J_{min} = J_b$, $T_L = T_{Lb}$

9 Out put J_{min} and T_L

Results show that the difference between on-off search technique and "golden section method" was 0.049% and 2.7% for J_{min} and T_L respectively, besides, the "golden section method" needs much less iteration steps to get the final result than the other one and computation time was saved considerably. However, it should be noted that before using "golden section method", one has to ensure that the problem to be solved is a single variable optimization problem. This method can be used to examine the results that were obtained earlier (Figure 5.1).

5.7 Further investigation of the on-off control profiles

In order to test the methodology of generating the heuristic on-off control profiles for different load conditions, several runs were made by changing the load configurations. Since the first load profile shown in Figure 5.1a was referred to as case1, the new loads are identified here as case2 and case3 load profiles shown in Figures 5.7a and 5.8a. Although these two load profiles are somewhat different than the first one, same methodology for computing "optimal on-off control" solution will be used. For load profiles shown in Figures 5.7a and 5.8a, again we expect to obtain the heuristic on-off control strategies for U_3, which satisfy the boundary condition (5.4) and meet the minimum cost criterion expressed in (5.3). The steady-state solutions for U_3 were found from Figure 5.2 or equation (5.6). The optimal lead time and on time for both cases were determined. Results for case2 and case3 are plotted in Figures 5.7b and 5.8b.

Figures 5.7b and 5.8b show the cost J as function of τ_{ld} and τ_{on} for case2 and

case3 respectively. They indicate that for lead time ranging between -1.4 to 0.4 hour, a convex function is obtained, and there is a point at which the minimum cost value J_{min} accrues. The resulting chilled water temperature T_{ch} and U_3 for two cases are shown in Figures 5.9 and 5.10 (solid line). The T_{ch} profiles reflect two load patterns. When sudden changes in load occur as in Figure 5.9a we can expect a rapid decrease in T_{ch} (Figure 5.9b). On the other hand when the load changes are gradual, T_{ch} changes are smooth. So, it can be concluded that the temperature distribution might be affected by the load shape and magnitude, but the boundary condition was met for both load cases because after 2.5h, the load curves become same. In Figures 5.9c and 5.10c, the heuristic on-off control profiles of U_3 are presented. It is apparent that in both cases, the U_3 was turn on at 30 minutes, in term of lead time, -0.5 hour ahead of the load. The duration of on time of U_3 for case3 is about 18 minutes less than that for case2, since the cooling load level is not as high as in case2. The chiller was turned off earlier in case2 in order to allow chilled water temperature T_{ch} to go to steady-state value 8°C. Comparisons of optimal T_{ch} and U_3 (identified as J_{min}) to that of another case were also made in Figures 5.9b,c and Figure 5.10b,c (dot lines).

The test results shown above demonstrate that the technique based on one-dimensional two variable search gave minimum cost under fluctuating load conditions.

5.8 Application of heuristic on-off control profiles

It is of interest to implement the heuristic on-off control technique described in the last section, for a typical day operation. To this end, the first step that is necessary

to take is to determine optimal switching solution over intervals of one to two hours until 24-hour period is covered. Next, we are going to show how the on-off control strategy is applied for a 24 hour period load.

5.8.1 Multiple usage of heuristic on-off control technique for daily load

Consider a step change load profile as shown in Figure 5.11a. For the day with this load demand curve, known a priori, we wish to find the heuristic switching control sequence for U_3. In this case, the cost function for minimizing the 24-hour pattern of energy use is defined as:

$$J = \int_0^{24} \alpha_1 \, U_3 \, dt + \alpha_2 \, (T_{ch} - T_{chset})^2 \, dt \qquad (5.8)$$

The terms in equation (5.8) are same as those in equation (5.3). We also expect the solution to this problem satisfy the following boundary condition:

$$T_{ch(22)} - T_{chss} = \pm \, 0.05^{\circ}c \qquad (5.9)$$

Moreover, the constraint on the chilled water temperature T_{ch} is taken to be:

$$7.0\ ^{\circ}c \le T_{ch} \le 9.0\ ^{\circ}c \qquad (5.10)$$

For the daily load profile shown in Figure 5.11a, we propose an optimal unconstrained control solution by repeated application of the heuristic on-off control technique, more specifically, once every two hours, between period 10 ~ 22 hours. In this way, the control solution for U_3 which satisfies boundary condition (5.9) and meets the minimum cost criterion (5.8) was found. Meanwhile, the minimum cost J_{min} for the day

would be computed by integration minimum cost values of each searched interval. Figure 5.11b,c,d,e present the on-off control profile of U_3 and resulting chilled water temperature T_{ch}. As we see in the Figure 5.11b, with the optimal solution of U_3, the temperature T_{ch} is beyond the constraint limit (5.10). The magnitude of net overshoot T_{os} is found to be 0.35 ~ 0.58 °C, and those overshoots occur between 12 ~ 18 hours, which indicates that during high load period, direct application of the control technique developed earlier can not solve the constraint problem. In order to generate the control solution which not only to be optimal or near-optimal, but also fulfil the constraint as in equation (5.10), it will be necessary to use a switching strategy as explained in next section.

5.8.2 Lead time switching approach for constrained near-optimal solution

There are three unacceptable overshoots in T_{ch} curve shown in Figure 5.11b. By examining the T_{ch} curve and corresponding U_3 profile, it was noted that those overshoots appear at three points. They are 0.35°C at 12.8 hour, 0.5°C at 14.7 hour, and 0.58°C at 16.8 hour. It seems that if we switch the chiller τ_{ld} ahead of time, the overshoots might be reduced. Therefore the chiller was switched ahead of time at each overshoot. At first step, τ_{ld1} and τ_{ld2} were switched from 12.8 to 12.7 hour, and τ_{ld2} was switched from 14.7 to 14.4 hour. The resulting T_{ch} and U_3 is shown in Figure 5.11d,e. In these figures the effect of switching τ_{ld1} and τ_{ld2} can be seen from T_{ch} responses where the first two overshoots are diminished. The second step, τ_{ld3} was switched from 16.8 to 16.4 hour and its result on T_{ch} and U_3 are shown in Figure 5.11f,g. From Figure 5.11f, it is noted that a new overshoot in T_{ch} occurred. In order to reduce the last overshoot, the third step was

taken by switching τ_{ld4} from 19.0 to 18.5 hour. The final result of T_{ch} and U_3 are shown in Figure 5.11h,i. These figures show that by a trial and error process the temperature T_{ch} is basically maintained in the range of 7.0 to 9.0 °C. The cost value J obtained from the modified operation scheme is 0.16% higher than the one without constraint J_{min}. So, for load profile shown in Figure 5.11a, we have found by trial and error the constrained control solution for U_3 which is near-optimal.

Figure 5.12 shows the lead time needed, as function of net overshoot of temperature T_{ch}. The data was obtained from several simulation results. Now, we are going to illustrate how the τ_{ld} switching approach can be made easier by considering another load profile. Consider, the daily load profile shown in Figure 5.13a and Figure 5.14a. In Figure 5.13a, it is assumed that at lunch time (12 hour) people are out of the building, the load therefore is decreased and remains the same until two hours later, at 14 hour the people are back. Meanwhile, due to solar radiation effects in the afternoon, the cooling load suddenly increased from 14 hour and remains high until 16 hours. In Figure 5.14a, the load was assumed to decrease right after the maximum value. In order to find the near-optimal on-off control profile for both cases, firstly, multiple use of the heuristic control technique was applied to each case. Having obtained an initial unconstrained solution for U_3 and the corresponding temperature configurations, as shown in Figure 5.13b,c and Figure 5.14b,c, respectively, we have determined the required switching time τ_{ld} for each overshoot point, using Figure 5.12. The manner in which the solution proceeded is shown in through Figure 5.13b,d and f. Figure 5.13f is the final solution which shows that T_{ch} is within constraints. The corresponding U_3 profile is given

in Figure 5.13. Like wise, the solution for obtained with load profile shown in Figure 5.14a are also presented in Figure 5.14b,c,d,e. It was found that final cost values of J were slightly higher than those for without constraint.

5.9 Implementation

In the above we have presented a methodology by which optimal on-off control strategies for chilled water system can be computed. However, to illustrate the technique we chose a reduced-order model. It is of interest to see if the optimal on-off control strategy determined from the reduced-order model can be implemented on the full-order model developed in chapter 3. Before doing this it would be necessary to make sure that the reduced-order model behaves similar or almost similar to the full-order model. To do this, first we need to make sure that the parameters in reduced-order model are properly chosen so that open loop response are identical or close to the that of full-order model. By regulating the storage capacity C_{ch}, compressor speed AN, we have plotted the open loop responses of chilled water temperature T_{ch} for both models shown in Figure 5.15a,b,c. for three different loads U_m=0.3, U_m=0.5 and U_m=0.8. It is apparent that steady-state time required is same for both models. However, the trajectories of T_{ch} are somewhat different, and for larger load U_m=0.8, the difference between two T_{ch} curves is more evident. This is because the full-order model is large and complex as such the system characteristic is effected by several parameters compared to the reduced-order model. Therefore, it can be considered that both models are close enough for the purpose of designing optimal on-off control using the reduced-order model. Since the control

element in full-order model is compressor motor speed AN, it is necessary to find out the steady-state optimal solution for speed AN in order to implement the control technique on the full-order model. For the steady-state set point temperature of 8°C, the result of optimal solution is shown in Figure 5.16. Note that AN as a function of U_m only was considered to simplify the problem. However there could be other variables which affect the speed AN. This requires further investigation which is left for future research.

5.9.1 Results and discussion

Several simulation results are presented with different load profiles. In each case first the optimal on-off control strategy was found by using the reduced-order model. Then this optimal on-off control sequence was implemented on the full-order model. The resulting solutions of T_{ch} profile were compared. These are shown in Figures 5.17 ~ 5.22. We can see from those figures that, the temperature T_{ch} of full-order model return to the steady-state value at 8°C exactly at 2.5 hour, the boundary condition (5.4) therefore is satisfied. In addition from the comparison of the T_{ch} profiles between both models, it is found that when load remains low, say during period of 0 ~ 1.5 hour and 2.5 ~ 3.5 hour, the T_{ch} response of full-order model are quite close to that of reduced-order model, however, when load increases, the temperature T_{ch} of full-order model are obviously lower than that of reduced-order model. This could be explained in that the full-order model was developed more thoroughly and is considered to be more accurate representation of chiller dynamics. The maximum temperature difference in T_{ch} between two models is about 0.2°C, 0.6°C and 0.4°C for load profiles shown in Figures 5.17a, 5.18a,

and 5.19a, respectively.

The simulation results for the daily load are shown in Figures 5.20a,b,c, Figures 5.21a,b,c, and Figure 5.22a,b,c. It can be noted that, by implementing the constraint near-optimal on-off control profiles on the full-order model, the response of T_{ch} are basically kept close within constraint. This could be considered as satisfying the constraint requirement (5.10). The comparison of temperature T_{ch} profiles between two models are also given in the figures. They indicate that both T_{ch} curves look very close and the largest difference between them is 0.15 ~ 0.25 °C. These results show that the heuristic on-off control methodology developed in the study is simple and near optimal and can be used for operation of chilled water cooling systems with storage.

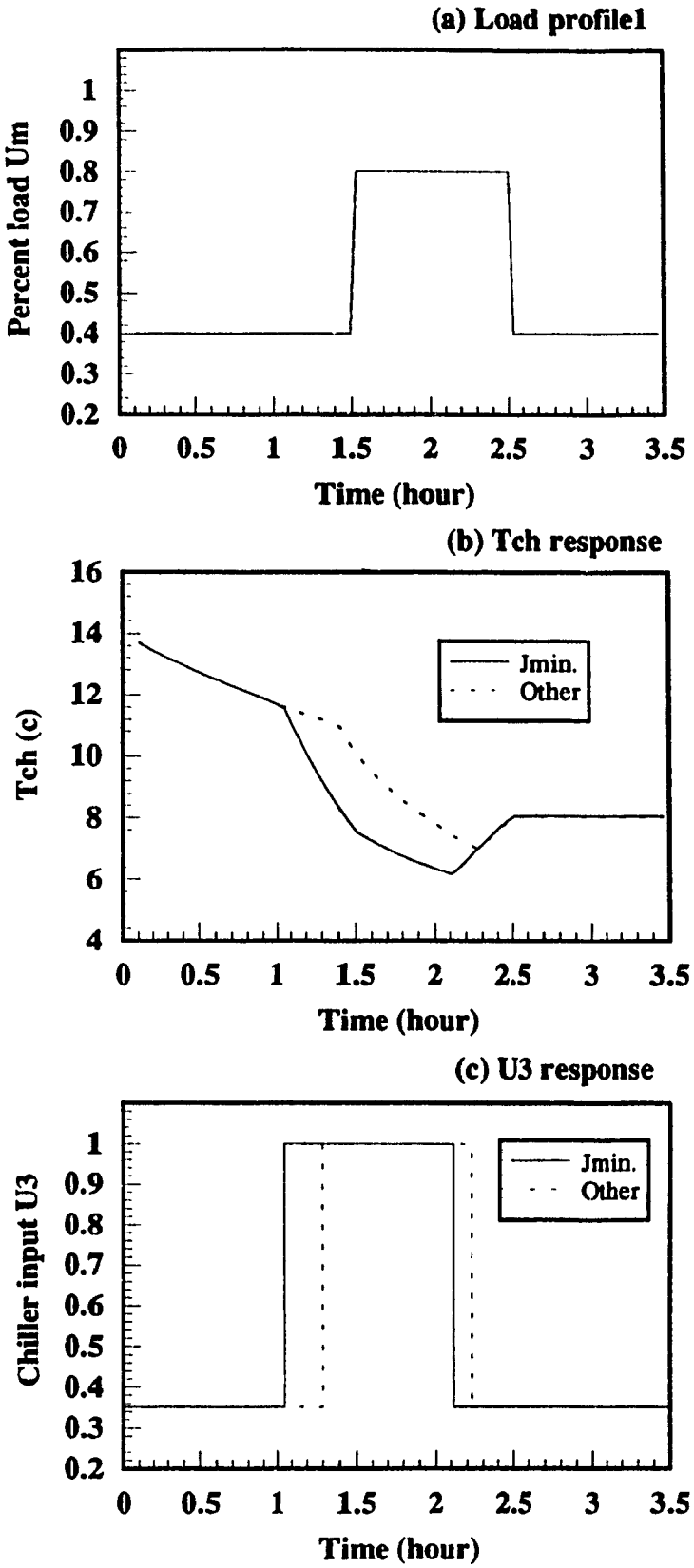

Figure 5.1 Comparsion of Tch and U3 responses between optimal (Jmin) and not optimal (other) case for load profile1

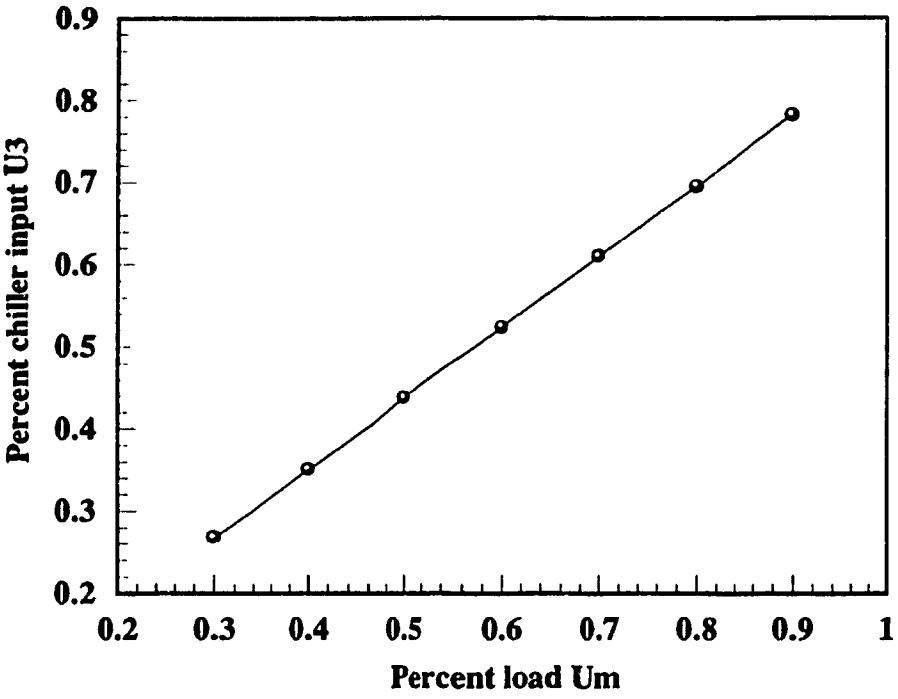

Figure 5.2 Steady-state optimal value of U3 as function of Um

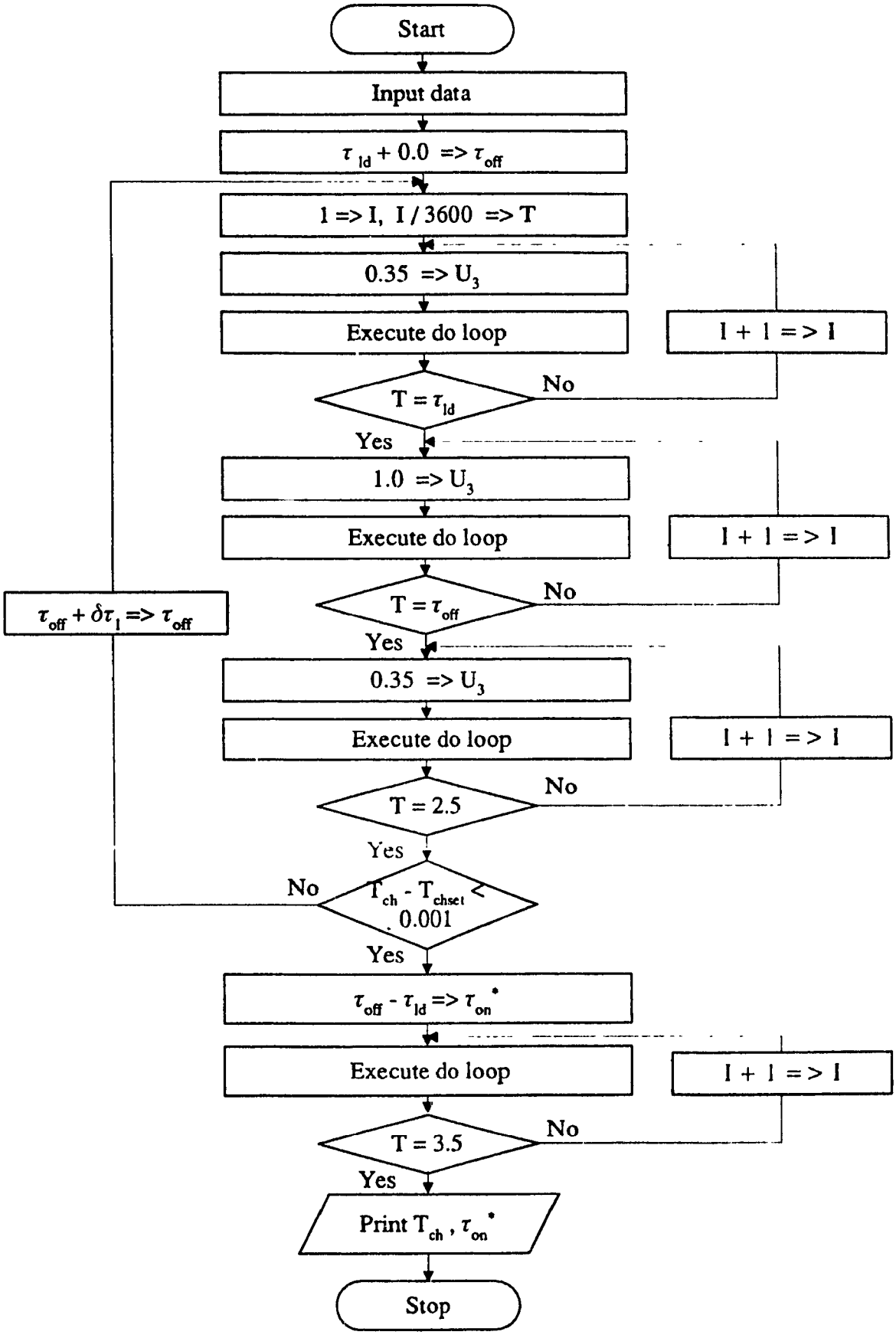

Figure 5.3 Flow chart of the program for searching optimal on time

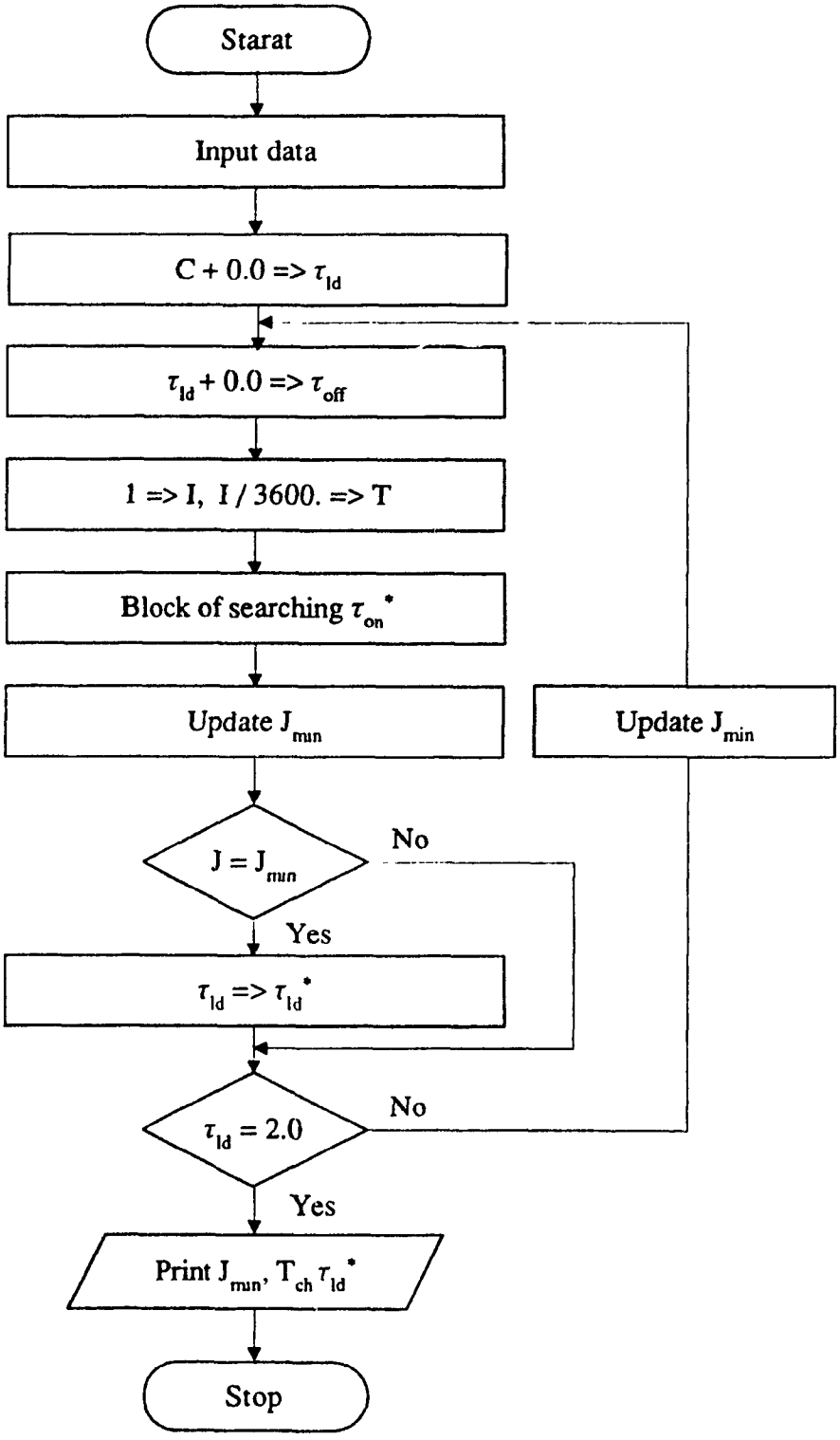

Figure 5.4 Flow chart of the program for searching optimal lead time

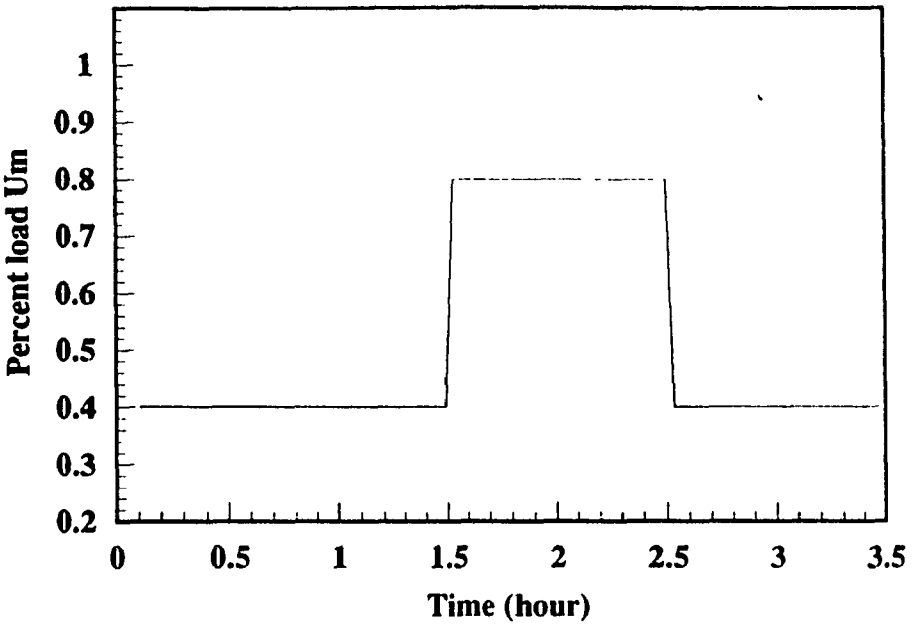

(a) Load profile1

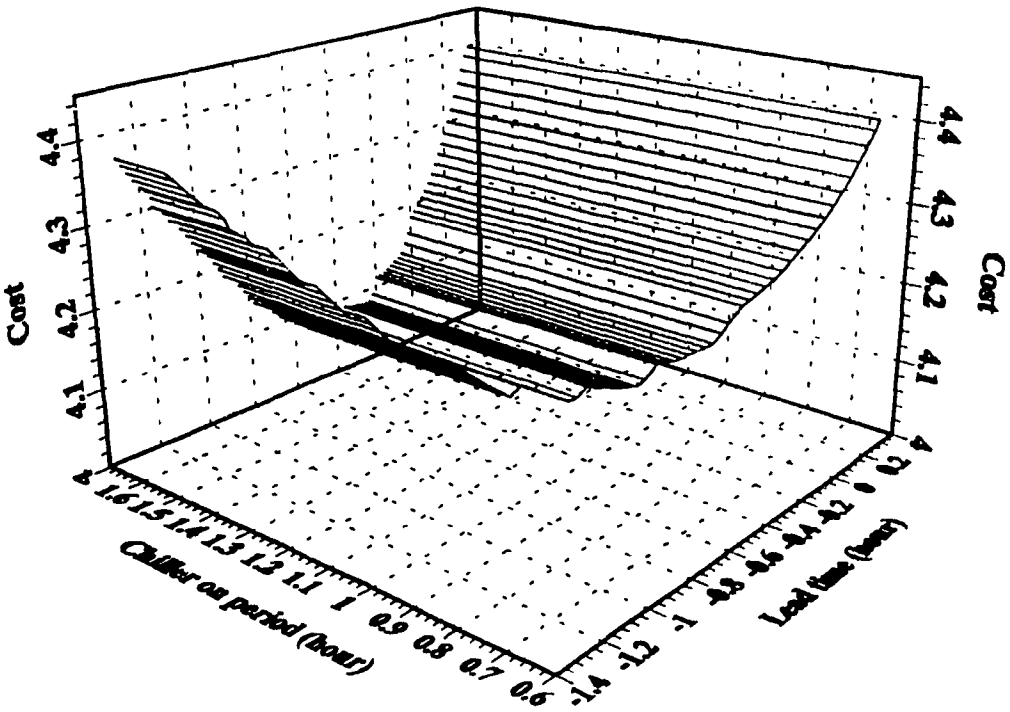

(b) Configuration of the cost

Figure 5.5 Chiller energy cost as function of lead time and on time for load profile1

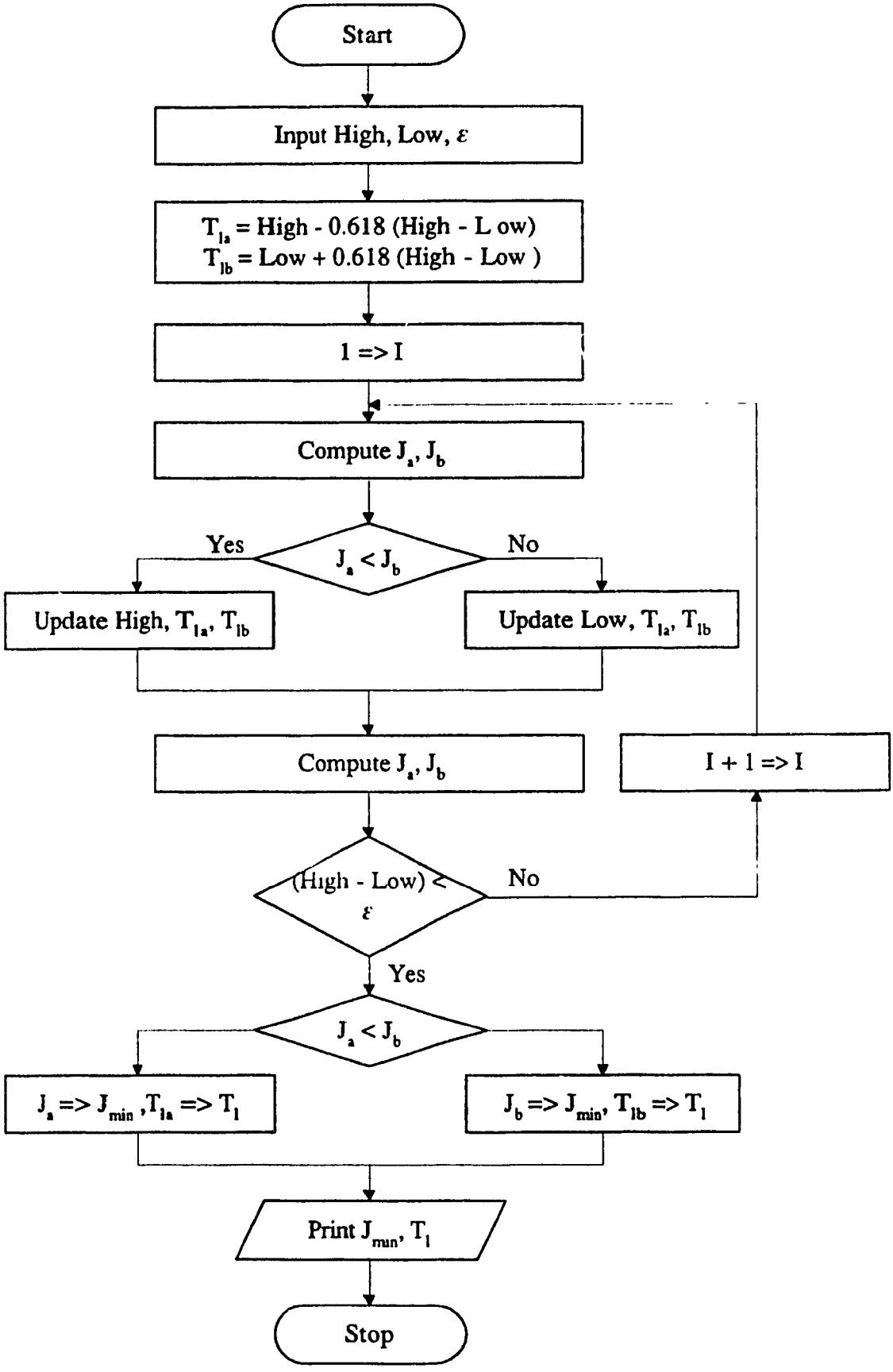

Figure 5.6 flow chart 01 the program for finding Jmin and Tl by "Gold section" method

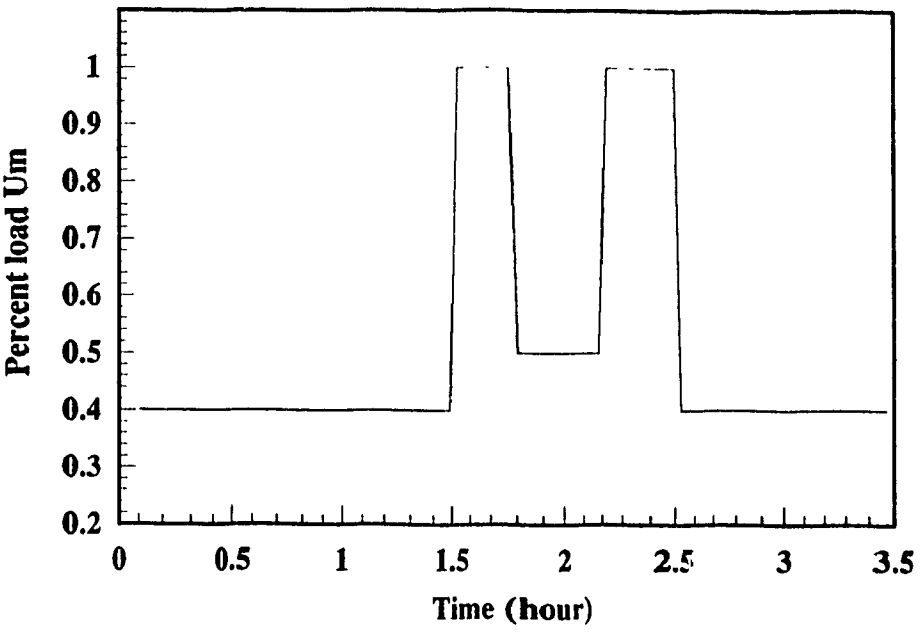

(a) Load profile2

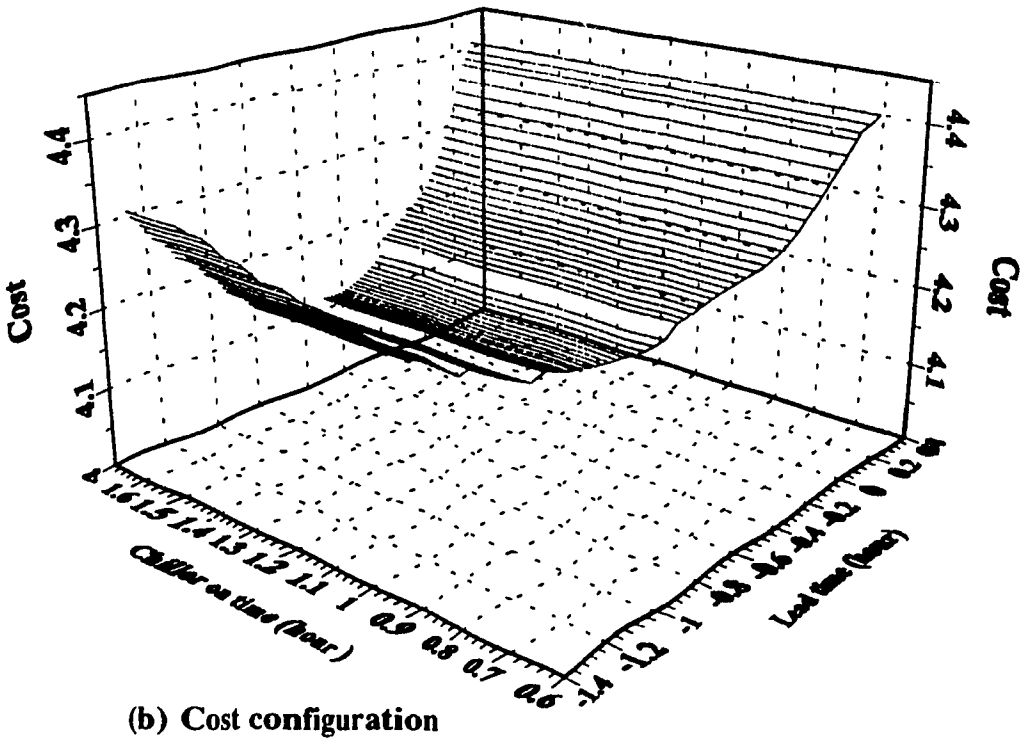

(b) Cost configuration

Figure 5.7 Chiller energy cost as function of lead time and on time for load profile2

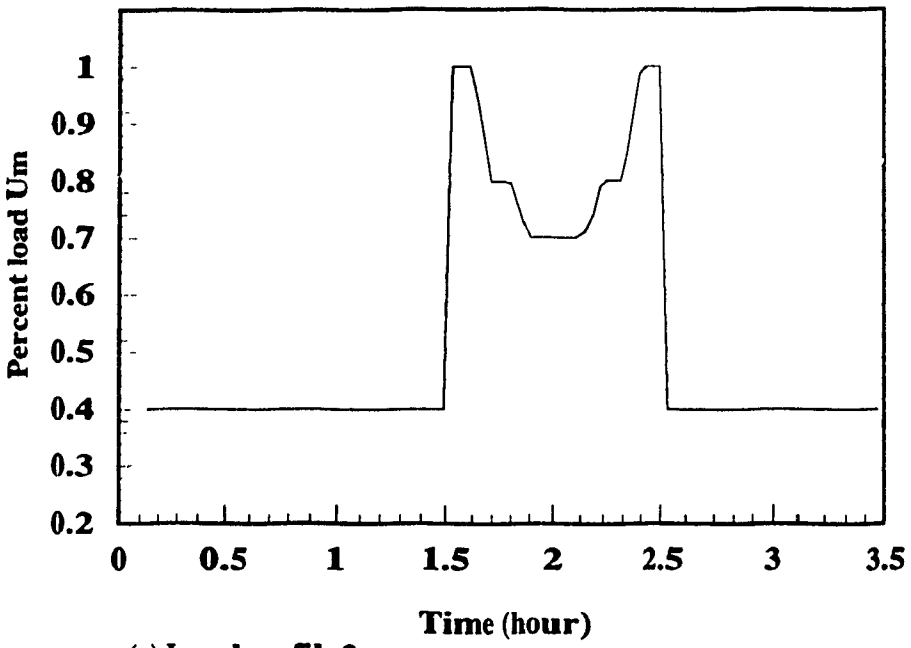

(a) Load profile3

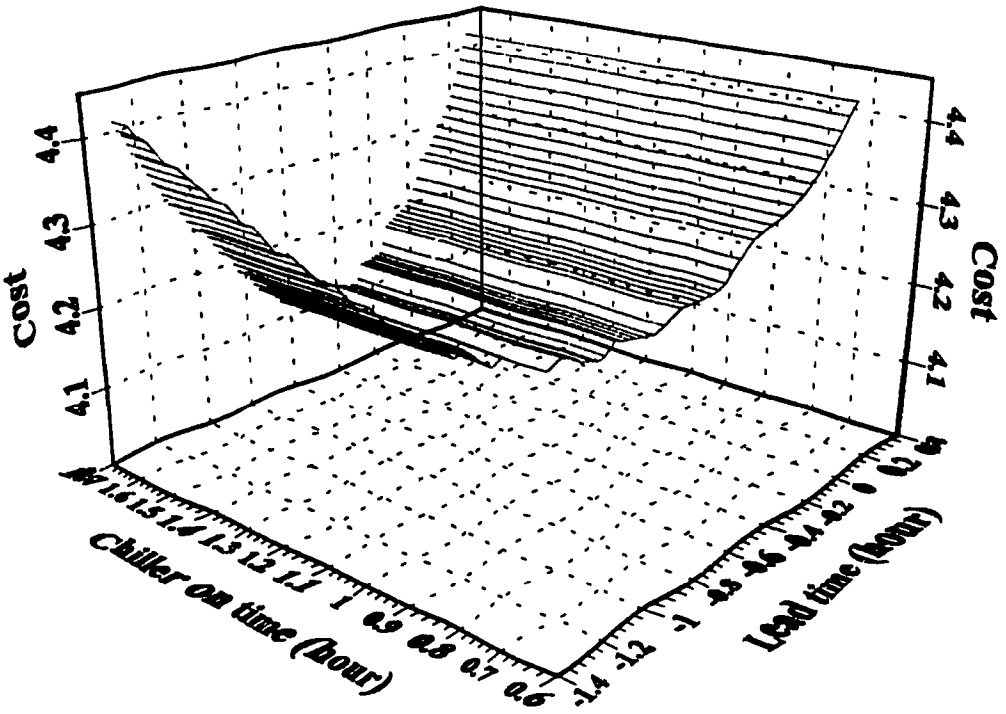

(b) Cost configuration

Figure 5.8 Chiller energy cost as function of lead time and on time for load profile3

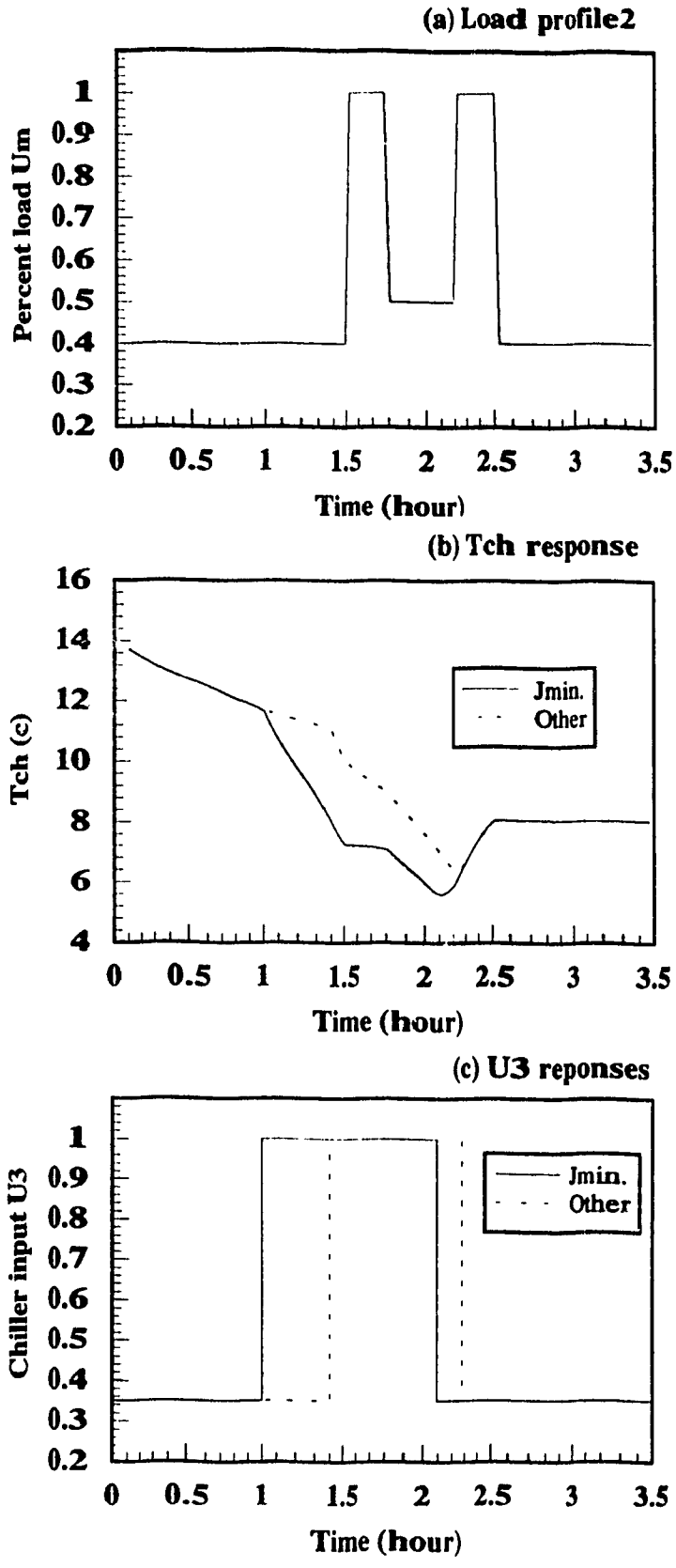

Figure 5.9 Comparsion of Tch and U3 responses between optimal (Jmin) and not optimal (other) case for load profile2

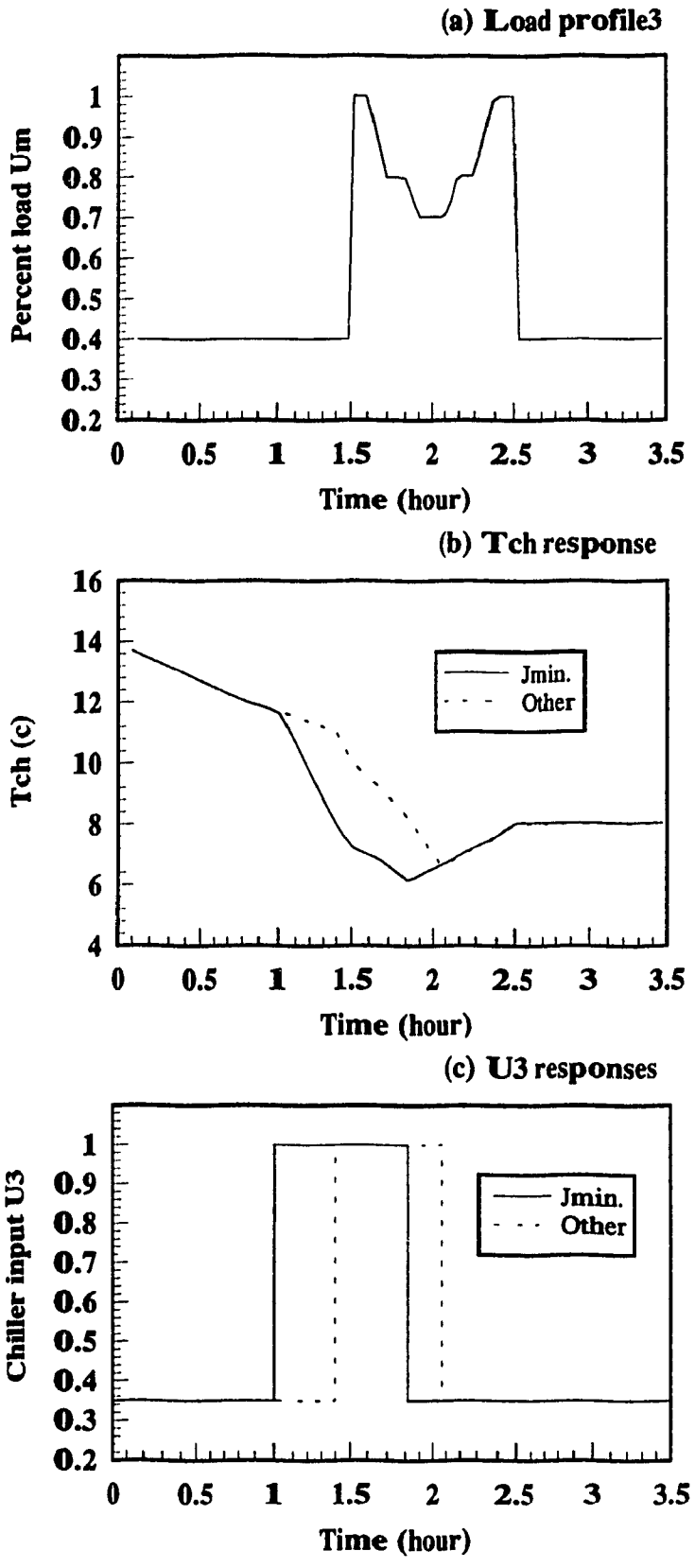

Figure 5.10 Comparsion of Tch and U3 responses between optimal (Jmin) and not optimal (other) case for load profile3

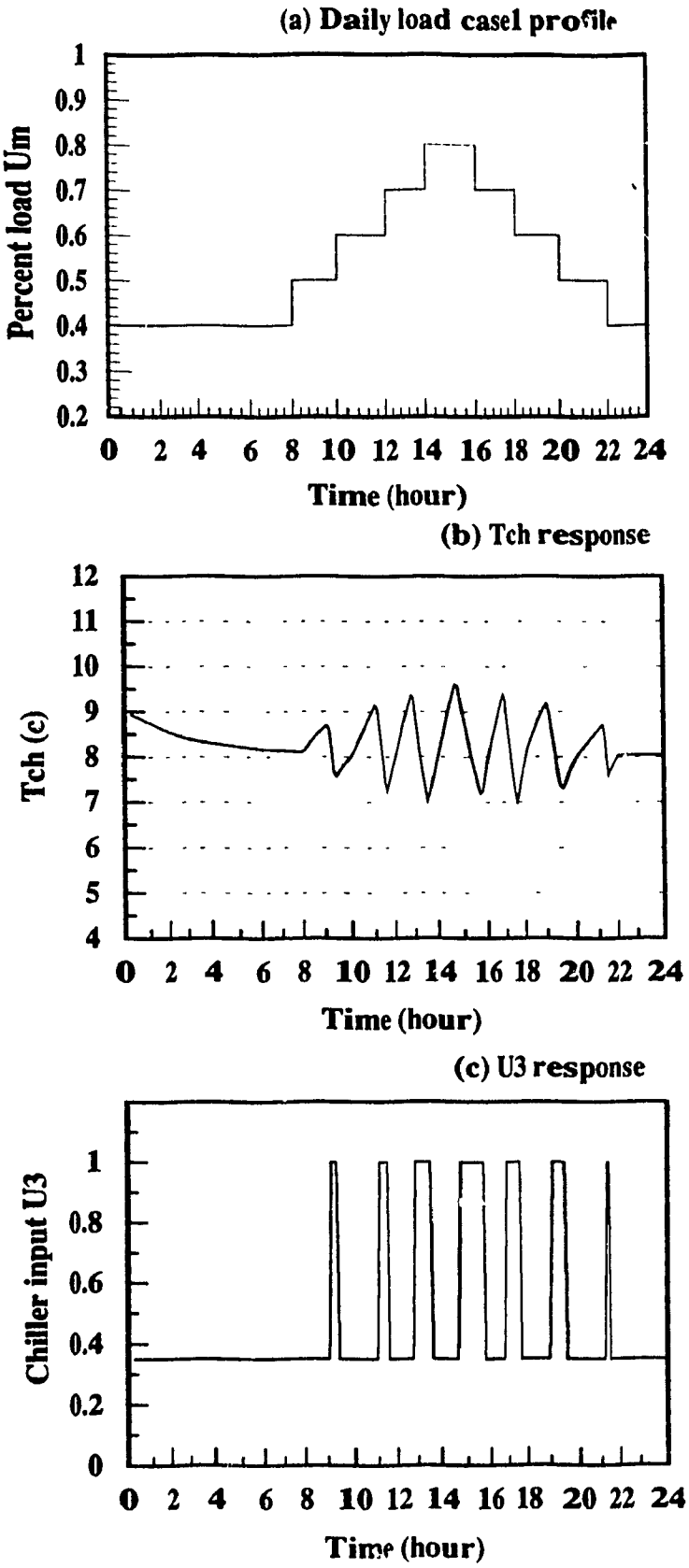

Figure 5.11 a,b,c Optimal unconstrained Tch and U3 responses

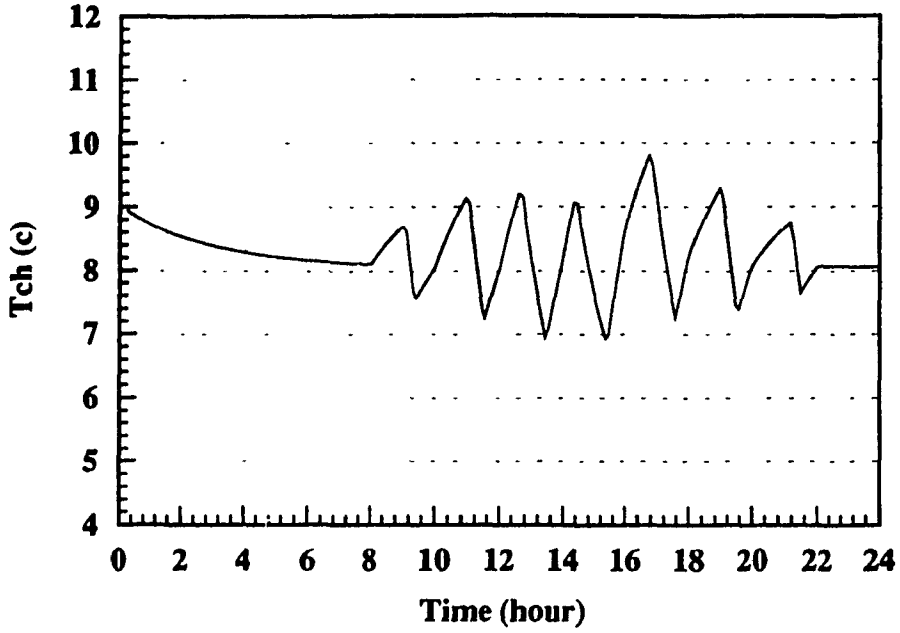

(d) Tch response

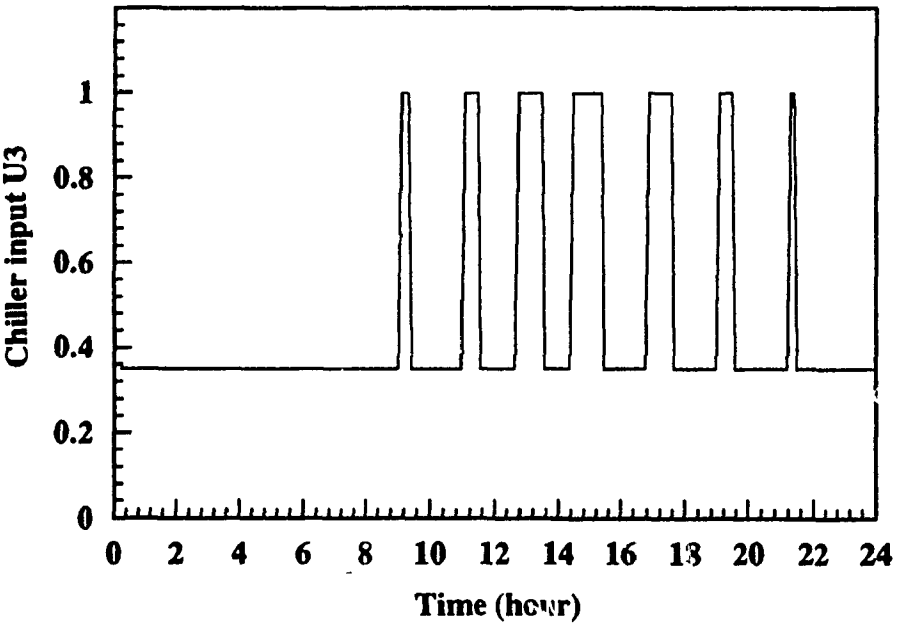

(e) U3 resopnse

Figure 5.11 d,e Optimal unconstrained Tch and U3 responses (first trial)

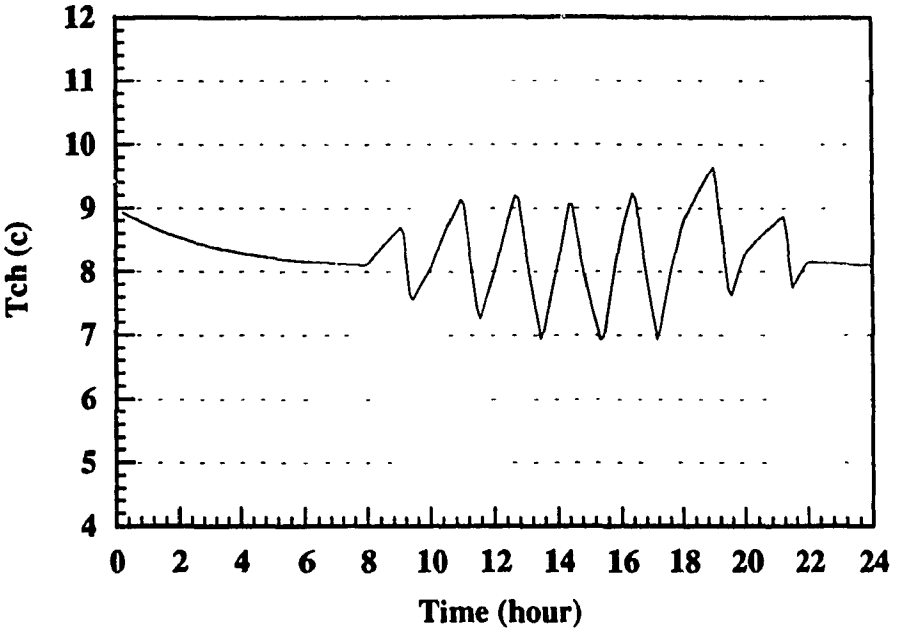

(f) Tch response

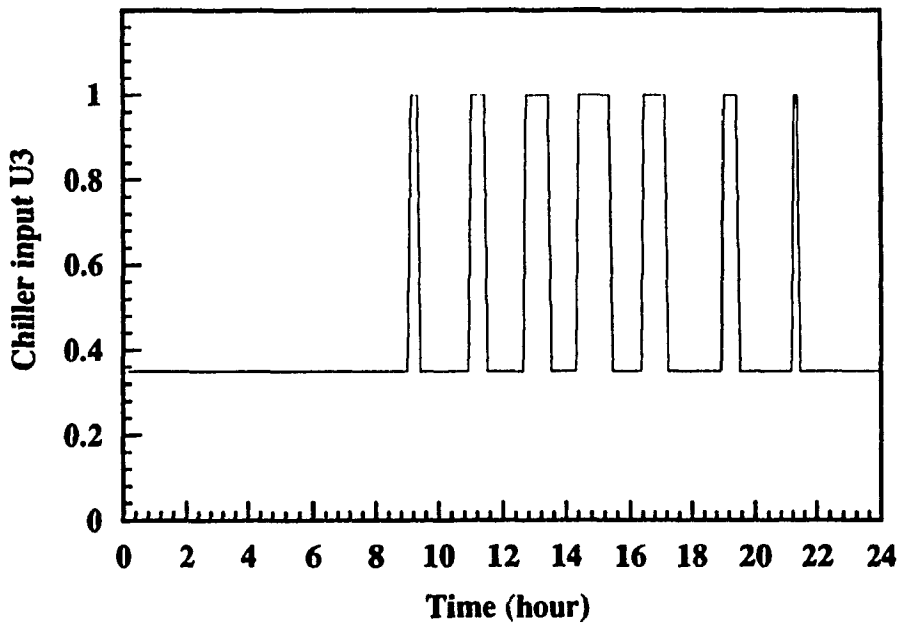

(g) U3 response

Figure 5.11 f,g Optimal unconstrained Tch and U3 responses (second trial)

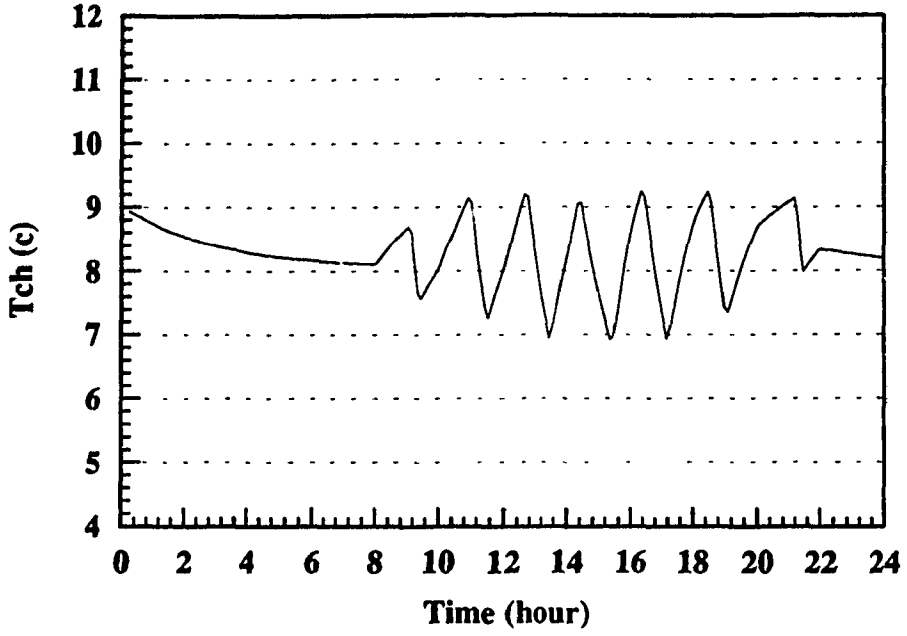

(i) Tch response

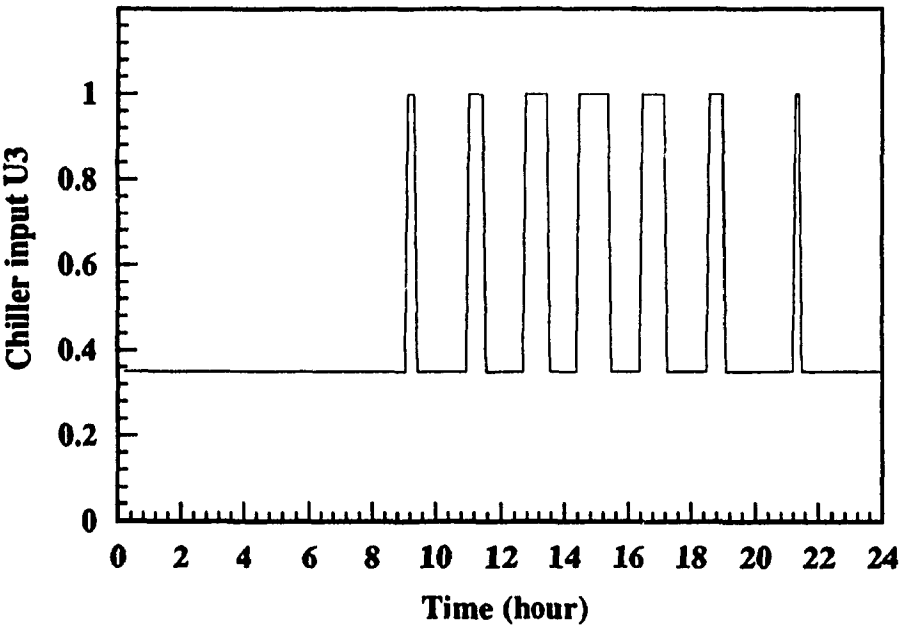

(h) U3 reponse

figure 5.11 h,i Optimal constrained Tch and U3 responses (third and final trial)

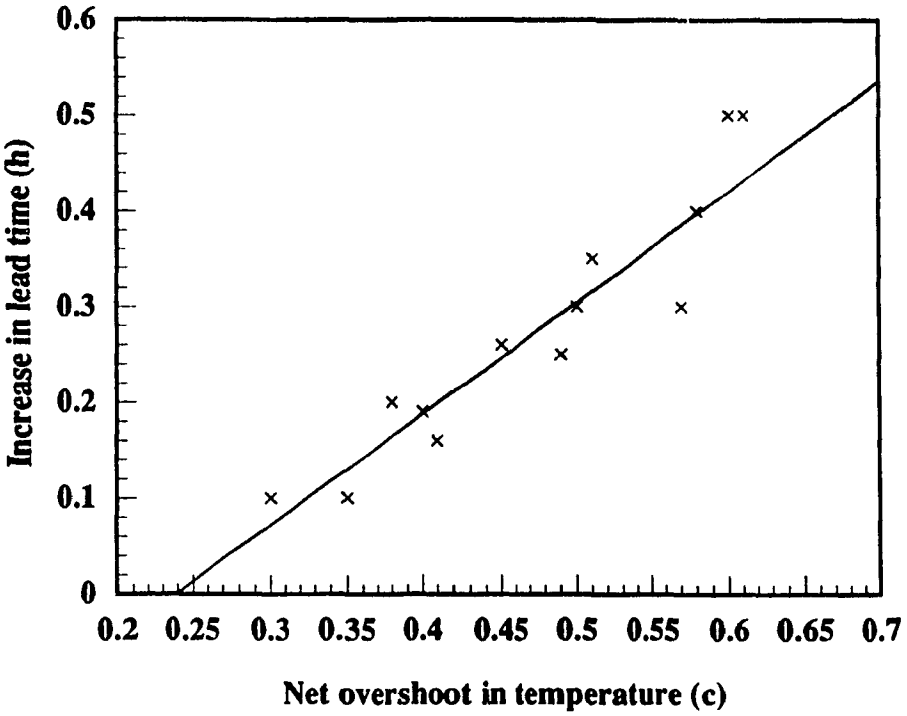

Figure 5.12 Lead time as a function of net overshoot in temperature

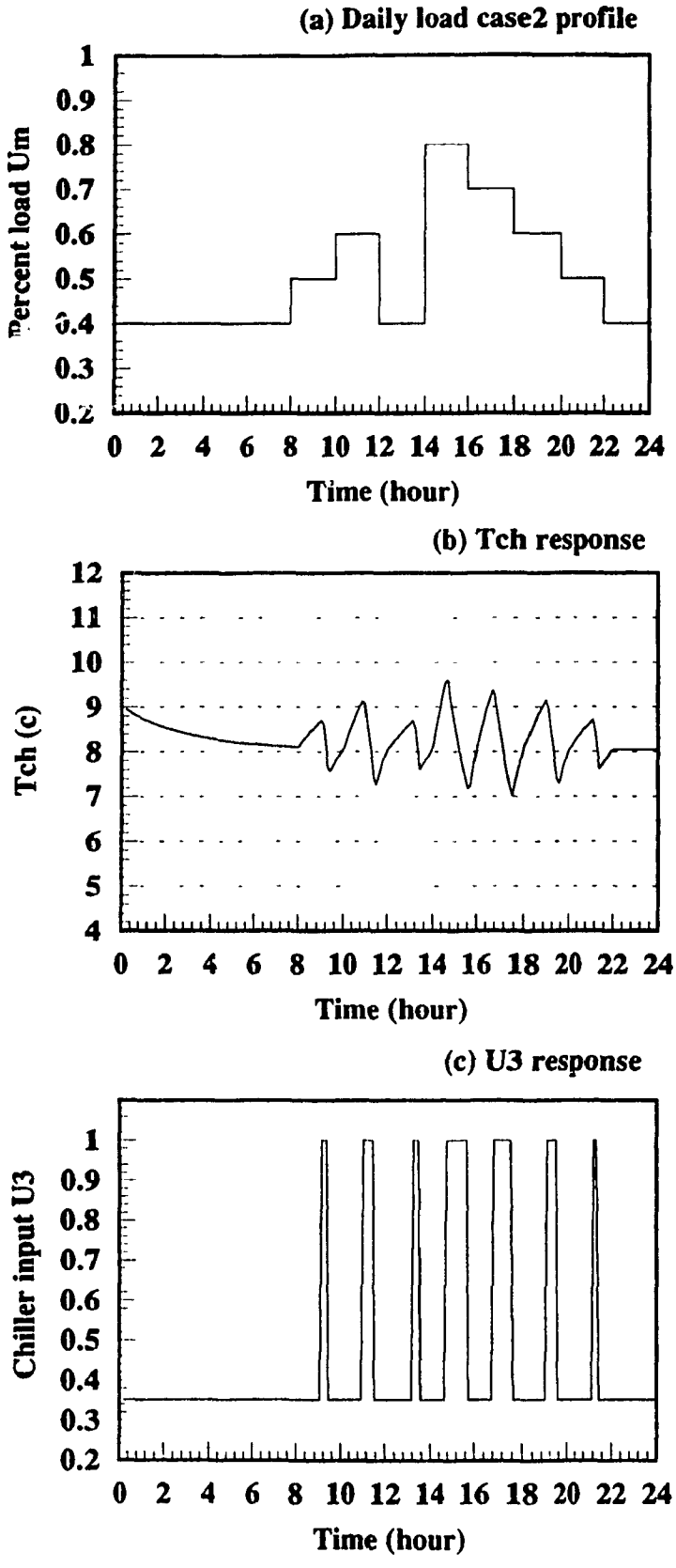

Figure 5.13 a,b,c Optimal unconstrained Tch and U3 responses

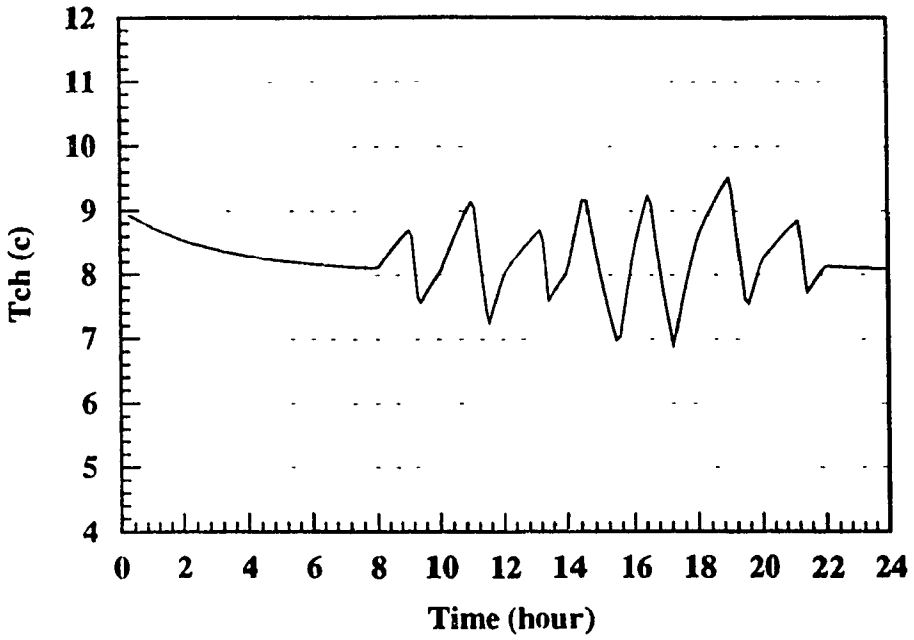

(d) Tch response

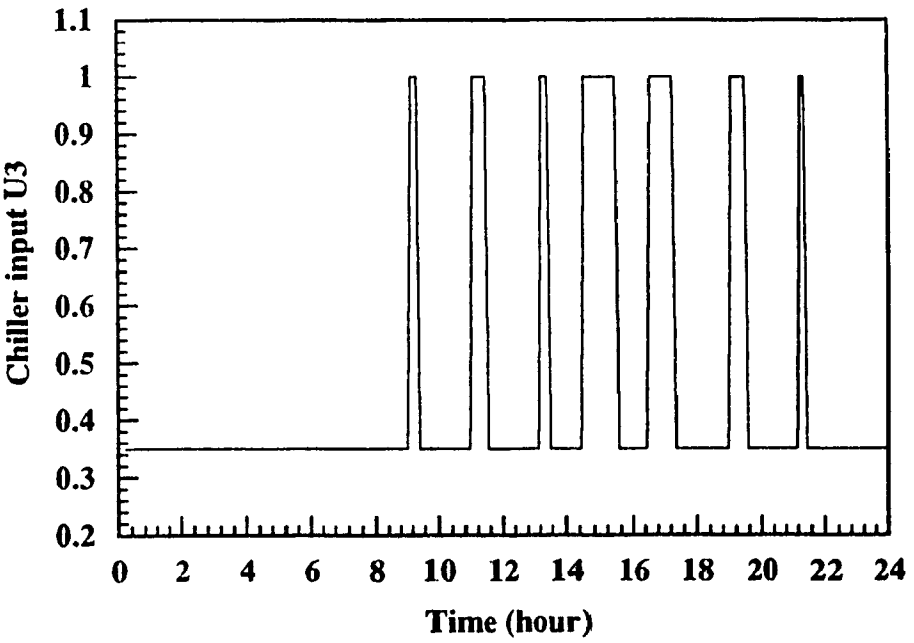

(e) U3 response

Figure 5.13 d,e Optimal unconstrained Tch and U3 responses (first trial using the results from Fig. 5.12)

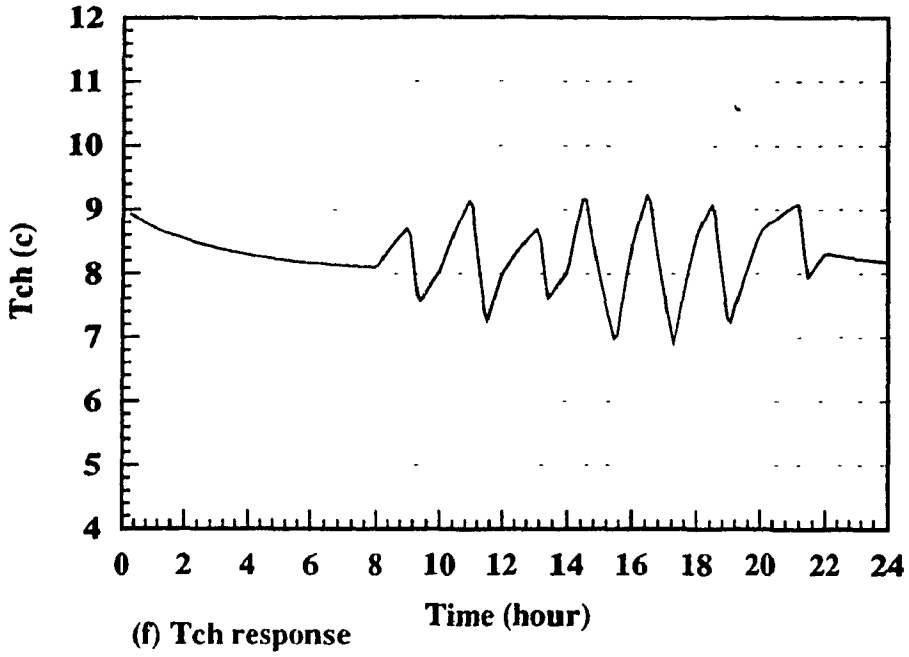

(f) Tch response

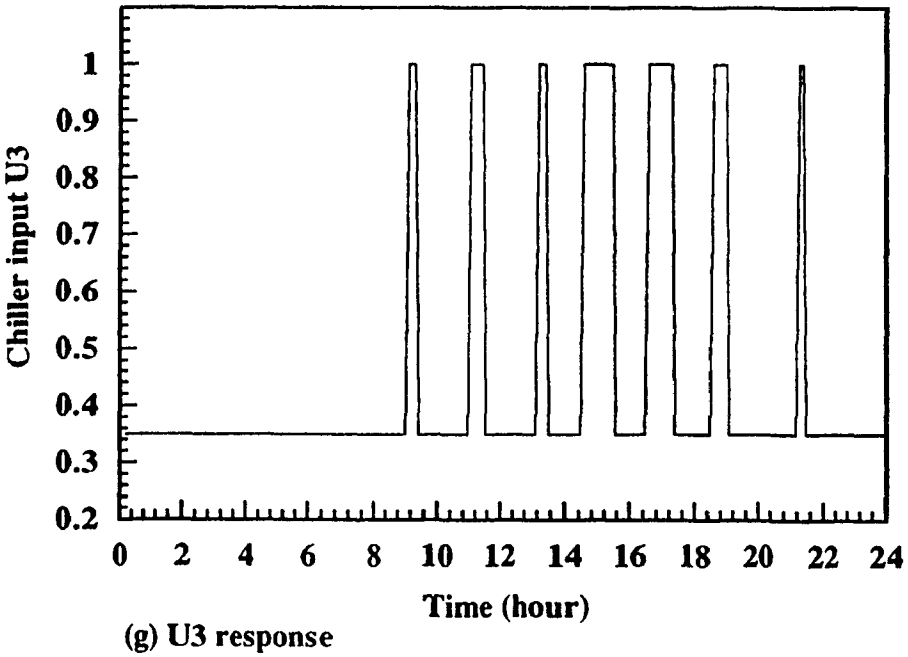

(g) U3 response

Figure 5.13 f,g Optimal unconstrained Tch and U3 responses (second and final trial using the results from Fig.12)

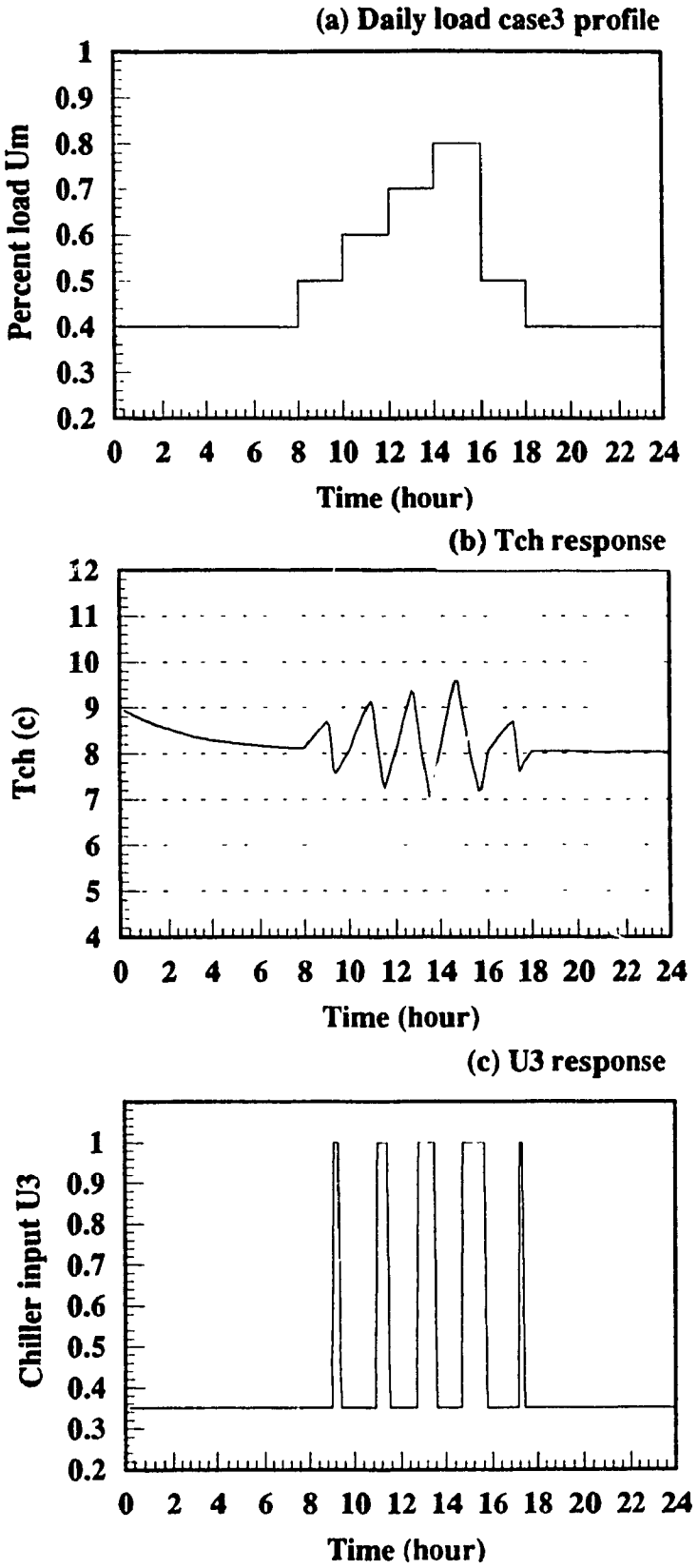

Figure 5.14 a,b,c Optimal unconstrained Tch and U3 responses

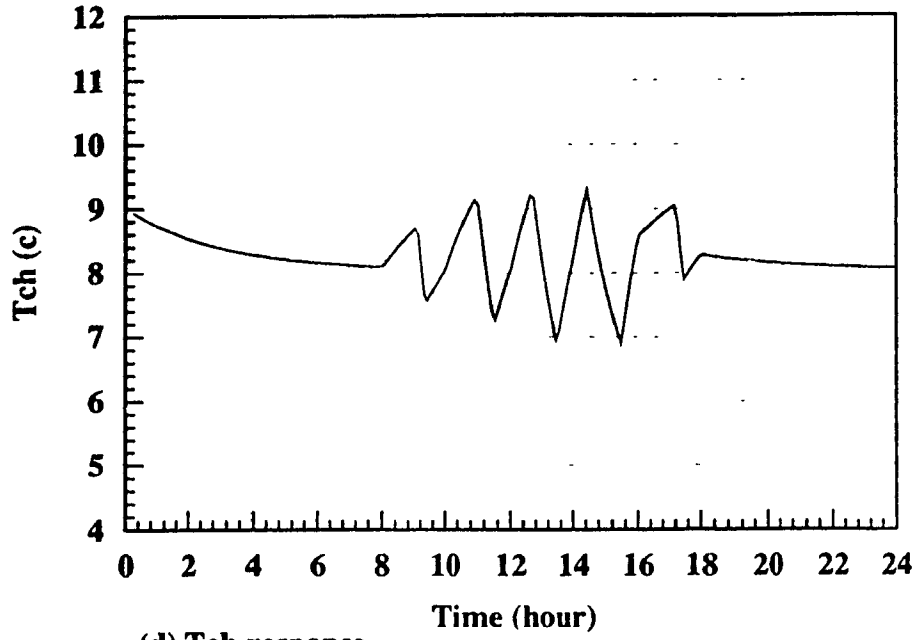

(d) Tch response

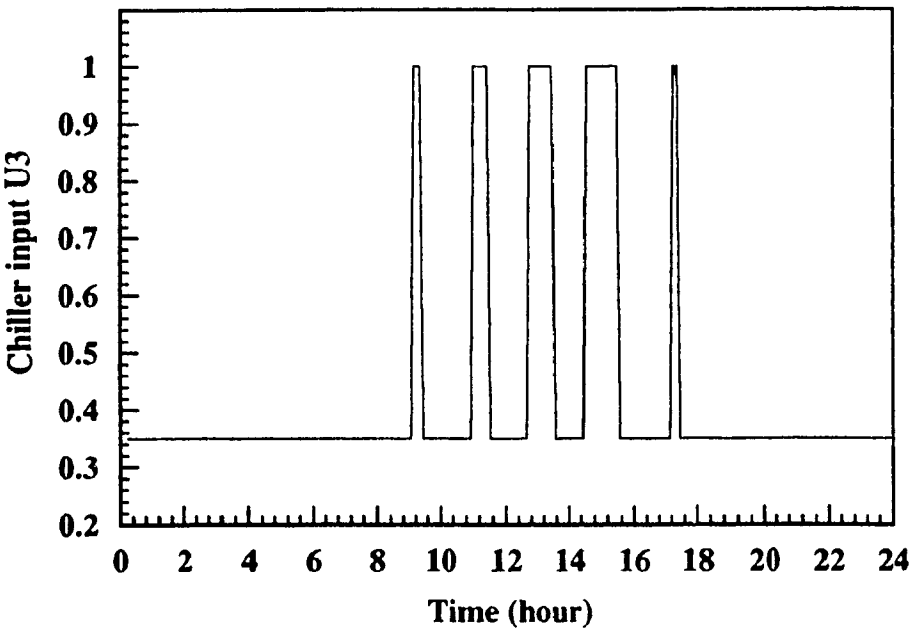

(e) U3 response

Figure 5.14 d,e Optimal unconstrained Tch and U3 responses (using the results from Fig. 5.12)

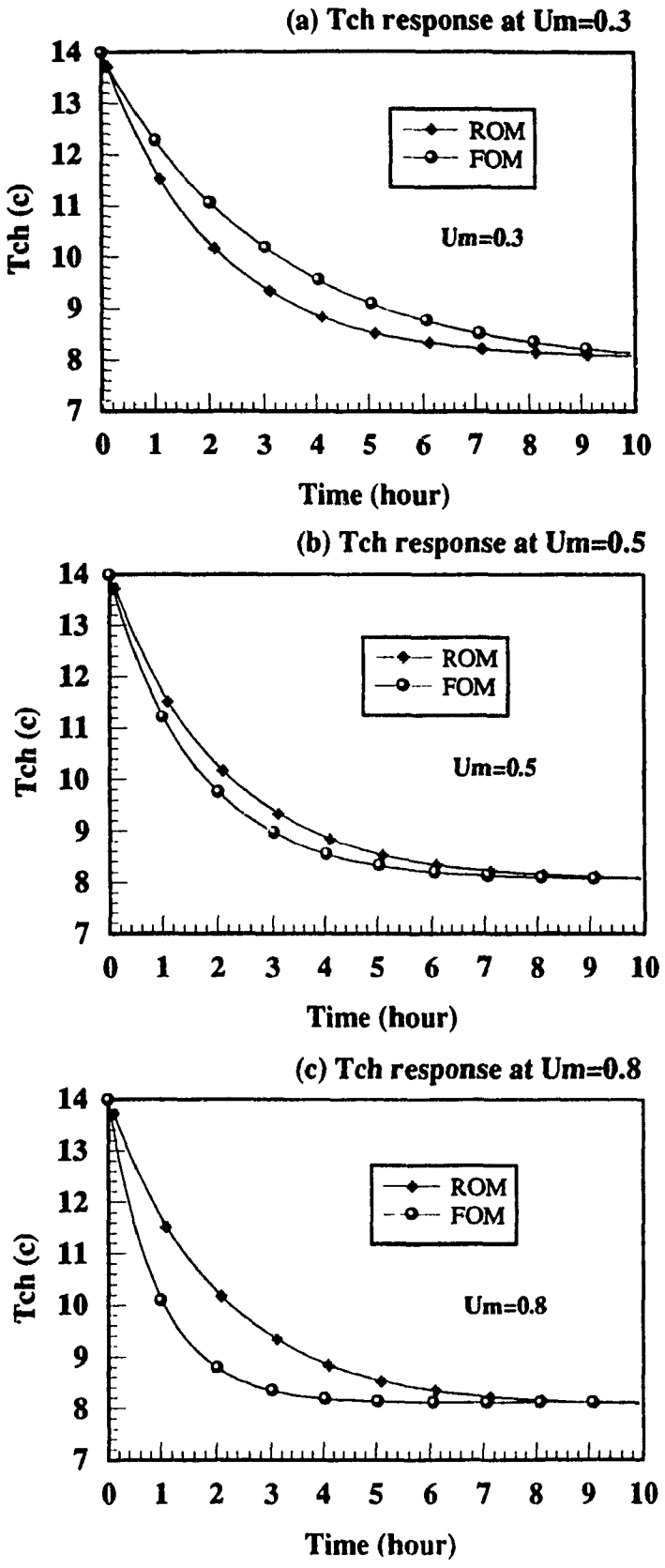

Figure 5.15 a,b,c Open loop responses of Tch for three load cases

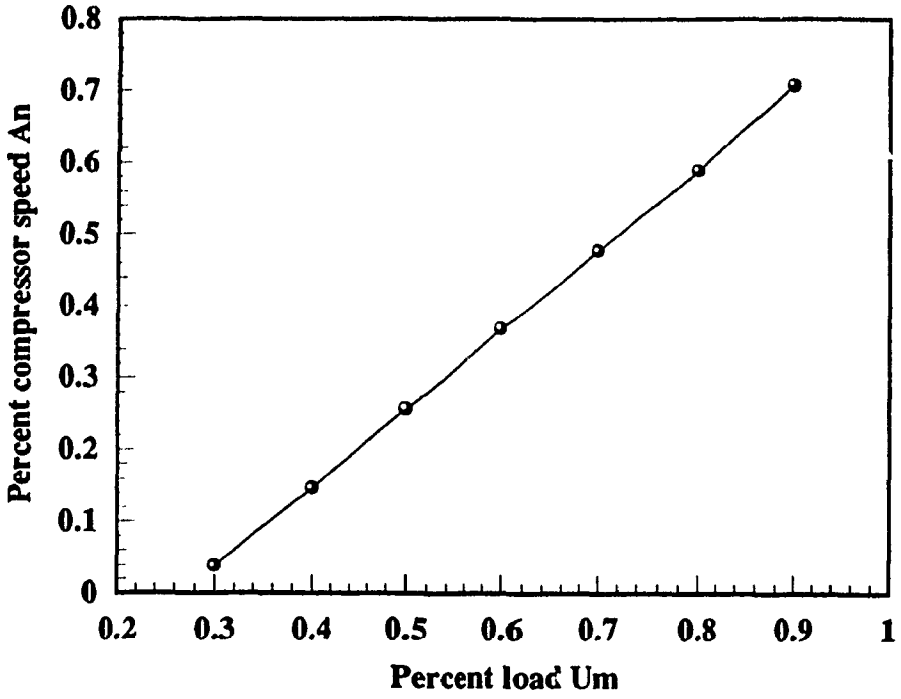

Figure 5.16 Steady-state optimal value of An as function of Um

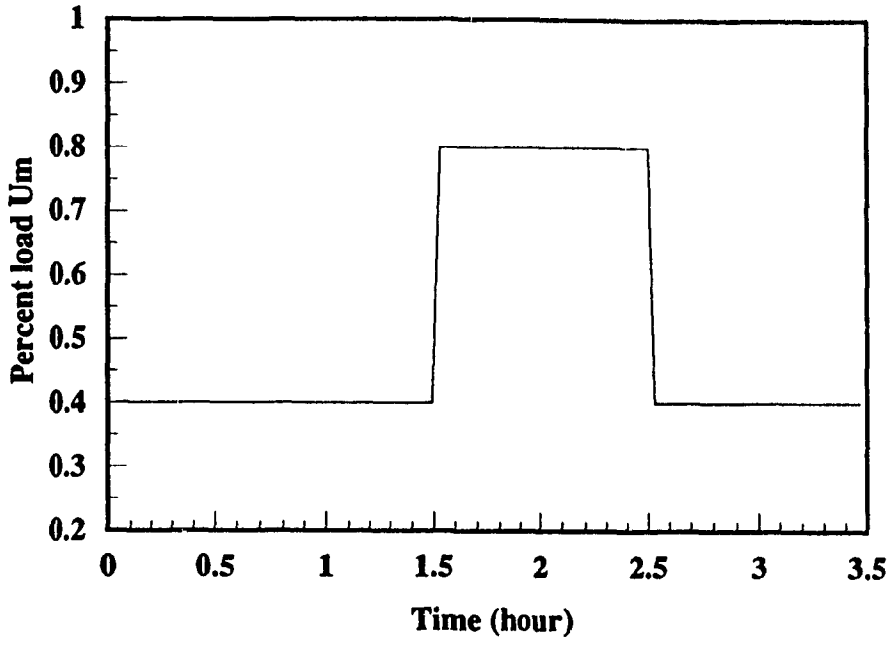

(a) Load profile1

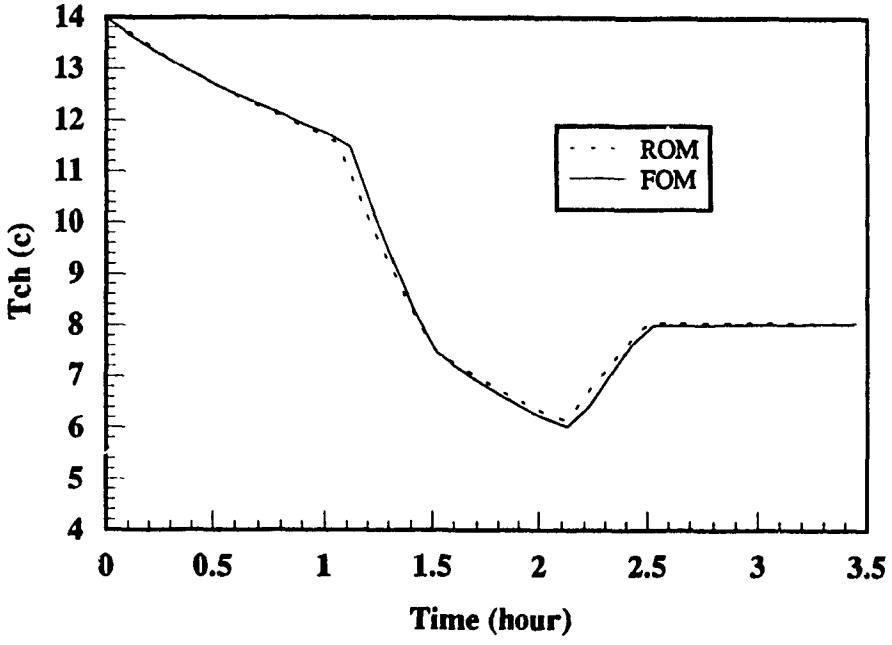

(b) Tch response

Figure 5.17 a,b Comparsion of Tch responses between two models for load profile1

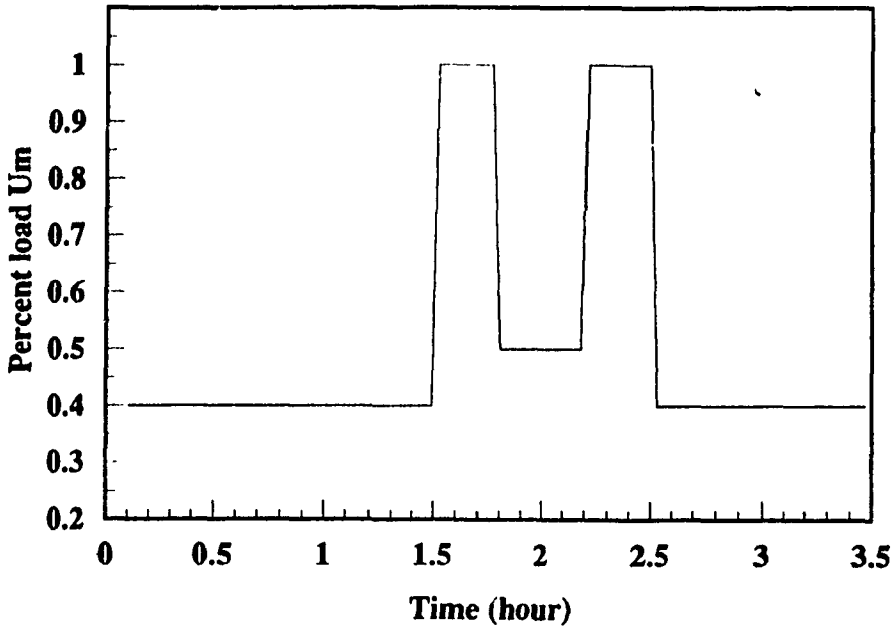

(a)Load profile2

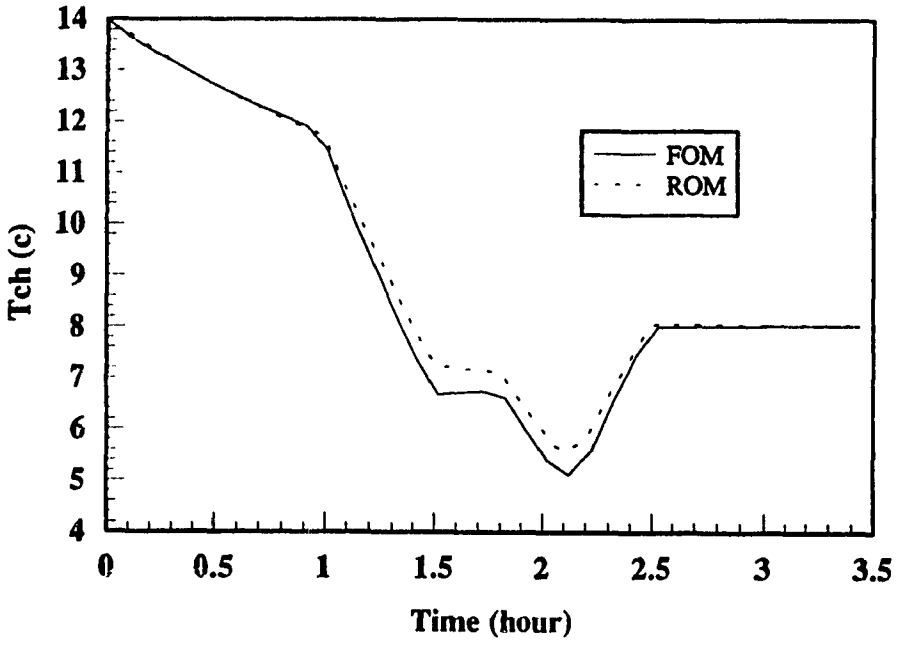

(b) Tch response

Figure 5.18 a,b Comparison of Tch responses between two models load profile2

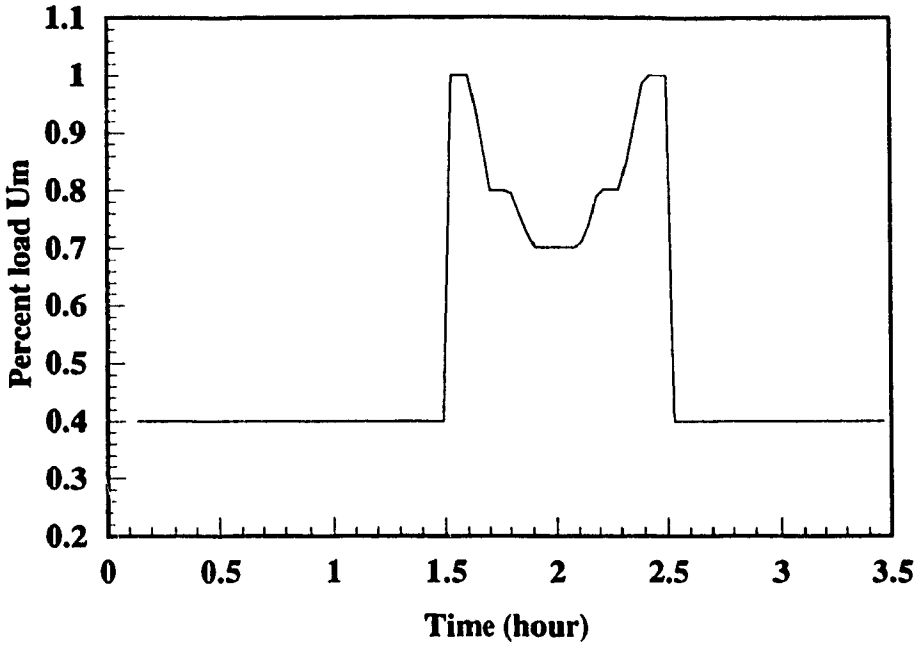

(a) Load profile3

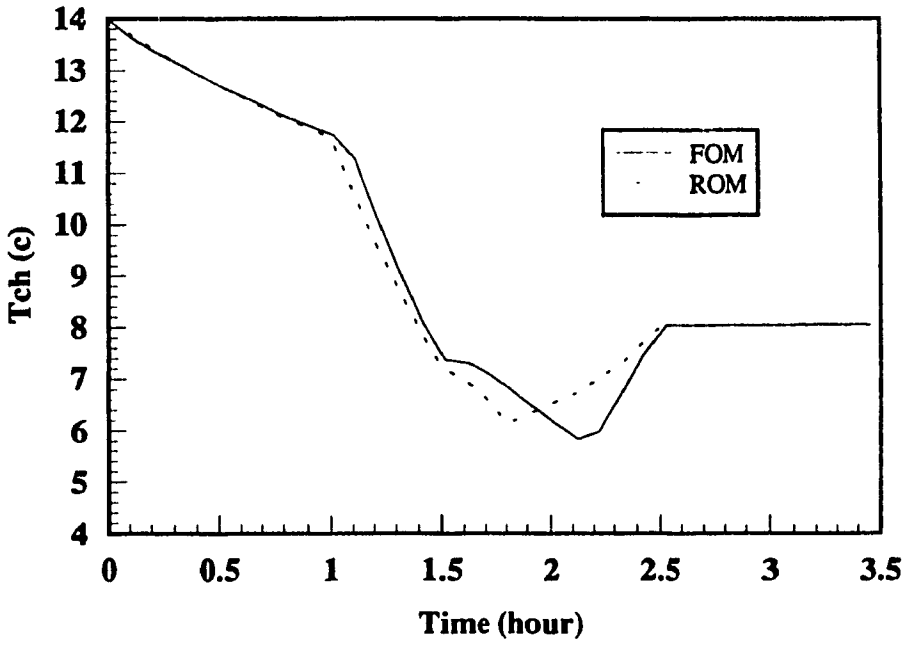

(b) Tch response

Figure 5.19 a,b Comparison of Tch responses between two models load profile3

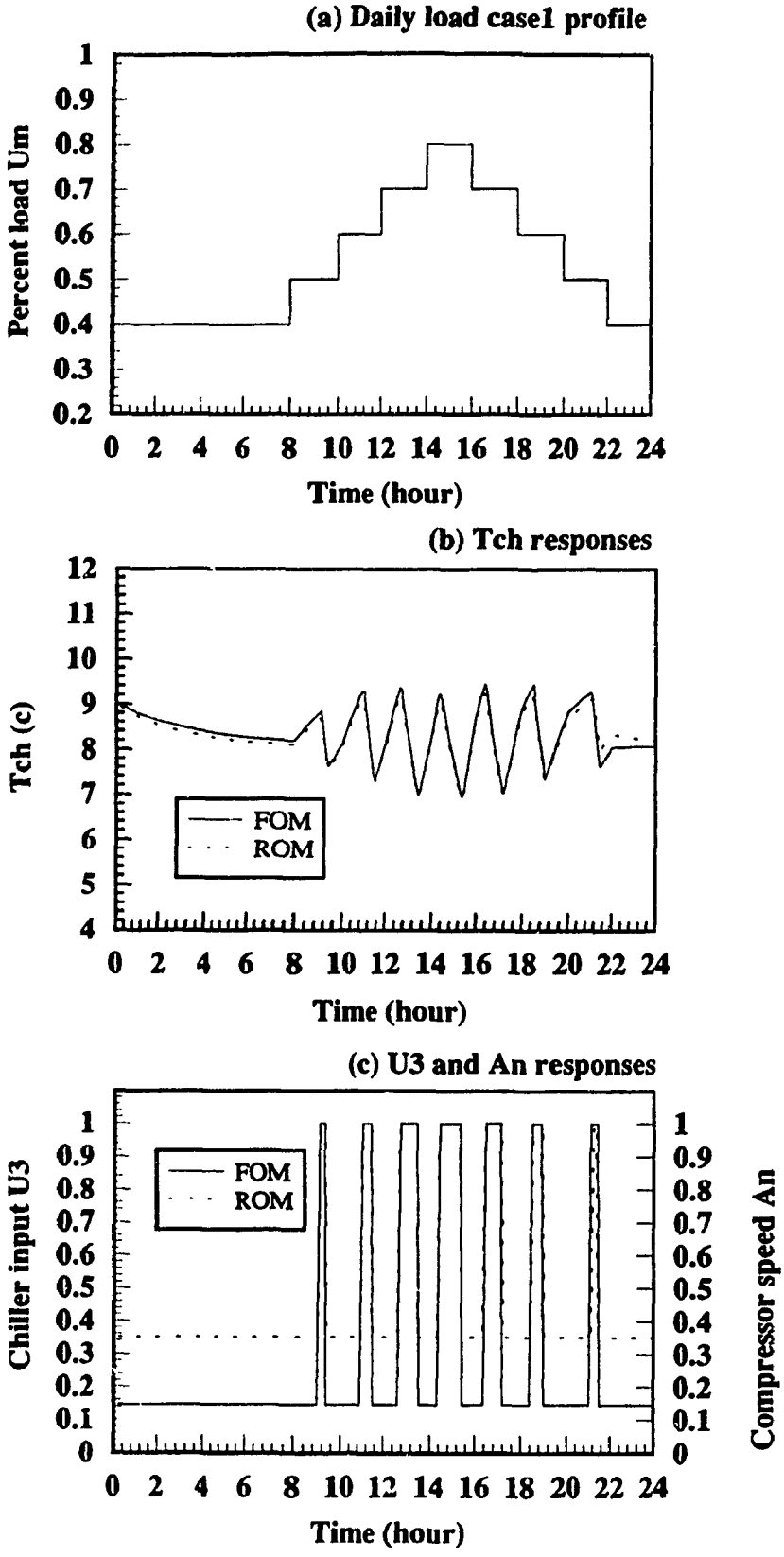

Figure 5.20 Comparsion of Tch and energy input respones of two models for daily load (case1)

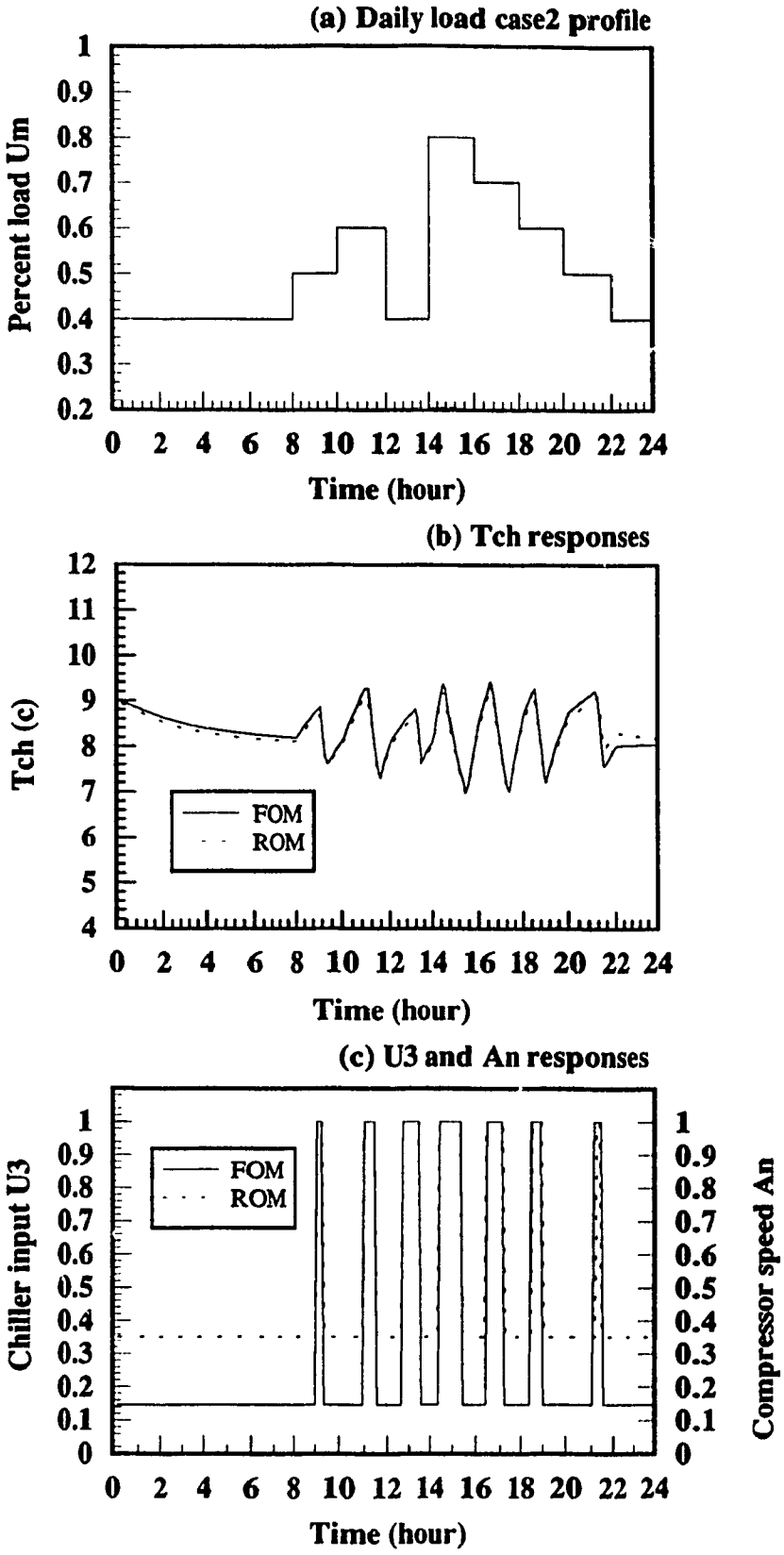

Figure 5.21 Comparison of Tch and energy input responses of two models for daily load (case2)

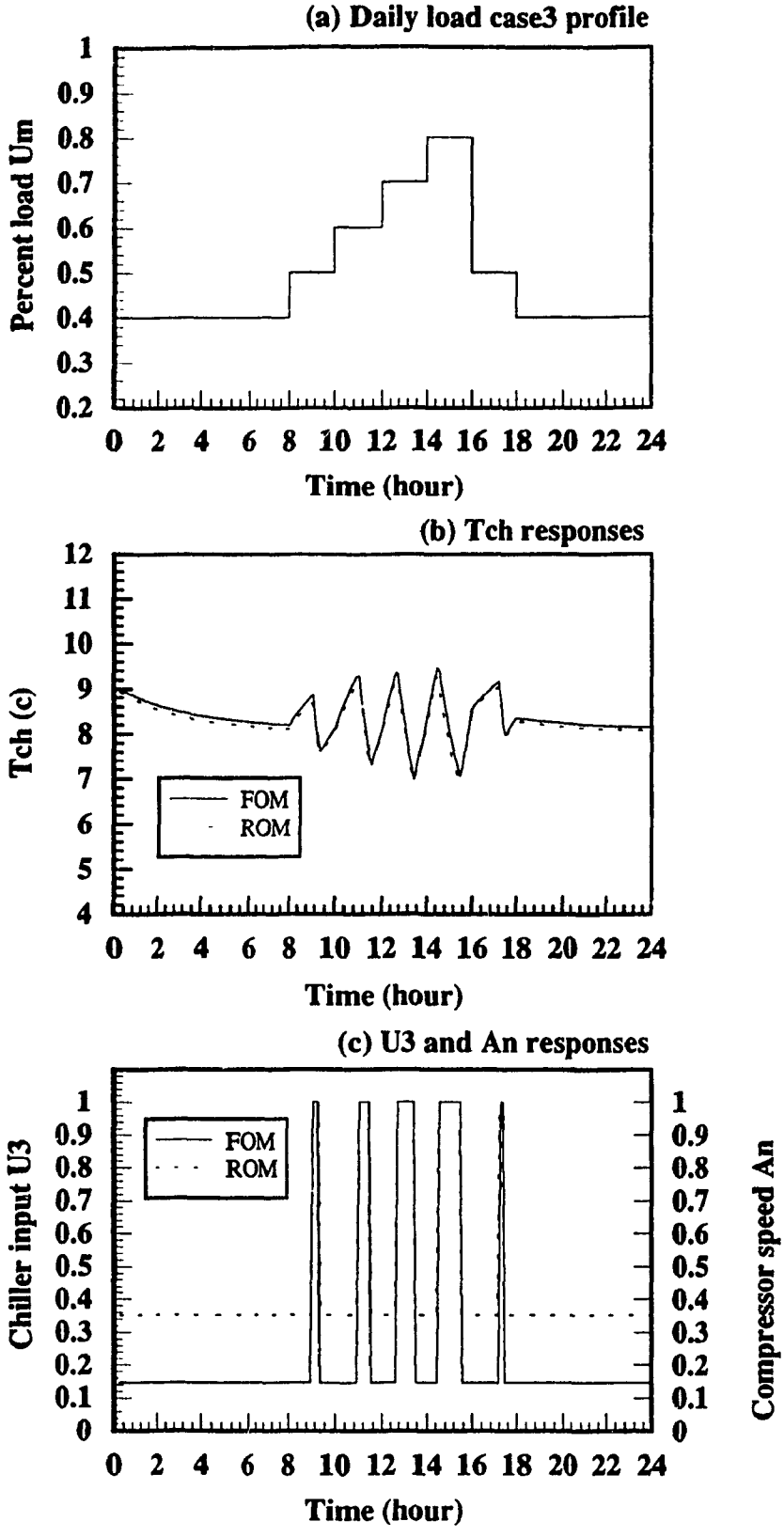

Figure 5.22 Comparsion of Tch and energy input responses for two models for daily load case3

CHAPTER 6

CONCLUSIONS

AND RECOMMENDATIONS

6.1 Conclusions

The main goal of this study was to formulate an analytical model of a chilled water cooling system that could predict transient response characteristics of the refrigeration system.

The chilled water cooling system model has been developed containing of a vapour compression refrigeration system (reciprocating compressor, a shell-and-tube condenser, a dry expansion evaporator), and evaporative cooler and a chilled water storage tank.

A computer program was developed based on the analytical model and it was run for different cases. The simulation results have shown that the model predicts the expected dynamic characteristics of the system for various operating conditions and it provides significant information and understanding about the system performance and stability. From the results, it can be summarized that:

1 The steady-state time of the system was found to be the order of 200s to 450s for the chosen range of load. It is relatively longer compare with other systems modeled in previous works, because of the storage tank.

2 The range of the COP obtained was from 3.5 to 4.9 as mass flow rate of the refrigerant varied from 0 to 100% of full value.

3 Results show that the degree of superheat at exit of evaporator is roughly proportional to the cooling load or (capacity of expansion valve).

4 The temperature of chilled water storage tank was effected significantly by the change of compressor motor speed and percent load.

5 A higher temperature of tube wall in evaporation region was observed because of

the consideration of two regions instead of only one.

6 Temperatures and all other property values of refrigerant in the critical point of the thermodynamic cycle were found to be in the reasonable range.

The development of a heuristic on-off control strategy based on a reduced-order system and its implementation on the chilled water cooling system has been studied. The results show that:

1 The heuristic on-off control strategy developed based on one dimensional searching method has shown to be "optimal" when the chiller system is operating under time varying load.

2 The daily chilled water temperature response indicate that the multiple application of the unconstrained optimal on-off control strategy with some fine tuning can give near optimal constrained solution.

3 The results of implementation of the heuristic on-off control profile on the full order model show that, for the short period load configurations the maximum chilled water temperature differences between full and reduced order model are 0.15, 0.5, and 0.3°C; for the daily load profiles the differences are 0.2, 0.18, and 0.1°C. Thus the on-off control technique can be successfully applied to control the speed of compressor motor AN.

The main contributions of this study is the development of an analytical model of the chilled water cooling system which is useful to study the effect of design changes in the system; the effect of changes in the component size; and the effect of changes in operating conditions. The analysis covers varied aspects of the entire system, such as the

physical phenomena inside the heat exchangers, including single and two phase conditions; the transient vapour and liquid mass flow of refrigerant throughout the operation; and the coefficient of the performance of the system. Another important contribution of this work is the development of a simple and yet optimal on-off control strategy for CWCS. The heuristic on-off control technique shows how to use a simple method to solve more complicated problems in terms of optimization & control.

6.2 Recommendations for future work

Based on the above study, the refinement of the model could be made by further investigation of empirical parameters, experimental results and more detailed theoretical analysis on each component of the system and the control analysis.

In order to improve the present study the following recommendations are made:

1 Improvement of the evaporator and condenser models. The model that is discussed in previous chapters were based on some simplifying assumptions which may not consider detailed physical phenomena that occur inside the heat exchangers in real practice. For example, in condenser model, only evaporation phase is assumed occupied, but the desuperheating and the subcooling phases have been neglected. Thus, more complicated derivation of the necessary equations will be required.

2 Modification of the compressor model. It is advisable to adapt the compressor model to a more practical one, by making the present model to a transient model.

3 Evaluation of heat transfer coefficients. It will be necessary to investigate the heat transfer coefficients for different phases in heat exchangers. The work could be

made by the experimental measurements.

4 Pressure drop calculations. The pressure drops of heat exchangers and refrigerant tubes could be considered to make the simulation more effective.

5 Improvement of evaporative cooler model. The evaporative cooler model could be formulated more detailed by considering it as numbers of small control volume instead of a lumped model.

6 Better techniques for searching optimal switching times for problems with multiple parameters have to be looked into.

REFERENCES

Allen, J.J., and Hamilton, J.F., 1983. "Steady-state reciprocating water chiller models." ASHRAE Transactions Vol. 89, Part 2A, pp. 398-407

Alves, G.E. "Concurrent liquid-gas flow in a pipe line contactor." Chemical Engineering Progress, 1954, Vol. 50, No. 9

Anderson, S.W., Rich, D.G., and Geary, D.F. "Evaporation of refrigerant 22 in a horizontal 3/4 Inch OD tube." ASHRAE Transactions 1966, Vol. 72, Part 1, pp. 22-36

ASHRAE, "1991 Application Handbook" American Society of Heating, Refrigerating and Air-conditioning Engineers, 39.1

Azer, N.Z., Abis, L.V., and Soliman, H.M. "Local heat transfer coefficients during annular flow condensation." ASHRAE Transaction 1972, Vol. 78, Part 2, pp. 135-144

Bae, S. "Refrigerant forced-convection condensation inside horizonal tubes." ASHRAE Transactions 1971, Vol.77, Part 2 pp. 104-115

Bonne, U., Patani, A., Jacobson, R., and Muller, P. "Electric-driven heat pump system: simulation and controls." ASHRAE Transactions LA-80-5 4 Los Angeles, Califomia (May 1980)

Braun, J.E., Klein, S.A., Beckman, W.A, and Mitchell, J.W. "Methodologies for optimal control of chilled water systems without storage." ASHRAE Transactions 1989, Vol. 95, Part 1, pp. 652-662

Braun, J.E., Klein, S.A., Mitchell, J.W., and Beckman, W.A. "Applications of optimal control to chilled water systems without storage." ASHRAE Transactions 1989, Vol. 95, Part 1 pp. 663-675

Braun, J.E., "A comparison of chiller-priority, storage-priority, and optimal control of an ice-storage system." ASHRAE Transactions 1992, Vol. 98, Part 1, pp. 893-902

Braun, J. E., Mitchell, J.W., Klein, S.A., and Beckman, W.A. "Performance and control characteristics of a large cooling system." ASHRAE Transactions 1987, Vol. 93, Part 2, pp. 1830-1852

Cascia, M.A. "Optimizing chiller plant energy savings using adaptive DDC algorithms." ASHRAE Transactions 1988, Vol. 94, Part 2, pp. 1937-1946

Cecchini, C. and Marchal, D. "A simulation model of refrigerating and air-conditioning

equipment based on experimental data." ASHRAE Transactions 1991, Vol. 97, Part 2. pp.388-393

Chi, J., 1979. "DEPAC - A computer model for design and performance analysis of central chillers." ASME paper No. 79-WA/HT-28

Chi, J., and Didion, D. 1982. "A simulation model of the transient performance of a heat pumps." International Journal of Refrigeration Vol. 5 No. 3, May. pp. 176-184

Clark, D.R., Hurley, H.W., and Hill, C.R. "Dynamic models for HVAC system components." ASHRAE Transactions 1985, Vol. 91, Part 1B, pp. 737-750

Dabiri, A.E. 1982. "A steady-state computer simulation model for air-to-air heat pumps." ASHRAE paper TO-82-8 No.3 p. 973-987

Daviri A.E., and Rice, C.K., "A compressor simulation model with corrections for the level of suction gas superheat." ASHRAE Transaction 1981, Vol. 87, Part 2, pp. 771-780

Dhar, M. 1978. "Transient analysis of refrigeration system." Ph.D. Thesis, Purdue University.

Dhar, M., and Soedel, W., 1979. "Transient anal[illegible]pour compression refrigeration system: Part 1 - mathematical model." X[illegible]al congress of refrigeration Proceedings Vol. 2

Domanski, D., and Didion, D., 1983 "C[illegible]g of the vapour compression system with constant flow area expansion d[illegible] Building Sciences Series 155

Dowing, R.C. "Refrigerant equations." ASHRAE Transactions 1974, Part 2, pp. 158-169

Ellison, R.D., and Creswick, F.A. 1978. "A computer simulation of stead-state performance of air-to-air heat pumps, ORNL/CON-16, OAK Ridge, TN: Oak Ridge Natl. Lab.

Fischer, S.K., and Rice, C.K., 1980. "A steady-state computer design model for air-to-air heat pumps." Oak Ridge National Laboratory ORNL/CON-80

Flower, J.E. 1978. "Analytical modelling of heat pump units as design aid and for performance prediction, UCRI-52618, Livermore, CA: Lawrence Livermore Lab.

Freeman, T.L., Beckman, W.A., Mitchell, J.W., and Duffie, J.A. 1975. "Computer modelling of heat pumps and the simulation of solar-heat pump systems." ASME paper 75-WA/Sol-3, New York, American Society of Mechanical Engineers

Gear, C.W. "Numerical initial value problems in ordinary differential equations." 1971 Prentice-Hall

Goh, P.A. 1990, "Modelling and control of a variable air volume (VAV) system." Master's thesis, Centre for Building Studies, Concordia University

Gupta, V.K., and Prasad, M. 1983. "Optimum thermodynamic performance of three-stage refrigerating system." International Journal of Refrigeration Vol. 6 No. 2 March, pp. 103-107

Hamilton, J.F., and miller, J.L. "A simulation program for modelling an air-conditioning systems." ASHRAE Transactions 1990, Vol. 96, Part 1, pp. 213-221

Hiller, C.C., and Glicksman, L.R. 1976. "Improving heat pump performance via compressor capacity control-analysis and tests." MIT-EL-76-002

Holman, J.P. "Heat transfer" 6th Edition, p. 498, McGraw-Hill Book Company, 1986

Hwang, B.C., Wu, C., Jackson, W.L., and Chen, F.C. 1986. "Modelling and simulation of a naval shipboard heat pump." International Journal of Modelling and Simulation, June

Jackson, W.L, Chen, F.C., and Hwang, B.C. "The simulation and performance of a centrifugal chiller." ASHRAE Transactions 1987, Vol. 93, Part 2, pp. 1751-1761

Johnson, G.A. "Optimization Techniques for a centrifugal chiller plant using a programmable
controller." ASHRAE Transactions 1985, Vol. 91, Part 1, pp. 835-847

Katsounes, G.T., and Erth, R.A. "Computer calculations of the thermodynamic properties of refrigerants 12, 22, and 502." ASHRAE Transactions 1971, Vol. 77, Part 2, p. 88

Kirshenbaun, M. "Chilled-water production in ice-based thermal storage systems."ASHRAE Transactions 1991, Vol. 97, Part 2, pp. 422-427

Krakowm K.I., and Lin, S. "A computer model for the simulation of multiple source heat pump performance." ASHRAE Transactions 1983, Vol. 89 Part 2A pp. 590-600

Krakow, K.I., and Lin, S. "A multiple (solar, air, and water) source heat pump for cold climates." ASHRAE Transactions 1983, Vol. 89, Part 2 pp. 574-581

Krakow, K.I., and Lin, S. "A numerical model of heat pumps having various means of refrigerant flow control and capacity control." ASHRAE Transactions 1987, Vol. 93, Part 2, pp. 574-510

Kuehl, S.J., and Goldschmidt, V.W., "Transient response of fixed area expansion devices." ASHRAE Transactions 1990, Vol. 96, Part 1, pp. 743-750

Kuehl, S.J., and Goldschmidt, V.M. "Modelling of steady flows of R-22 through capillary tubes."
ASHRAE Transactions Vol. 97, Part 1, pp. 139-148

Li, R.Y., Lin, S., and Chen, Z.H. "Numerical modelling of thermodynamic nonequilibrium flow of refrigerant through capillary tubes." ASHRAE Transactions 1990, Vol. 96, Part 1, pp. 542-549

Lau, A.S., Beckman, W.A., and Mitchell, J.W., "Development of computerized control strategies for a large chilled water plant." ASHRAE Transactions 1985, Vol. 91 Part 1B, pp. 766-780

Lee, W., Bonner, S.A., and Leonard, R.G. 1971. "Dynamic analysis and simulation of a gas regulator." Proceeding international Symposium of flow, Its measurement and Control, ISA, Pittsburgh, Pennsylvania, May

London, A.L., Kays, M.W., and Jonson, "Heat transfer and flow friction characteristics of some compact heat exchanger surfaces, Part 3 design data for five surfaces." ASME Transactions 1952, Vol. 74, p. 1167

Macarthur, J.W. 1984. "Transient heat pump behaviour: A theoretical investigation." International Journal of Refrigeration Vol. 7, No. 2 March, pp. 123-132

Martain, J.J. "Correlations and equations used in calculating thermodynamic properties of 'Freon' refrigerants." Thermodynamic and Transport Properties of Gases, Liquids, and Solids, pp. 110-122 ASME, New York City, 1959

McHarnes, R.C., Eiseman, B.J., and Martin, J.J. "Thermodynamic properties of 'Freon' refrigerants - I 'Freon' 12." Refrigeration Engineering 1955, Vol. 63, p. 31

Mitchell, J. "Analysis of energy use and control characteristics of a large variable speed drive chiller system." ASHRAE Journal January 1988, pp. 33-34

Oliver, P.P., Sepsy, C.F., and Jones, C.D., 1973. "A thermodynamic computer simulation of an air-to-air heat pump system for a commercial building." NSF-RA-N-73-375, National science Foundation, November

Pate, M.B., and Tree, D.R., "An analysis of choked flow conditions in a capillary tube-suction line heat exchanger ASHRAE Transactions 1987, Vol. 93, Part 1, pp. 368-380

Rawlings, L. "Strategies to optimize ice storage." ASHRAE Journal May 1985, pp. 39-48

Sami, S.M., Duong, T.N., Mercadia, Y., and Galanis, N. "Prediction of the transient response of heat pumps." ASHRAE Transactions 1978, Vol. 93, Part 2, pp. 471-490

Sami, S.M., and Duong, T. 1986. "Development of DAHP; transient computer program to
simulate heat pump performance." T.R. MEC/86/7

Sami, S.M., Mercadier, Y., Galanis, N., and Duong, T. 1986. "Heat pumps: review of analytical and experimental methods." T.R. MEC/85/7

Saraf, G.R., and Dhar, P.L. "Simulation of a shill-and-tube condenser." Simulation, March 1979, p. 83

Simmonds, P. "A control strategy for chilled water production." ASHRAE Journal January 1994 pp. 30-36

Spethmann, D.H. "Optimized control of multiple chillers." ASHRAE Transactions 1985, Vol. 91, Part 2B, pp. 848-856

Spethmann, D.H. "Optimal control for cool storage." ASHRAE Transactions 1989, Vol. 95, Part 1, pp. 1189-1193

Spethmann, D.H. "Application considerations in optimal control of cool storage." ASHRAE Transactions 1993, Vol. 99, Part 1, pp. 1009-1015

Spethmann, D.H. "Optimized control of multiple chillers." ASHRAE Transactions 1985, Vol. 91,
Part 2B pp. 848-856

Tanaka, N., Ikenchi, M., and Yamanaka, G. "Experimental study on the dynamic characteristics of a heat pump." ASHRAE Transactions 1982, Vol. 88, Part 2 pp. 323-331

Tobias, J.R. "Dynamic simulation of a direct expansion vapour compression air conditioning system." Proc. Piltsburgh conference on Modelling and Simulation, April 1973, pp. 430-434

Traviss, D.P. "Flow regimes in horizontal two-phase flow with condensation." ASHRAE Transactions 1973, Vol. 97, Part 2, pp. 31-39

Utesch, A.L. "Direct digital control of a large centrifugal chiller." ASHRAE Transactions 1990, Vol. 96, Part 2, pp. 797-799

Wang, Y.T., and Willson, D.R. "Heat pump control." IEE Proceedings Vol. 130, Part D, No. 6, November 1983, PP. 328-332

Williams, V.A. "Optimization of chiller plant's energy consumption utilizing a central EMCS and DDC." ASHRAE Transactions 1985, Vol. 91, Part 2B, pp. 857-861

Wong, S.P.W., and Wang, S.K., "System simulation of the performance of a centrifugal chiller using a shill-and-tube type water-cooled condenser and R-11 as refrigerant." ASHRAE Transactions 1989, Vol. 95, Part 1 pp. 445-454

Yasuda, H., and Touber, S., 1982. "Simulation model of a vapour compression refrigeration system." Laboratory for Refrigerating Engineering and Air Conditioning Rept. No. WTHD 133

Yasuda, H., and Touber, S., "Simulation model of a vapour compression refrigeration system." ASHRAE Transactions 1983, Vol. 89, Part 2A, pp. 408-425

Young, D.J. "Development of a northern climate residential air source heat pump." ASHARE Transactions 1980, Vol. 86, Part 1 pp. 671-686

Zaheer-uddin, M., and Wang, J.C.Y. 1992. "Start-stop control strategies for heat recovery in multi-zone water-loop heat pump systems." Heat Recovery Systems & CHP Vol.12 No.4

Zaheer-uddin, M., Rink, R.E., and Gourishankar, V.G. " Heuristic control profiles for integrated boilers." ASHRAE Transactions 1990, Vol. 96, Part 2 pp. 205-211

Zeng, Z.S. "A study of a air-conditioning control system using a variable speed compressor and a variable speed evaporator fan." 1993, Master's thesis, Dept. of Mechanical Engineering, Concordia University

APPENDIX

FORTRAN PROGRAM

```
*******************************************************************************
*
*     CHILLED WATER COOLING SYSTEM (CWCS) SYSTEM SIMULATION PROGRAM
*
*     THIS IS THE MAIN PROGRAM FOR THE ANALYSIS OF THE CWCS SYSTEM
*     PERFORMANCE ACCORDING TO THE SCHEMATIC DIAGRAM IN THE THESIS
*
*     PURPOSE:
*        TO SIMULATE THE SYSTEM DYNAMIC CHARACTERISTICS INCLUDING
*        EACH SYSTEM COMPONENT
*
*     SUBROUTINES OF THE COMPONENTS
*
*        SUBROUTINE --- COMP (COMPRESSOR)
*        SUBROUTINE --- COND (CONDENSER)
*        SUBROUTINE --- EVCO (EVAPORATIVE COOLER)
*        SUBROUTINE --- EVA  (EVAPORATOR: EVAPORATION REGION)
*        SUBROUTINE --- SUHT (EVAPORATOR: SUPERHEAT REGION)
*        SUBROUTINE --- EXPA (EXPANSION VAVLE)
*        SUBROUTINE --- STOR (CHILLED WATER STORAGE)
*
*     SUBROUTINES OF REFRIGERANT R-12 THERMODYNAMIC PROPERTIES
*
*        SUBROUTINE --- R12HP
*        SUBROUTINE --- R12LP
*        SUBROUTINE --- PHTH
*        SUBROUTINE --- PLTL
*        SUBROUTINE --- SHEAT
*
*     DATA REQUIRED:
*
*        COMPRESSOR PARAMETERS
*        CONDENSER PARAMETERS
*        EVAPORATIVE COOLER PARAMETERS
*        EVAPORATOR PARAMETERS
*        EXPANSION VALVE PARAMETERS
*        STORAGE PARAMETERS
*
*******************************************************************************
      PROGRAM MODEL

      IMPLICIT DOUBLE PRECISION (A-H,O-Z)

      DOUBLE PRECISION K,KR

      CHARACTER*12 FILEIN,FILEOUT,FILEPLOT
      PARAMETER (N=13)

      DIMENSION Y(8,N),SAVE(10,N),SAVE01(N),SAVE02(N),YMAX(N),
     &          TEM(N),ERROR(N),PW(N,N),X0(N)
```

```
      COMMON  /VVV/MT,NSTEP,V,H,EPS
      COMMON  /COMP/AN,ANMAX,FRV,VD,K
      COMMON  /COND/HIC,AIC,HOC,AOC,U2,U2MAX,CC,
     &            VC,CWA,CPW,SCOL1,SCOL2
      COMMON  /EVAP/HE,AIE,HWA,AOE,HES,DW,CW,AW,CS,AR,
     &            VOE,LTO,NS,U4,U4MAX,LAM,AOE1
      COMMON  /COOL/HC,A,TAC,CPA,U1,U1MAX,CWO,tao
      COMMON  /STOR/UM,UMMAX,TCITY,CCH
      COMMON  /TXV/CTXV,DTSS
      COMMON  /PARA/PS,PD,TL,COP,CAP,TRE,TRC,
     &            HL,WC,DCL1,FAIL,FAIG,TE,TSH,DTSH,
     &            DS,DZ,KR,TWO,VOC,Y0,VS,TEVM,
     &            TEST,TCH,DCV,HCV,CV,DCL,HCL,CL,HCI,
     &            DEV,HEV,DEL,HEL,A1,A2,A3,
     &            QE,QC,UCOM,UCI,ANN,PNN,QNN

C     SET INITIAL CONDITIONS

      TEM(1)=39.0+273.15
      TEM(2)=36.0+273.15
      TEM(3)=32.0+273.15
      TEM(4)=2.0+273.15
      TEM(5)=6.0+273.15
      TEM(6)=8.0+273.15
      TEM(7)=10.0+273.15
      TEM(8)=10.0+273.15
      TEM(9)=10.0+273.15
      TEM(10)=10.50+273.15
      TEM(11)=10.50+273.15
      TEM(12)=10.50+273.15
      TEM(13)=14.0+273.15

      IOIN=10
      IOOUT=20
      IOPLOT=30

C     INPUT THE FILE NAME

C     WRITE(*,*) 'ENTER THE INPUT FILE NAME'
C     READ(*,'(A12)') FILEIN

      WRITE(*,*) 'ENTER THE OUTPUT FILE NAME --- dATA'
      READ(*,'(A12)') FILEOUT

C     OPEN THE INPUT AND OUTPUT FILE

C     OPEN(IOIN,FILE=FILEIN,STATUS='OLD')
      OPEN(IOOUT,FILE=FILEOUT,STATUS='NEW')


C     INPUT PARAMETERS OF COMPONENT MODELS
```

```
*       ******************** PARAMETERS OF COMPRESSOR ********************

        AN=1.
        ANMAX=1200.0
        FRV=0.05
        VD=0.0006
        K=1.15

*       ******************** SPECIFICATION OF CONDENSER ********************

        HIC=5111*1.2*1.5
        AIC=7.5*2.
        HOC=6120.0
        AOC=3.5/1.5
        U2=1.0
        U2MAX=7000.0
        CC=20.7
        CWA=500.0
        CPW=4.2
        VC=2.5
        SCOL1=4.
        SCOL2=5.

*       ********************* PARAMETERS OF EVAPORATOR *********************

        HE=250.*20.44
        HE=HE*2.
        AIE=0.47
        HWA=6200.0
        HWA=HWA*2.
        AOE=0.534*2.
        HES=180.0*20.
        CPW=4.2
        DW=8910.0
        CW=0.39
        AW=0.0005
        CS=0.6
        AR=0.00177
        LTO=8.0
        VOE=0.75
        CPW=4.2
        NS=2
        LAM=0.3938


*       ***************** PARAMETERS OF EVAPORATIVE COOLER *****************

        HC=360.*20.44*1.5
        A=1.5*2.*20.
        TAC=28.0+273.15
```

```
      CPA=1.0
      U1=1.0
      U1MAX=2368.69*10.
      CWO=83.7
      CPW=4.2

*     ******************** PARAMETERS OF STORAGE ****************************

      UM=1.0
      UMMAX=1150.
      TCITY=20.+273.15
      CCH=18.0
      CPW=4.2
      U4=1.0
      U4MAX=6000.

*     *************** PARAMETERS OF EXPANSION VAVLE ***********************

      CTXV=4.5
      DTJS=6.0

*     ********************************************************************************

      DO 111 I=1,N
      Y(1,I)=TEM(I)
      X0(I)=TEM(I)
111   CONTINUE

C     CLOSE(IOIN)

      T = 0.0

      WRITE(IOOUT,*) 'TIME=',T

      WRITE(IOOUT,*)
      WRITE(IOOUT,14) (Y(1,II),II=1,N)

C     WRITE(IOPLOT) N
C     WRITE(IOPLOT) T
C     WRITE(IOPLOT) (Y(1,I),I=1,N)



15    H=1.E-5
      EPS=1.0E-2
      T=0.
      MF=2
      JSTART=0
      MAXD=8
      IF(MF.NE.0) MAXD=7
      WRITE(*,*) 'INPUT TEND'
```

```
      READ(*,*) TEND
      TSTEP=5.
      TPLOT=5.
      T1=TSTEP
      TP=TPLOT
      V=0.
      NSTEP=0.
      MT=0.
      HMIN=1.E-8
      HMAX=0.4
      DO 1 I=1,N
1     YMAX(I)=1.

2     CALL DIFSB(N,T,Y,TEM,SAVE,SAVE01,SAVE02,H,HMIN,HMAX,EPS,MF,
     &          YMAX,ERROR,KF,JSTART,MAXD,PW)
      IF(KF.LE.0) THEN
            if(kf.eq.-1) WRITE(*,*) 'the step < Hmix'
            if(kf.eq.-2) WRITE(*,*) 'maximum order to large'
            if(kf.eq.-3) WRITE(*,*) 'con not converge'
            if(kf.eq.-4) WRITE(*,*) 'eps to small'

            WRITE(*,*) 'KFLAG=',KF,'    TIME=',T
            STOP
      ENDIF

      NSTEP=NSTEP+1

      IF(ABS(TP-T).LE.1E-10.OR.T.GT.TP) GO TO 10
      GO TO 2
10    AH=T/FLOAT(NSTEP)


      DO 9111 I=1,N
      TEM(I)=Y(1,I)
9111  CONTINUE

      TP=T+TPLOT
C           IF(TP.GE.300.0) THEN
C                       HMAX=0.8
C           ENDIF

      DO 9222 I=1,5
      Y(1,I)=Y(1,I)-273.15
9222  CONTINUE

      DO 9888 I=6,13
      Y(1,I)=Y(1,I)-273.15
9888  CONTINUE

      TSH=TSH-273.15
      TL=TL-273.15
```

```
      TCH=TCH-273.15

      IF(T.GT.T1.OR.ABS(T1-T).LE.1E-8) THEN

            WRITE(IOOUT,*) 'TIME=',T
            WRITE(IOOUT,14) (Y(1,I),I=1,N)
            WRITE(*,*) 'TIME=',T,(Y(1,I),I=1,N)

C     ENDIF


C           WRITE(IOOUT,14) (SAVE01(I),I=1,N)

14          FORMAT(1X,6E12.5)

              IF(T.GE.10.0.AND.T.LE.100) THEN
                TSTEP=30.
                T1=T+TSTEP
              ELSE IF(T.GT.100.)THEN
                TSTEP=50.
                T1=T+TSTEP


      ENDIF
      ENDIF

      DO 9444 I=1,5
      Y(1,I)=Y(1,I)+273.15
9444  CONTINUE

      DO 9999 I=6,13
      Y(1,I)=Y(1,I)+273.15
9999  CONTINUE

      TCH=TCH+273.15

      IF(T.LE.TEND) GO TO 2

      STOP
      END


      SUBROUTINE DIFFUN(T,X,DX,N)
      IMPLICIT DOUBLE PRECISION (A-H,O-Z)

      DIMENSION DX(N),X(N)
      COMMON  /VVV/MT,NSTEP,V,H,EPS

      COMMON /IODATA/IOIN,IOOUT,IOPLOT

      CALL FORMFX(N,DX,X,T,)
```

```
      V=V+1
      RETURN
      END

      SUBROUTINE PEDERV(T,X,PW,N)
      IMPLICIT DOUBLE PRECISION (A-H,O-Z)

      DIMENSION PW(N,N),X(N)

      RETURN
      END

      SUBROUTINE MATINV(PW,N,M,J)
      IMPLICIT DOUBLE PRECISION (A-H,O-Z)
      PARAMETER (NN=13)

      DIMENSION PW(N,N),B(NN),C(NN),ME(NN),MF(NN)

      COMMON  /VVV/MT,NSTEP,V,H,EPS

      EP=1.0E-8
      CALL INVERT(PW,B,C,ME,MF,N,EP)

      IF(EP.LT.0) THEN
            WRITE(*,*) 'MAXTRIX IS SINGEL'
            STOP
      ENDIF

      MT=MT+1
      RETURN
      END


      SUBROUTINE DIFSB(N,T,Y,TEM,SAVE,SAVE01,SAVE02,H,HMIN,HMAX,
     &      EPS,MF,YMAX,ERROR,KFLAG,JSTART,MAXDER,PW)

      IMPLICIT DOUBLE PRECISION (A-H,O-Z)

      DIMENSION Y(8,N),YMAX(N),SAVE(10,N),ERROR(N),PW(*),
     &  TEM(N),SAVE01(N),SAVE02(N),A(8),PERTST(7,2,3)

      DATA PERTST/2.0,4.5,7.333,10.42,13.7,17.15,1.0,
     &      2.0,12.0,24.0,37.89,53.33,70.08,87.97,
     &      3.0,6.0,9.167,12.5,15.98,1.0,1.0,
     &      12.0,24.0,37.89,53.33,70.08,87.97,1.0,
     &      1.0,1.0,0.5,0.1667,0.04133,0.008267,1.0,
     &      1.0,1.0,2.0,1.0,0.3157,0.07407,0.0139/

      DATA A(2)/-1.0/

      IRET=1
```

```
      KFLAG=1
      IF(JSTART.LE.0) GO TO 140
100   DO 110 I=1,N
      DO 110 J=1,K
110   SAVE(J,I)=Y(J,I)
      HOLD=HNEW
      IF (H.EQ.HOLD) GO TO 130
120   RACUM=H/HOLD
      IRET1=1
      GO TO 750
130   NQOLD=NQ
      TGLD=T
      RACUM=1.0
      IF (JSTART.GT.0) GO TO 250
      GO TO 170
140   IF(JSTART.EQ.-1) GO TO 160
      NQ=1
      N3=N
      N4=N*N
      DO 991 I=1,N
991   TEM(I)=Y(1,I)
      CALL DIFFUN(T,TEM,SAVE01,N)


      DO 150 I=1,N
150   Y(2,I)=SAVE01(I)*H
      HNEW=H
      K=2
      GO TO 100
160   IF(NQ.EQ.NQOLD) JSTART=1
      T=TGLD
      NQ=NQOLD
      K=NQ+1
      GO TO 120
170   IF(MF.EQ.0) GO TO 180
      IF(NQ.GT.6) GO TO 190
      GO TO (221,222,223,224,225,226),NQ
180   IF(NQ.GT.7) GO TO 190
      GO TO (211,212,213,214,215,216,217),NQ
190   KFLAG=-2
      RETURN
211   A(1)=-1.0
      GO TO 230
212   A(1)=-0.5
      A(3)=-0.5
      GO TO 230
213   A(1)=-0.4167
      A(3)=-0.75
      A(4)=-0.1667
      GO TO 230
214   A(1)=-0.375
```

```
      A(3)=-0.9167
      A(4)=-0.3333
      A(5)=-0.0417
      GO TO 230
215   A(1)=-0.3486
      A(3)=-1.0417
      A(4)=-0.4861
      A(5)=-0.1042
      A(6)=-0.0083
      GO TO 230
216   A(1)=-0.3299
      A(3)=-1.14167
      A(4)=-0.625
      A(5)=-0.1771
      A(6)=-0.025
      A(7)=-0.0014
      GO TO 230
217   A(1)=-0.3156
      A(3)=-1.235
      A(4)=-0.7519
      A(5)=-0.2552
      A(6)=-0.0486
      A(7)=-0.0049
      A(8)=-0.0002
      GO TO 230
221   A(1)=-1.0
      GO TO 230
222   A(1)=-0.6667
      A(3)=-0.3333
      GO TO 230
223   A(1)=-0.5455
      A(3)=A(1)
      A(4)=-0.0909
      GO TO 230
224   A(1)=-0.48
      A(3)=-0.7
      A(4)=-0.2
      A(5)=-0.02
      GO TO 230
225   A(1)=-0.4380
      A(3)=-0.8212
      A(4)=-0.3102
      A(5)=-0.0547
      A(6)=-0.0036
      GO TO 230
226   A(1)=-0.4082
      A(3)=-0.9206
      A(4)=-0.4167
      A(5)=-0.0992
      A(6)=-0.0119
      A(7)=-0.0006
```

```
230   K=NQ+1
      IDOUB=K
      MTYP=(4-MF)/2
      ENQ2=.5/FLOAT(NQ+1)
      ENQ3=.5/FLOAT(NQ+2)
      ENQ1=.5/FLOAT(NQ)
      PEPSH=EPS
      EUP=(PERTST(NQ,MTYP,2)*PEPSH)**2
      E=(PERTST(NQ,MTYP,1)*PEPSH)**2
      EDWN=(PERTST(NQ,MTYP,3)*PEPSH)**2
      IF(EDWN.EQ.0) GO TO 780
      BND=EPS*ENQ3/FLOAT(N)
240   IWEVAL=MF
      GO TO (250,680), IRET
250   T=T+H
      DO 260 J=2,K
      DO 260 J1=J,K
      J2=K-J1+J-1
      DO 260 I=1,N
260   Y(J2,I)=Y(J2,I)+Y(J2+1,I)
      DO 270 I=1,N
270   ERROR(I)=0.0
      DO 430 L=1,3
      DO 992 I=1,N
992   TEM(I)=Y(1,I)
      CALL DIFFUN(T,TEM,SAVE01,N)

      IF(IWEVAL.LT.1) GO TO 350
      IF(MF.EQ.2) GO TO 310
      DO 993 I=1,N
993   TEM(I)=Y(1,I)
      CALL PEDERV(T,TEM,PW,N3)
      R=A(1)*H
      DO 280 I=1,N4
280   PW(I)=PW(I)*R
290   DO 300 I=1,N
      N1=I*(N3+1)-N3
300   PW(N1)=1.0+PW(N1)
      IWEVAL=-1
      CALL MATINV(PW,N,N3,J1)
      IF(J1.GT.0) GO TO 350
      GO TO 440
310   DO 320 I=1,N
320   SAVE(9,I)=Y(1,I)
      DO 340 J=1,N
      R=EPS*EPS
      RR=ABS(SAVE(9,J))
      IF(EPS.LT.RR) R=EPS*RR
      Y(1,J)=Y(1,J)+R
      D=A(1)*H/R
      DO 994 I=1,N
```

```
994   TEM(I)=Y(1,I)
      CALL DIFFUN(T,TEM,SAVE02,N)
      DO 330 I=1,N
      N1=I+(J-1)*N3
330   PW(N1)=(SAVE02(I)-SAVE01(I))*D
340   Y(1,J)=SAVE(9,J)
      GO TO 290
350   IF(MF.NE.0) GO TO 370
      DO 360 I=1,N
360   SAVE(9,I)=Y(2,I)-SAVE01(I)*H
      GO TO 410
370   DO 380 I=1,N
380   SAVE02(I)=Y(2,I)-SAVE01(I)*H
      DO 400 I=1,N
      D=0.0
      DO 390 J=1,N
      N1=I+(J-1)*N3
390   D=D+PW(N1)*SAVE02(J)
400   SAVE(9,I)=D
410   NT=N
      DO 420 I=1,N
      Y(1,I)=Y(1,I)+A(1)*SAVE(9,I)
      Y(2,I)=Y(2,I)-SAVE(9,I)
      ERROR(I)=ERROR(I)+SAVE(9,I)
      IF(ABS(SAVE(9,I)).LE.(BND*YMAX(I))) NT=NT-1
420   CONTINUE
      IF(NT.LE.0) GO TO 490
430   CONTINUE
440   T=TGLD
      IF(H.GT.(HMIN*1.00001)) GO TO 4401
      IF((IWEVAL-MTYP).LT.-1) GO TO 460
4401  IF (MF.EQ.0) GO TO 4402
      IF(IWEVAL.NE.0) GO TO 4402
      GO TO 4403
4402  RACUM=RACUM*0.25
4403  IWEVAL=MF
      IRET1=2
      GO TO 750
460   KFLAG=-3
470   DO 480 I=1,N
      DO 480 J=1,K
480   Y(J,I)=SAVE(J,I)
      H=HOLD
      NQ=NQOLD
      JSTART=NQ
      RETURN
490   D=0.0
      DO 500 I=1,N
500   D=D+(ERROR(I)/YMAX(I))**2
      IWEVAL=0
      IF(D.GT.E) GO TO 540
```

```
      IF(K.LT.3) GO TO 520
      DO 510 J=3,K
      DO 510 I=1,N
510   Y(J,I)=Y(J,I)+A(J)*ERROR(I)
520   KFLAG=+1
      HNEW=H
      IF(IDOUB.LE.1) GO TO 550
      IDOUB=IDOUB-1
      IF(IDOUB.GT.1) GO TO 700
      DO 530 I=1,N
530   SAVE(10,I)=ERROR(I)
      GO TO 700
540   KFLAG=KFLAG-2
      IF(H.LE.(HMIN*1.00001)) GO TO 740
      T=TGLD
      IF(KFLAG.LE.-5) GO TO 720
550   PR2=(D/E)**ENQ2*1.2
      PR3=1.0E+20
      IF(NQ.GE.MAXDER) GO TO 570
      IF(KFLAG.LE.-1) GO TO 570
      D=0.0
      DO 560 I=1,N
560   D=D+((ERROR(I)-SAVE(10,I))/YMAX(I))**2
      PR3=(D/EUP)**ENQ3*1.4
570   PR1=1.E+20
      IF(NQ.LE.1) GO TO 590
      D=0.0
      DO 580 I=1,N
580   D=D+(Y(K,1)/YMAX(I))**2
      PR1=(D/EDWN)**ENQ1*1.3
590   CONTINUE
      IF(PR2.LE.PR3) GO TO 650
      IF(PR3.LT.PR1) GO TO 660
600   R=1.E+4
      IF(PR1.GT.1.E-4) R=1.0/PR1
      NEWQ=NQ-1
610   IDOUB=10
      IF(KFLAG.NE.1) GO TO 6101
      IF(R.LT.1.1) GO TO 700
6101  IF(NEWQ.LE.NQ) GO TO 630
      DO 620 I=1,N
620   Y(NEWQ+1,I)=ERROR(I)*A(K)/FLOAT(K)
630   K=NEWQ+1
      IF(KFLAG.EQ.1) GO TO 670
      RACUM=RACUM*R
      IRET1=3
      GO TO 750
640   IF(NEWQ.EQ.NQ) GO TO 250
      NQ=NEWQ
      GO TO 170
650   IF(PR2.GT.PR1) GO TO 600
```

```
      NEWQ=NQ
      R=1.E+4
      IF(PR2.GT.1.E-4) R=1.0/PR2
      GO TO 610
660   R=1.0E+4
      IF(PR3.GT.1.E-4) R=1.0/PR3
      NEWQ=NQ+1
      GO TO 610
670   IRET=2
      RR=HMAX/ABS(H)
      IF(R.GT.RR) R=RR
      H=H*R
      HNEW=H
      IF(NQ.EQ.NEWQ) GO TO 680
      NQ=NEWQ
      GO TO 170
680   R1=1.0
      DO 690 J=2,K
      R1=R1*R
      DO 690 I=1,N
690   Y(J,I)=Y(J,I)*R1
      IDOUB=K
700   DO 710 I=1,N
710   IF(YMAX(I).LT.ABS(Y(1,I))) YMAX(I)=ABS(Y(1,I))
      JSTART=NQ
      RETURN
720   IF(NQ.EQ.1) GO TO 780
      DO 995 I=1,N
995   TEM(I)=Y(1,I)
      CALL DIFFUN(T,TEM,SAVE01,N)

      R=H/HOLD
      DO 730 I=1,N
      Y(1,I)=SAVE(1,I)
      SAVE(2,I)=HOLD*SAVE01(I)
730   Y(2,I)=SAVE(2,I)*R
      NQ=1
      KFLAG=1
      GO TO 170
740   KFLAG=-1
      HNEW=H
      JSTART=NQ
      RETURN
750   RR=ABS(HMIN/HOLD)
      IF(RACUM.LT.RR) RACUM=RR
      RR=ABS(HMAX/HOLD)
      IF(RACUM.GT.RR) RACUM=RR
      R1=1.0
      DO 760 J=2,K
      R1=R1*RACUM
      DO 760 I=1,N
```

```
760   Y(J,I)=SAVE(J,I)*R1
      H=HOLD*RACUM
      DO 770 I=1,N
770   Y(1,I)=SAVE(1,I)
      IDOUB=K
      GO TO (130,250,640), IRET1
780   KFLAG=-4
      GO TO 470
      END


      SUBROUTINE INVERT(A,B,C,ME,MF,N,EP)

      IMPLICIT DOUBLE PRECISION (A-H,O-Z)

      DIMENSION A(N,N),B(N),C(N),ME(N),MF(N)

      DO 10 K=1,N
      Y=0.0
      DO 20 I=K,N
      DO 20 J=K,N
      IF(ABS(A(I,J)).LE.ABS(Y)) GO TO 20
      Y=A(I,J)
      I2=I
      J2=J
20    CONTINUE
      IF(ABS(Y).LT.EP) GO TO 32
      IF(I2.EQ.K) GO TO 33
      DO 11 J=1,N
      W=A(I2,J)
      A(I2,J)=A(K,J)
11    A(K,J)=W
33    IF(J2.EQ.K) GO TO 44
      DO 22 I=1,N
      W=A(I,J2)
      A(I,J2)=A(I,K)
22    A(I,K)=W
44    ME(K)=I2
      MF(K)=J2
      DO 50 J=1,N
      IF(J-K) 2,3,2
3     B(J)=1./Y
      C(J)=1.
      GO TO 4
2     B(J)=-A(K,J)/Y
      C(J)=A(J,K)
4     A(K,J)=0.0
      A(J,K)=0.0
50    CONTINUE
      DO 40 I=1,N
      DO 40 J=1,N
```

```
40    A(I,J)=A(I,J)+C(I)*B(J)
10    CONTINUE
       DO 60 L=1,N
       K=N-L+1
       K1=ME(K)
       K2=MF(K)
       IF(K1.EQ.K) GO TO 70
       DO 55 I=1,N
       W=A(I,K1)
       A(I,K1)=A(I,K)
55    A(I,K)=W
70    IF(K2.EQ.K) GO TO 60
       DO 66 J=1,N
       W=A(K2,J)
       A(K2,J)=A(K,J)
66    A(K,J)=W
60    CONTINUE
       RETURN
32    EP=-EP
       RETURN
       END

C     ************************************************************************

       SUBROUTINE FORMFX(MAXN,F,X,T)

       IMPLICIT DOUBLE PRECISION (A-H,O-Z)

       DOUBLE PRECISION  K,KR

       COMMON  /VVV/MT,NSTEP,V,H,EPS
       COMMON  /COMP/AN,ANMAX,FRV,VD,K
       COMMON  /COND/HIC,AIC,HOC,AOC,U2,U2MAX,CC,
     &         VC,CWA,CPW,SCOL1,SCOL2
       COMMON  /EVAP/HE,AIE,HWA,AOE,HES,DW,CW,AW,CS,AR,
     &         VOE,LTO,NS,U4,U4MAX,LAM,AOE1
       COMMON  /COOL/HC,A,TAC,CPA,U1,U1MAX,CWO,tao
       COMMON  /STOR/UM,UMMAX,TCITY,CCH
       COMMON  /TXV/CTXV,DTSS
       COMMON  /PARA/PS,PD,TL,COP,CAP,TRE,TRC,
     &         HL,WC,DCL1,FAIL,FAIG,TE,TSH,DTSH,
     &         DS,DZ,KR,VOC,TWO,Y0,vs,TEVM,
     &         TEST,TCH,DCV,HCV,CV,DCL,HCL,CL,HCI,
     &         DEV,HEV,DEL,HEL,A1,A2,A3,
     &         QE,QC,UCOM,UCI,ANN,PNN,QNN

       DIMENSION F(MAXN),X(MAXN)

       DO 1000 I=1,MAXN

       F(I)=0.0
```

```
1000   CONTINUE

*      ************************* FOR COMPRESSOR *******************************

       VD=0.0006

       TRC=X(1)
       CALL PHTH (PD,TRC)

       TRE=X(4)
       CALL PLTL (PS,TRE)

       TSH=X(7)
       CALL SHEAT (DS,VS,HS,PS,TSH)

       CALL COMP (EV,FRV,PD,PS,KR,K,WC,VS,VD,FAIG,DS,AN,ANMAX,
     &          TL,TSH,HL,HS)

*      ********************** FOR CONDENSER *********************************

       FCI=FAIG
       FCO=FAIL
       HCI=HL

       CCO=501.678
       ETA=0.8

       CALL R12HP (DCV,DCL,DDCV,DDCL,HCV,HCL,CV,CL,TRC)

       TRC1=TRC-SCOL1
       CALL R12HP (DCV1,DCL1,DDCV1,DDCL1,HCV1,HCL1,
     &          CV1,CL1,TRC1)

       CALL COND (MAXN,F,X(1),X(2),X(3),1,2,CCO,FCI,HCI,FCO,HCL,
     &          HIC,AIC,CC,U2,U2MAX,CPW,ETA)

*      ***************** FOR EVAPORATIVE COOLER ****************************

       CALL EVCO (MAXN,F,X(2),X(3),3,CWO,U2,U2MAX,CPW,ETA,HC,
     &          A,TAC,TAO,U1,U1MAX,CPA)

*      ********************** FOR EVAPORATOR (EVA) **************************

       FEO=FAIG
       FEI=FAIL
       CEO=10.

       CALL R12LP (DEV,DEL,DDEV,DDEL,HEV,HEL,CEV,CEL,TRE)

       TRC2=TRC-SCOL1-SCOL2
       CALL R12HP (DCV2,DCL2,DDCV2,DDCL2,HCV2,HCL2,CV2,CL2,TRC2)
```

```
      HEI=HCL
      LTE=5.6

      CALL EVA (MAXN,F,X(4),X(5),X(10),4,5,FEI,HEI,FEO,HEV,
     &          HE,AIE,LTE,DW,CW,AW,HWA,AOE,CEO)

*     ************************** FOR EVAPORATOR (SUHT) **********************

      NS=2
      I1=6
      I2=I1+NS

      J1=7
      J2=J1+NS

      DZ1=3.4
      DZ2=1.2
      AWA=0.005
      DWA=1000.0
      CS=3.

      CALL SUHT (MAXN,F,X(4),X(5),X(I1),X(J1),X(I2),X(J2),X(10),
     &          X(11),X(12),X(MAXN),I1,J1,I2,J2,10,11,12,DS,CS,AR,
     &          FEO,DZ1,HES,AIE,DZ2,HWA,DWA,CPW,AWA,AOE,DW,
     &          CW,AW,U4,U4MAX)

*     ************************* FOR EXPANSION VAVLE *************************

80    DTSH=TSH-TRE

      CALL EXPA (DPTXV,PD,PS,FAIL,CTXV,DTSH,DTSS,DCL2)

*     ***************************** FOR STORAGE *******************************

      CALL STOR (MAXN,F,X(12),X(MAXN),TCITY,MAXN,CCH,U4,U4MAX,CPW,
     &          UM,UMMAX)

C     *************************************************************************

      COP=(HS-HEI)/WC
      QE=(FAIL+FAIG)/2.*(HS-HEI)
      QC=(FAIL+FAIG)/2.*(HL-HCL)
      AVEF=(FAIL+FAIG)/2.

      DO 1111 I=1,MAXN
1111  F(I)=F(I)/3600.

      RETURN
      END
```

```
************************************************************************************
*
*     COMPRESSOR SIMULATION PROGRAM
*
*     PURPOSE:
*
*       TO SIMULATE THE PERFORMANCE OF COMPRESSOR DURING THE
*       OPERATION OF THE CHILLED WATER COOLING SYSTEM AND
*       FIND OUT THE OUTLET TEMPERATURE AND ENTHALPY OF THE
*       REFRIGERANT GAS
*
*     INPUT DATA:
*
*       AN ----- RATE OF THE MAXIMUM COMPRESSOR MOTOR SPEED
*       ANMAX -- MAXIMUM COMPRESSOR MOTOR SPEED
*       FRV ----
*       VD ----- CLEARANCE VOLUME OF THE COMPRESSOR CYLINDER
*       K ------ POLYTROPHIC CONSTANT, ASSUMED EQUAL TO
*             SPECIFIC HEAT RATION
*       PD ----- PRESSURE OF REFRIGERANT AT DISCHARGE SECTION
*       PS ----- PRESSURE OF REFRIGERANT AT SUCTION SECTION
*       VS ----- SPECIFIC VOLUME OF THE REFRIGERAT AT DISCHARGE
*             SECTION
*       TSH ---- DEGREE OF SUPERHEAT OF REFRIGERANT AT INLET OF
*             COMPRESSOR
*
*     OUTPUT DATA:
*
*       EV ----- CLEARANCE VOLUME EFFICIENCY
*       WC ----- WORK DONE OF COMPRESSOR MOTOR
*       FAIG --- MASS FLOW RATE OF REFRIGERANT GAS AT DISCHARGE
*             SECTION
*       TL ----- TEMPERATURE OF REFRIGERANT GAS LEAVING THE
*             COMPRESSOR
*       FAIG --- MASS FLOW RATE OF REFRIGERANT GAS AT DISCHARGE
*             SECTION
*       HL ----- ENTHALPY OF REFRIGERANT GAS LEAVING THE
*             COMPRESSOR
*
************************************************************************************

      SUBROUTINE COMP (EV,FRV,PD,PS,KR,K,WC,VS,VD,FAIG,DS,
     &            AN,ANMAX,TL,TSH,HL,HS)

      IMPLICIT DOUBLE PRECISION (A-H, O-Z)

      DOUBLE PRECISION K,KR

      EV= 1.-FRV*((PD/PS)**(1./K)-1.)
      KR=(K-1.)/K
      WC=1./KR*PS*VS*((PD/PS)**KR-1.)/1000.
```

```
      FAIG=DS*VD*AN*ANMAX*60.

      TL=TSH*(PD/PS)**KR
      HL=HS+WC

      RETURN
      END

*****************************************************************************
*
*     CONDENSER SIMULATION PROGRAM
*
*     PURPOSE:
*
*       TO SIMULATE THE PERFORMANCE OF REFRIGERANT AND COOLING
*       WATER INSIDE THE CONDENSER TUBES AND SHELL, GET THE
*       TRANSIENT RESPONSES OF THE TEMPERATURE OF SATURATED
*       REFRIGERANT UNDER THE CONDENSATION CONDITION, AND THE
*       TEMPERATURE OF THE CYCLING WATER
*
*     INPUT DATA:
*
*       HIC ---- HEAT TRANSFER COEFFICIENT OF THE REFRIGERANT
*             INSIDE THE CONDENSER TUBES
*       HOC ---- HEAT TRANSFER COEFFICIENT OF THE CONDENSER TUBES
*       AIC ---- HEAT EXCHANGE AREA BETWEEN THE REFRIGERANT
*             AND THE TUBES
*       AOC ---- HEAT EXCHANGE AREA BETWEEN THE CONDENSER TUBES AND
*             CYCLING WATER
*       U2 ----- RATIO OF MAXIMUM MASS FLOW RATE OF WATER
*       U2MAX -- MAXIMUM MASS FLOW RATE OF WATER
*       CC ----- THERMAL CAPACITY OF THE CONDENSER
*       CPW ---- SPECIFIC HEAT OF WATER
*       VC ----- VOLUME OF THE CONDENSER
*       SCOL1 -- DEGREE OF THE SUBCOOLING OF THE REFRIGERANT IN
*             IN CONDENSER
*       FAIG --- MASS FLOW RATE OF REFRIGERANT GAS AT DISCHARGE
*             SECTION
*       HL ----- ENTHALPY OF REFRIGERANT GAS LEAVING THE
*             COMPRESSOR
*       TL ----- TEMPERATURE OF REFRIGERANT GAS LEAVING THE
*             COMPRESSOR
*
*
*     OUTPUT DATA:
*
*       TRCC --- TEMPERATURE OF THE SATURATED REFRIGERANT INSIDE
*             CONDENSER TUBES
*       TCC ---- TEMPERATURE OF THE CONDENSER TUBES
*
*****************************************************************************
```

```
      SUBROUTINE COND (NMAXN,F,TRCC,TCC,TWO,I,J,CCO,FCI,HCI,FCO,HCL,
     &          HIC,AIC,CC,U2,U2MAX,CPW,ETA)


      IMPLICIT DOUBLE PRECISION (A-H,O-Z)

      DIMENSION F(NMAXN)

      F(I)=1./CCO*(FCI*HCI-FCO*HCL
     &    -HIC*AIC*(TRCC-TCC))

      F(J)=1./CC*(HIC*AIC*(TRCC-TCC)
     &    -U2*U2MAX*CPW*ETA*(TCC-TWO))

      RETURN
      END

*****************************************************************************
*
*     EVAPORATIVE COOLER SIMULATION PROGRAM
*
*     PURPOSE:
*
*       TO SIMULATE THE PERFORMANCE OF EVAPORATIVE COOLER DURING
*       THE HEAT EXCHANGE BETWEEN CYCLING WATER AND THE COOLER,
*       AND TO FIND OUT THE TEMPERATE RESPONSE OF THE WATER
*       LEAVING THE CONDENSER
*
*     INPUT DATA:
*
*       HC ----- HEAT TRANSFER COEFFICIENT BETWEEN TUBES AND
*             SPRAY WATER
*       A ------ HEAT TRANSFER AREA OF THE EVAPORATIVE COOLER
*       TAC ---- TEMPERATE OF AMBIENT AIR OF THE EVAPORATIVE
*             COOLER
*       CWO ---- THERMAL CAPACITY OF THE EVAPORATIVE COOLER
*       CPA ---- SPECIFIC HEAT OF AIR
*       CPW ---- SPECIFIC HEAT OF WATER
*       U1 ----- RATIO OF MAXIMUM MASS FLOW RATE OF CYCLING
*             AIR
*       U1MAX -- MAXIMUM MASS FLOW RATE OF CYCLING AIR
*
*     OUTPUT DATA:
*
*       TWO ---- TEMPERATURE OF THE CYCLING WATER INSIDE THE
*             CONDENSER SHELL
*       TAO ---- TEMPERATURE OF THE OUTGOING AIR FROM EVAPORATIVE
*             COOLER
*
*****************************************************************************
```

```
      SUBROUTINE EVCO (NMAXN,F,TCC,TWO,I,CWO,U2,U2MAX,CPW,
     &                 ETA,HC,A,TAC,TAO,U1,U1MAX,CPA)


      IMPLICIT DOUBLE PRECISION (A-H,O-Z)

      DIMENSION F(NMAXN)

      F(I)=1./CWO*(U2*U2MAX*CPW*ETA*(TCC-TWO)
     &    -HC*A*(TWO-0.5*TAC-0.5*TAO))


      TAO=TAC+(U2*U2MAX*CPW*ETA*(TCC-TWO))/
     &    (U1*U1MAX*CPA)


      RETURN
      END

*************************************************************************
*
*     EVAPORATOR (EVAPORATION REGION) SIMULATION PROGRAM
*
*     PURPOSE:
*
*       TO SIMULATE THE PERFORMANCE OF HEAT EXCHANGE BETWEEN
*       REFRIGERANT AND EVAPORATOR TUBES INSIDE THE EVAPORATION
*       REGION
*
*     REMARKS:
*
*       SIMULATION PROCESS AND THE RESPONSE OF THE CYCLING CHILLED
*       WATER IS NOT SHOWN IN THIS SUBROUTINE, IT WILL BE GIVEN IN
*       THE SUBROUTINE OF SUPERHEAT REGION
*
*     INPUT DATA:
*
*       HE ----- HEAT TRANSFER COEFFICIENT BETWEEN REFRIGERANT
*              AND TUBES INSIDE EVAPORATION REGION
*       AIE ---- HEAT TRANSFER AREA INSIDE EVAPORATOR (EVAPORATION
*              REGION) TUBES
*       HWA ---- HEAT TRANSFER COEFFICIENT BETWEEN EVAPORATOR TUBES
*              AND CHILLED WATER
*       AOE ---- HEAT TRANSFER AREA BETWEEN EVAPORATOR TUBES AND
*              CYCLING WATER
*       CPW ---- SPECIFIC HEAT OF WATER
*       DW ----- DENSITY OF THE EVAPORATOR MATERIAL
*       CW ----- THERMAL CAPACITY OF EVAPORATOR MATERIAL
*       AW ----- CROSS SECTIONAL AREA OF REFRIGERATOR TUBE
*       LTE ---- LENGTH OF THE EVAPORATION REGION
*       CPW ---- THERMAL CAPACITY OF WATER
```

```
*
*     OUTPUT DATA:
*
*       TREE --- TEMPERATURE OF SATURATED REFRIGERANT INSIDE
*              EVAPORATION REGION
*       TEE ---- TEMPERATURE OF EVAPORATOR TUBES
*
*************************************************************************************

      SUBROUTINE EVA (NMAXN,F,TREE,TEE,TWAE1,I,J,FEI,HEI,
     &              FEO,HEV,HE,AIE,LTE,DW,CW,AW,HWA,AOE,CEO)

      IMPLICIT DOUBLE PRECISION (A-H,O-Z)

      DIMENSION F(NMAXN)

      DOUBLE PRECISION LTE

      F(I)=(FEI*HEI-FEO*HEV+HE*AIE*(TEE-TREE)*LTE)
c     &     /((0.75*DEV*CEV+(1.-0.75)*DEL*CEL
c     &     +0.75*DDEV*HEV+(1.-0.75)*DDEL*HEL)*AR*LTE)
     &     /CEO

      F(J)=1./(DW*CW*AW)*(HWA*AOE*(TWAE1-TEE)
     &    -HE*AIE*(TEE-TREE))

      RETURN
      END

*************************************************************************************
*
*     EVAPORATOR (SUPERHEAT REGION) SIMULATION PROGRAM
*
*     PURPOSE:
*
*       TO SIMULATE THE PERFORMANCE OF HEAT EXCHANGE BETWEEN
*       REFRIGERANT AND EVAPORATOR TUBES; AND BETWEEN THE TUBES AND
*       CYCLING CHILLED WATER INSIDE SUPERHEAT REGION
*
*     REMARK:
*
*       IN SUPERHEAT REGION, THE REFRIGERANT, TUBES AND CHILLED
*       WATER ARE SIMUi ATED AS SMALL CONTROL VOLUMES. WHERE
*       I1, J1, AND J REFER THE REFRIGERANT, TUBE, AND WATER AT
*       NOD 1. I2, J2, AND K REFER THE REFRIGERANT, TUBE, AND
*       WATER AT NOD 2. I REFERS THE WATER AT EVAPORATION REGION
*
*     INPUT DATA.
*
*       HES ---- HEAT TPANSFER COEFFICIENT BETWEEN REFRIGERANT
*              AND TUBES IN SUPERHEAT REGION
```

```
*       CS ----- SPECIFIC HEAT OF REFRIGERANT VAPOUR IN SUPERHEAT
*             REGION
*       NS ----- NUMBER OF THE SMALL VOLUMES
*       DW ----- DENSITY OF THE EVAPORATOR MATERIAL
*       CW ----- THERMAL CAPACITY OF EVAPORATOR MATERIAL
*       AW ----- CROSS SECTIONAL AREA OF REFRIGERATOR TUBE
*
*      OUTPUT DATA:
*
*       TS1 ---- TEMPERATURE OF REFRIGERANT AT NOD 1
*       TES1 --- TEMPERATURE OF EVAPORATOR TUBE AT NOD 1
*       TS2 ---- TEMPERATURE OF REFRIGERANT AT NOD 2
*       TES2 --- TEMPERATURE OF EVAPORATOR TUBE AT NOD 2
*       TWAE1 -- TEMPERATURE OF CHILLED WATER AT EVAPORATION
*             REGION
*       TWAE2 -- TEMPERATURE OF CHILLED WATER AT NOD1
*       TWAE3 -- TEMPERATURE OF CHILLED WATER AT NOD2
*
**********************************************************************************

      SUBROUTINE SUHT (NMAXN,F,TREE,TEE,TS1,TS2,TES1,TES2,TWAE1,
     &          TWAE2,TWAE3,TCH,I1,J1,I2,J2,I,J,K,DS,CS,AR,FE0,
     &          DZ1,HES,AIE,DZ2,HWA,DWA,CPW,AWA,AOE,DW,CW,AW,
     &          U4,U4MAX)

      IMPLICIT DOUBLE PRECISION (A-H,0-Z)

      DIMENSION F(NMAXN)

      F(I1)=1./(DS*CS*AR)*((FE0*CS)/DZ1*(TREE-TS1)
     &    +HES*AIE*(TES1-TS1))

      F(J1)=1./(DS*CS*AR)*((FE0*CS)/DZ2*(TS1-TS2)
     &    +HES*AIE*(TES2-TS2))

      F(I2)=1./(DW*CW*AW)*(HWA*AOE*(TWAE2-TES1)
     &     -HES*AIE*(TES1-TS1))

      F(J2)=1./(DW*CW*AW)*(HWA*AOE*(TWAE3-TES2)
     &     -HES*AIE*(TES2-TS2))

      F(I)=1./(DWA*CPW*AWA)*(U4*U4MAX*CPW*(TCH-TWAE1)
     &     -HWA*AOE*(TWAE1-TEE))

      F(J)=1./(DWA*AWA*DZ1)*(U4*U4MAX*(TWAE1-TWAE2))
     &     -1./(DWA*CPW*AWA)*(HWA*AOE*(TWAE2-TES1))

      F(K)=1./(DWA*AWA*DZ2)*(U4*U4MAX*(TWAE2-TWAE3))
     &     -1./(DWA*CPW*AWA)*(HWA*AOE*(TWAE3-TES2))

      RETURN
```

```
      END
*****************************************************************************
*
*     SIMULATION OF THE EXPANSION VALVE
*
*     PURPOSE:
*
*      TO SIMULATE THE PERFORMANCE OF EXPANSION VALVE DURING THE
*      OPERATION OF THE CHILLED WATER COOLING SYSTEM
*
*     INPUT DATA:
*
*      CTXV --- GENERAL ORIFICE FLOW AREA COEFFICIENT
*      DTSS --- STEADY-STATE SUPERHEAT OF THE EXPANSION VALVE
*
*     OUTPUT DATA:
*
*      FAIL --- MASS FLOW RATE OF THE SATURATED REFRIGERANT LIQUID
*            THROUGH THE EXPANSION VALVE
*
*****************************************************************************

      SUBROUTINE EXPA (DPTXV,PD,PS,FAIL,CTXV,DTSH,DTSS,DCL2)

      IMPLICIT DOUBLE PRECISION (A-H,O-Z)

      DPTXV=(PD-PS)/1.E+6
      FAIL=CTXV*(DTSH-DTSS)*(DCL2*DPTXV)**0.5

      RETURN
      END
*****************************************************************************
*
*     SIMULATION OF STORAGE
*
*     PURPOSE:
*
*      TO SIMULATION THE RESPONSE OF THE CHILLER WATER DURING THE
*      OPERATION OF THE SYSTEM,
*
*     INPUT DATA:
*
*      UM ----- RATIO OF MAXIMUM MASS FLOW RATE OF THE WATER FROM
*            THE APPLICATION FACILITIES
*      UMMAX -- MASS FLOW RATE OF THE WATER FROM THE APPLICATION
*            FACILITIES
*      TCITY -- TEMPERATURE OF THE WATER FROM THE APPLICATION
*            FACILITIES
*      CCH ---- THERMAL CAPACITY OF THE STORAGE
```

```
*       CPW ---- THERMAL CAPACITY OF THE WATER
*       U4 ----- RATIO OF MAXIMUM MASS FLOW RATE OF CYCLING WATER
*       U4MAX -- MAXIMUM MASS FLOW RATE OF CYCLING WATER
*
*     OUTPUT DATA:
*
*       TCH ---- TEMPERATURE OF CHILLED WATER STORAGE
*
*************************************************************************

      SUBROUTINE STOR (NMAXN,F,TWAE3,TCH,TCITY,J,CCH,U4,U4MAX,CPW,
     &          UM,UMMAX)

      IMPLICIT DOUBLE PRECISION (A-H,O-Z)

      DIMENSION F(NMAXN)

      F(J)=1./CCH*(-U4*U4MAX*CPW*(TCH-TWAE3)
     &     +UM*UMMAX*CPW*(TCITY-TCH))

      RETURN
      END

*************************** R12 HIGH PRESSURE ***************************
*
*     THIS SUBROUTINE COMPUTES THERMO-DYNAMICAL PROPERTY OF
*     REFRIGERANT R-12 FOR HIGH PRESSURE REGION
*     273.2+25. < TRC < 273.2+45.
*
*     INPUT DATA:
*
*       TRC ---- CONDENSATION TEMPERATURE
*
*     OUTPUT DATA:
*
*       DCV ---- DENSITY OF VAPOUR
*       DCL ---- DENSITY OF LIQUID
*       DDCV --- D(DCV)/DTRC
*       DDCL --- D(DCL)/DTRC
*       HCV ---- ENTHALPY OF VAPOUR
*       HCL ---- ENTHALPY OF LIQUID
*       CV ----- SPECIFIC HEAT OF VAPOUR
*       CL ----- SPECIFIC HEAT OF LIQUID
*
*************************************************************************

      SUBROUTINE R12HP(DCV,DCL,DDCV,DDCL,HCV,HCL,CV,CL,TRC)

      IMPLICIT DOUBLE PRECISION (A-H,O-Z)

      DCV=1.2088*TRC-325.203
```

```
      DCL=-3.8273*TRC+2453.293
      DDCV=1.2088
      DDCL=-3.8273
      HCV=0.27758*TRC+502.799
      HCL=0.99042*TRC+147.454
      CV=0.27758
      CL=0.99042

      RETURN
      END

************************************ R12 LOW PRESSURE ***************************
*
*     THIS SUBROUTINE COMPUTES THERMO-DYNAMICAL PROPERTY OF
*     REFRIGERANT R-12 FOR LOW PRESSURE REGION
*
*
*     INPUT DATA:
*
*      TRC ---- EVAPORATION TEMPERATURE
*
*     OUTPUT DATA:
*
*      DEV ---- DENSITY OF VAPOUR
*      DEL ---- DENSITY OF LIQUID
*      DDEV --- D(DEV)/DTRE
*      DDEL --- D(DEL)/DTRE
*      HEV ---- ENTHALPY OF VAPOUR
*      HEL ---- ENTHALPY OF LIQUID
*      CEV ----- SPECIFIC HEAT OF VAPOUR
*      CEL ----- SPECIFIC HEAT OF LIQUID
*
*******************************************************************************

      SUBROUTINE R12LP (DEV,DEL,DDEV,DDEL,HEV,HEL,CEV,CEL,TRE)
      IMPLICIT DOUBLE PRECISION (A-H,O-Z)

      DEV=0.547*TRE-131.778
      DEL=-3.172*TRE+2260.70
      DDEV=0.547
      DDEL=-3.172
      HEV=0.46423*TRE+446.65
      HEL=0.93307*TRE+163.67
      CEV=0.46423
      CEL=0.93307

      RETURN
      END
```

```
*****************************************************************************
*
*      THIS SUBROUTINE CALCULATES SATURATE PRESSURE FROM TEMPERATURE
*      FOR R-12
*
*      INPUT DATA:
*
*       TH ---- CONDENSATION TEMPERATURE
*
*      OUTPUT DATA:
*
*       PH ---- PRESSURE
*
*****************************************************************************

        SUBROUTINE PHTH(PH,TH)
        IMPLICIT DOUBLE PRECISION (A-H,O-Z)

        PH=(0.172*TH-44.479)*9.80665E+4

        RETURN
        END

*****************************************************************************
*
*      THIS SUBROUTINE CALCULATES SATURATE PRESSURE FROM TEMPERATURE
*      FOR R-12
*
*      INPUT DATA:
*
*       TL ---- EVAPORATION TEMPERATURE
*
*      OUTPUT DATA:
*
*       PL ---- PRESSURE
*
*****************************************************************************

        SUBROUTINE PLTL(PL,TL)
        IMPLICIT DOUBLE PRECISION (A-H,O-Z)

        PL=(0.1036*TL-25.135)*9.80665E+4

        RETURN
        END

*****************************************************************************
*
*      THIS SUBROUTINE CALCULATE DENSITY AND ENTHALPY OF SUPERHEATED
*      VAPOUR
*
```

```
*      INPUT DATA:
*
*        P ----- PRESSURE OF SUPERHEATED VAPOUR
*        T ----- TEMPERATE OF SUPERHEATED VAPOUR
*
*      OUTPUT DATA:
*
*        V ----- SPECIFIC VOLUME OF SUPERHEATED VAPOUR
*        D ----- DENSITY OF SUPERHEATED VAPOUR
*        H ----- ENTHALPY OF SUPERHEATED VAPOUR
*
*************************************************************************************

      SUBROUTINE SHEAT (D,V,H,P,T)
      IMPLICIT DOUBLE PRECISION (A-H,O-Z)

      PATA=P*1.0197162E-1
      V=7.0113*T/PATA-(295.47E-5+629.62E-10*PATA)
     &  *(273.1/T)**5.5+0.0009
      D=1./V
      HCAL=108.97+0.0736*T+0.0001195*T**2-PATA
     &    *(0.00119/T-0.0000114)
      H=HCAL*4.18605

      RETURN
      END
```